The University of Osaka
Institutional Knowledge Archive

Title	Advancing bottom-up approach for the development of multi-scale building stock energy model
Author(s)	Bin Perwez, Usama
Citation	大阪大学, 2023, 博士論文
Version Type	VoR
URL	https://doi.org/10.18910/92956
rights	
Note	

The University of Osaka Institutional Knowledge Archive : OUKA

https://ir.library.osaka-u.ac.jp/

The University of Osaka

Doctoral Dissertation

Advancing bottom-up approach for the development of multi-scale building stock energy model

USAMA BIN PERWEZ

June 2023

Graduate School of Engineering,

Osaka University

Energy Systems Area

Division of Sustainable Energy and Environmental Engineering

Abstract

Building stock energy modelling (BSEM) has gained a lot of attention recently with the development of a range of methodologies due to its multi-dimensional capabilities and the potential to incorporate various decarbonization strategies and climate mitigation scenarios. With the advancement of data-driven techniques, BSEMs involve a higher degree of complexity with varying model structure and output that requires comprehensive reporting guidelines to improve the interpretation and consistency of these models. In BSEM, several bottom-up methodologies have been developed to assess the energy demand and emission reduction potential of the stock but, often have transitional limitations either to shift from aggregated to disaggregated stock boundary conditions or involve a differentiated description of practices and policies across a range of scales and sectors. This thesis aims to advance the methodological capability of BSEM in terms of data coherence, scalability and coordination, which can provide transparency and capture value with the least cost and effort. Based on the above background, the key data acquisition techniques of BSEM are assessed to assist in the selection of the BSEM approach depending on the data availability and quality, and then, a novel bottom-up BSEM approach is developed to incorporate scalability and integration of multiple building-oriented elements within the model. Moreover, to exhibit the model applicability and integration of the developed model, a bottom-up BSEM approach is coupled with a physical approach of building integrated photovoltaics (BIPV) potential estimation to assess the carbon neutrality of commercial building stock at scale. The thesis is comprised of six chapters whose summary is explained as follows:

Chapter 1 provides a comprehensive overview of transitional strategies and measures to decarbonize the commercial building stock. After this, a quadrant-based classification of BSEM is outlined and further review of methods related to carbon neutrality assessment and BIPV estimation are discussed.

In Chapter 2, key data acquisition techniques of BSEM and their use cases are identified and then, illustrated the development process of three major BSEM approaches. The crossover framework was further developed to assess the accuracy and added value of quality and quantity of data on the model performance of commercial BSEM.

In Chapter 3, an automated dynamic building simulation framework using a GIS-synthetic hybrid model is developed to integrate spatial and synthetic modelling approaches for facilitating the concurrent consideration of multiple building-oriented elements at multiple scales.

In Chapter 4, a multi-model framework of the BSEM-BIPV coupled scheme is developed to illustrate the process of model coupling for the assessment of carbon-neutral building stock, which can involve a higher degree of coordination to adequately manage the modelling functionality and integration, resolution and data coherence.

Chapter 5 presents an integrated discussion to explain the contributions and practical perspective of the advancement of BSEM approaches. The chapter further highlights the importance of the role of data acquisition, multi-scale modelling and purpose-driven coupling for enhancing the model development process of BSEM.

Chapter 6 provides a summary of contributions related to formulated research objectives.

Overall, this thesis has contributed to the advancement of BSEM by providing comprehensive reporting guidelines in terms of accuracy, granularity and multi-dimensionality aspects. This has enhanced the capability of the BSEM to be further extended to any demographic landscape or spatial resolution and evolve into a long-term transitional workflow. Thus, enabling long-term spatial energy resource planning and decision-making in terms of sufficiency, efficiency and renewables for commercial building stock across various scales.

Keywords: Building stock energy modelling; Hybrid building stock modelling; Bottom-up model; Data-driven approach; GIS modelling; Synthetic modelling; Multi-scale; Commercial buildings.

List of Publications

Journal Articles

1. **Perwez U**, Yamaguchi Y, Ma T, Dai Y, Shimoda Y. (2022). Multi-scale GIS-synthetic hybrid approach for the development of commercial building stock energy model. Applied Energy, vol. 323, 119536. https://doi.org/10.1016/j.apenergy.2022.119536

2. Yamaguchi Y, Shoda Y, Yoshizawa S, Imai T, **Perwez U**, Shimoda Y, Hayashi Y. (2023). Feasibility assessment of net zero-energy transformation of building stock using integrated synthetic population, building stock, and power distribution network framework. Applied Energy, vol. 333, 120568. https://doi.org/10.1016/j.apenergy.2022.120568

3. Shono K, Yamaguchi Y, **Perwez U**, Ma T, Dai Y, Shimoda Y. (2023). Large-scale building-integrated photovoltaics installation on building façades: Hourly resolution analysis using commercial building stock in Tokyo, Japan. Solar Energy, vol. 253, pp. 137-153. https://doi.org/10.1016/j.solener.2023.02.025

4. **Perwez U**, Shono K, Yamaguchi Y, Shimoda Y. (2023). Multi-scale UBEM-BIPV coupled approach for the assessment of carbon neutrality of commercial building stock. Energy and Buildings, 113086. https://doi.org/10.1016/j.enbuild.2023.113086

Conference Proceedings

1. **Perwez U**, Yamaguchi Y, Shimoda Y. (2020). Development of Geo-spatial building stock model for Japanese Commercial Buildings. Proceedings of 2nd Annual Conference of Society of Airconditioning and Sanitary Engineering (SHASE), vol. 10. https://doi.org/10.18948/shasetaikai.2020.10.0_25

2. **Perwez U**, Yamaguchi Y, Shimoda Y. (2021). Cross-over analysis of building-stock modelling approaches for bottom-up engineering model. Proceedings of Building Simulation 2021: 17th Conference of IBPSA, vol. 17, pp. 1781-1788. https://doi.org/10.26868/25222708.2021.30586

Acknowledgment

I would like to thank everyone who has supported me since I began my doctoral studies here at Osaka University, Japan. Your love, support and encouragement have made my experience here much more enjoyable and rewarding. Sometimes nothing seems to go in the right direction; you need to have patience and persistence, which would not have been possible without the support of my wife, daughter and friends.

First and foremost, I would like to express special thanks to my supervisor Dr. Yoshiyuki Shimoda for his continuous support throughout my doctoral studies. I admire his passion and dedication to his research and students, and consider him as my mentor and a source of inspiration to excel in academia. Dr. Yohei Yamaguchi was the first person who introduced me to the field of building stock energy modelling. He got me started on the commercial BSEM project and pushed me to tackle some interesting problems. I would like to pay special thanks to Dr. Masanobu Kii for their guidance and service on my committee. I need to thank my lab member, Keita Shono, for his kind suggestions and the discussions we had on different topics. During my stay at Shimoda lab, I would like to acknowledge Shiho Takai and Miyuki Okumura for their cooperation in my administrative issues at Osaka University, Japan. Along with this, I am also very grateful to the Ministry of Education, Culture, Sports, Science and Technology (MEXT) of Japan for awarding a Japanese Government MEXT (Monbukagakusho) Research Scholarship that resulted in the funding of my four-year doctoral studies.

Finally, I pay due respect and thanks to my parents, Perwez Mehdi and Asma Perwez, for their care and prayers during my PhD journey. Upon completion of this long journey, I owe my sentiments of deep appreciation to my wife, Sarah, and my little princess, Aimal, for their love and encouragement that has been the backbone of my life. Thank you for always believing in me.

Dedicated to my Parents, wife, daughter and adored siblings whose tremendous support and cooperation led me to this wonderful accomplishment

Table of Contents

Abstract i
List of Publications iii
Acknowledgment iv
Table of Contents vi
Figures ix
Tables xiii
Equations xiv
Nomenclature xv
1 Introduction 1
1.1 Background 1
1.2 Towards carbon-neutral building stock 1
1.2.1 Sufficiency 2
1.2.2 Efficiency 3
1.2.3 Renewables 3
1.3 Overview of building stock energy modelling (BSEM) 4
1.3.1 Bottom-up/white-box (Q4) model 5
1.4 Methods to analyze carbon neutrality of building stock 7
1.5 Methods for assessment of BIPV potential 7
1.6 Literature review 8
1.6.1 Cross-over analysis of bottom-up BSEMs 8
1.6.2 Development of multi-scale approach for bottom-up BSEM 10
1.6.3 Carbon neutrality assessment using bottom-up BSEM and BIPV model 12
1.7 Research gap 14
1.8 Aim and objectives 15
1.9 Contributions 16
1.10 Thesis outline 17
2 Cross-over analysis of bottom-up BSEMs 19
2.1 Purpose 19
2.2 Overview of bottom-up BSEMs 19
2.3 Methodology 20
2.3.1 Data collection 21
2.3.2 Building stock initialization 22
2.3.3 Building stock characterization 22
2.3.4 Building stock evaluation 24
2.3.5 Building stock energy simulations 24

2.4 Results and discussion 25
2.5 Conclusion 29
3 Development of multi-scale approach for bottom-up BSEM 31
3.1 Purpose 31
3.2 Methodology 32
3.2.1 Data 33
3.2.2 Hybrid stock modelling 34
3.2.3 Building stock energy modelling and simulation 37
3.2.4 Building stock scenarios 39
3.3 Results 40
3.3.1 GIS building stock analysis 41
3.3.2 Synthetic building stock analysis 43
3.3.3 Building stock energy modelling and simulation 46
3.3.4 Building stock scenarios 51
3.4 Discussion 57
3.5 Conclusions 60
3.6 Appendix 61
3.6.1 Appendix A 61
3.6.2 Appendix B 62
3.6.3 Appendix C 65
3.6.4 Appendix D. Settings for building stock energy simulation 65
3.6.5 Appendix E 66
3.7 Supplementary data 66
4 Carbon neutrality assessment using bottom-up BSEM and BIPV model 67
4.1 Purpose 67
4.2 Methodology 68
4.2.1 UBEM model 69
4.2.2 BIPV potential estimation approach 70
4.2.3 Decarbonization scenarios and strategies 71
4.2.4 Carbon neutrality assessment 73
4.3 Results 74
4.3.1 Building stock analysis 74
4.3.2 Aggregated evaluation 75
4.3.3 Multi-scale evaluation 81
4.4 Discussion 88
4.4.1 Development of UBEM-BIPV coupled approach 88

4.4.2 Relationship between decarbonization strategies 89
4.4.3 Scalability 89
4.4.4 Future work and limitations 90
4.5 Conclusion 90
4.6 Appendix 91
4.6.1 Appendix A. Development of a physical-based BIPV potential estimation 91
4.6.2 Appendix B. Types of HVAC systems and other measures. 92
4.6.3 Appendix C. Description of commercial RBMs for UBEM model 94
4.7 Supplementary data 94
5 Integrated discussion 95
5.1 Role of data acquisition 95
5.2 Multi-scale modelling 96
5.3 Purpose-driven coupling 97
5.4 Future work and limitations 98
6 Conclusion 100
References 103

Figures

FIGURE 1-1. OVERVIEW OF SER FRAMEWORK..... 2
FIGURE 1-2. QUADRANT-BASED CLASSIFICATION OF BSEM..... 4
FIGURE 1-3. THESIS OUTLINE. 17
FIGURE 2-1. OVERVIEW OF THE TRANSITIONAL SHIFT FROM AGGREGATED TO DISAGGREGATED BOUNDARY CONDITIONS..... 20
FIGURE 2-2. CROSS-OVER FRAMEWORK TO ASSESS BUILDING STOCK-LEVEL APPROACHES. 21
FIGURE 2-3. STRUCTURE OF BUILDING STOCK USING DIFFERENT APPROACHES..... 26
FIGURE 2-4. DISTRIBUTION OF HVAC STOCK USING DIFFERENT BUILDING STOCK APPROACHES: (A) COOLING SYSTEMS; (B) HEATING SYSTEMS; AND (C) FUEL TYPE..... 29
FIGURE 2-5. COMPARISON OF AGGREGATED ENERGY DEMAND AND CARBON EMISSIONS ACROSS THE STOCK FOR DIFFERENT BOTTOM-UP BSEMS..... 29
FIGURE 3-1. SCHEMATIC OVERVIEW OF GIS-SYNTHETIC HYBRID APPROACH..... 32
FIGURE 3-2. SIMPLIFIED WORKFLOW OF DATASETS USED IN GIS-SYNTHETIC HYBRID FRAMEWORK..... 33
FIGURE 3-3. K-MEANS OPTIMUM CLUSTERING USING DISTANCE-METRIC MEASUREMENT CRITERIA. (WHERE X- AND Y-AXIS PRESENT K (OR CLUSTER) VALUE AND NORMALIZED INDEX RESPECTIVELY; TOP AND BOTTOM FIGURES SHOW THE VARIATION OF INTERNAL VALIDATION INDICES AND UNIFIED VALIDATION INDEX RESPECTIVELY, FOR FOUR DIFFERENT MEASURES OF DISTANCE AND CLUSTERING METRICS (EUCLIDEAN, MANHATTAN, CORRELATION, AND SPEARMAN).)..... 42
FIGURE 3-4. OVERVIEW OF BUILDING TYPOLOGIES OF COMMERCIAL BUILDING STOCK ACROSS DIFFERENT SCALES. 42
FIGURE 3-5. SEGMENT-WISE COMPOSITION OF NEIGHBOURHOOD CONTEXT FOR DIFFERENT SCALES (NOTATION: D IS THE ADJACENT AVERAGE DISTANCE BETWEEN TARGET BUILDING AND NEIGHBOURHOOD; H IS THE AVERAGE NEIGHBOURHOOD HEIGHT; AND TB IS THE AVERAGE HEIGHT OF TARGET BUILDING)..... 43
FIGURE 3-6. LONG-TERM STOCK DISTRIBUTION OF BUILDING VINTAGE FOR COMMERCIAL BUILDINGS ACROSS DIFFERENT SCALES..... 44
FIGURE 3-7. DISTRIBUTION OF HVAC SYSTEMS IN THE COMMERCIAL BUILDING STOCK FOR DIFFERENT SCALES. 45
FIGURE 3-8. DISTRIBUTION OF ESMS IN THE COMMERCIAL BUILDING STOCK FOR DIFFERENT SCALES..... 46
FIGURE 3-9. (A) VALIDATION OF RBMS FOR DIFFERENT SCALES: I) OFFICE; II) HOTEL; III) HOSPITAL AND IV) SCHOOL.; (B) CUMULATIVE FREQUENCY DISTRIBUTION OF EUI ACROSS

THE STOCK FOR DIFFERENT SCALES: I) NATIONAL; II) TOKYO; AND III) CHUO; (C) AGGREGATED-LEVEL EVALUATION OF THE MODEL FOR DIFFERENT SCALES: I) NATIONAL; II) TOKYO; AND III) CHUO. 48
FIGURE 3-10. ANNUAL EUI OF RBMS FOR NATIONAL (A), TOKYO (B), AND CHUO (C) IN TERMS OF; I) END-USE AND II) FUEL TYPE. 49
FIGURE 3-11. LONG-TERM PRIMARY ENERGY CONSUMPTION ACROSS DIFFERENT SCALES; A) SEGMENT-WISE AND B) END-USE (WHERE 2030E AND 2030P REPRESENT ELECTRIFICATION AND POTENTIAL SCENARIOS FOR THE 2030 YEAR RESPECTIVELY)..... 50
FIGURE 3-12. VARIATION OF ENERGY CONSUMPTION BY THE IMPLEMENTATION OF DIFFERENT SCALES (NATIONAL AND TOKYO) ON A REFERENCE SCALE (OR CHUO): A) ANNUAL PRIMARY ENERGY CONSUMPTION AND CARBON EMISSIONS; B) SCALE UNCERTAINTY RELATIVE TO CHUO SCALE (WHERE EACH DOT REPRESENTS A SPECIFIC RBM CLUSTER WHICH IS SORTED FROM HIGHEST TO LOWEST CVRMSE VALUE). 51
FIGURE 3-13. ILLUSTRATIVE BUILDING-BY-BUILDING MAPPING OF THE SPATIAL DISTRIBUTION OF PRIMARY ENERGY CONSUMPTION BY THE IMPLEMENTATION OF DIFFERENT SCALES (NATIONAL AND TOKYO) ON A REFERENCE SCALE (OR CHUO). 52
FIGURE 3-14. OAT ANALYSIS FOR QUANTIFYING ENERGY EPIDEMIOLOGY (WITH CHUO AS REFERENCE SCALE): A) CLUSTER-WISE PRIMARY ENERGY DIFFERENCE DUE TO VARIOUS PARAMETERS BY IMPLEMENTING NATIONAL (I) AND TOKYO (II) OFFICE BUILDING STOCK (NOTATION: BLACK AS POSITIVE AND RED AS NEGATIVE); B) AVERAGE IMPACT FACTORS OF VARIOUS PARAMETERS. 54
FIGURE 3-15. LONG-TERM ENERGY EPIDEMIOLOGY EFFECTS: A) ANNUAL PRIMARY ENERGY CONSUMPTION AND CARBON EMISSIONS; AND B) SCALE UNCERTAINTY RELATIVE TO CHUO SCALE (WHERE EACH DOT REPRESENTS A SPECIFIC CLUSTER WHICH IS SORTED FROM HIGHEST TO LOWEST CVRMSE VALUE). 55
FIGURE 3-16. OAT EFFECT ON THE STOCK-WISE UNCERTAINTY FOR NATIONAL (I), TOKYO (II) AND CHUO (III) (WHERE EACH DOT REPRESENTS A SPECIFIC CLUSTER WHICH IS SORTED FROM HIGHEST TO LOWEST CV RMSE VALUE)..... 55
FIGURE 3-17. OAT EFFECT ON THE ELEMENT-WISE UNCERTAINTY ACROSS THE SCALE. 56
FIGURE 3-18. COMBINED EFFECT ON THE MODEL PREDICTION: A) STOCK-WISE UNCERTAINTY FOR NATIONAL (I), TOKYO (II) AND CHUO (III); AND B) ELEMENT-WISE UNCERTAINTY ACROSS THE SCALE. 57
FIGURE 4-1. SCHEMATIC OVERVIEW OF UBEM-BIPV COUPLED APPROACH. 69

FIGURE 4-2. COMPOSITION OF COMMERCIAL BUILDING STOCK FOR DIFFERENT SCENARIOS: (A) BUILDING USAGE (APPENDIX C); (B) ENVELOPE; (C) HVAC SYSTEM HEAT SOURCE (APPENDIX TABLE B1); AND (D) VENTILATION MEASURES (APPENDIX TABLE B4). 75
FIGURE 4-3. (A) CUMULATIVE FREQUENCY DISTRIBUTION OF EUI ACROSS THE COMMERCIAL BUILDING STOCK; (B) AVERAGE HOURLY REGIONAL ELECTRICITY DEMAND OF COMMERCIAL BUILDING STOCK. 76
FIGURE 4-4. (A) ANNUAL PRIMARY ENERGY CONSUMPTION OF COMMERCIAL BUILDING STOCK ACROSS DIFFERENT PATHWAYS (NOTE: NEGATIVE VALUES INDICATE THE REDUCTION INDUCED BY EACH MEASURE BETWEEN THE TRANSITION OF PATHWAY)..... 77
FIGURE 4-5. AVERAGE HOURLY REGIONAL ELECTRICITY AND GAS DEMAND CONSIDERING SEASONAL CHANGES AND THE IMPACT OF VARIOUS MEASURES ON COMMERCIAL BUILDING STOCK (NOTE: NEGATIVE VALUES INDICATE THE REDUCTION INDUCED BY EACH MEASURE BETWEEN THE TRANSITION OF PATHWAY). 78
FIGURE 4-6. SENSITIVITY ANALYSIS OF KEY DESIGN AND PLANNING PARAMETERS OF BIPV ON A YEARLY SUPPLY POTENTIAL. 78
FIGURE 4-7. (A) COMPOSITION OF BIPV MODULE AREA FOR DIFFERENT SUPPLY STRATEGIES; (B) BIPV ANNUAL GENERATION FOR DIFFERENT SUPPLY STRATEGIES AT THE REGIONAL LEVEL; AND (C) LOAD DURATION CURVE OF DIFFERENT SUPPLY STRATEGIES..... 79
FIGURE 4-8. ANNUAL ENERGY BALANCE (A) AND EMISSION REDUCTION POTENTIAL (B) OF COMMERCIAL BUILDING STOCK ACROSS DIFFERENT DEMAND AND SUPPLY-SIDE STRATEGIES AT THE REGIONAL LEVEL..... 80
FIGURE 4-9. (A) AVERAGE MONTHLY DYNAMIC ENERGY BALANCE; (B) PERFORMANCE ASSESSMENT; AND (C) LOAD DURATION CURVE OF COMMERCIAL BUILDING STOCK ACROSS DIFFERENT DEMAND AND SUPPLY-SIDE STRATEGIES AT THE REGIONAL LEVEL..... 81
FIGURE 4-10. (A) DISTRIBUTION OF EUI; AND (B) COMPARISON OF AVERAGE DAILY LOAD FACTOR ACROSS DIFFERENT SCALES. 82
FIGURE 4-11. ILLUSTRATIVE CITY SCALE MAP OF THE SPATIAL DISTRIBUTION OF PRIMARY ENERGY CONSUMPTION FOR VARIOUS PATHWAYS. 83
FIGURE 4-12. REDUCTION POTENTIAL OF DEMAND-SIDE MEASURES ACROSS DIFFERENT SCALES: A) ACTIVE; AND B) PASSIVE MEASURES. 83
FIGURE 4-13. AVERAGE HOURLY BIPV GENERATION ACROSS DIFFERENT SCALES: I) DISTRICT; II) CITY; AND III) REGIONAL LEVEL (SHOWING THE AMOUNT OF ADDED POTENTIAL WITH THE CHANGE IN INTEGRATION LEVEL)..... 85

FIGURE 4-14. ANNUAL EMISSION REDUCTION POTENTIAL UNDER DIFFERENT INTENSITIES, (A) CEI=0.47 AND (B) CEI=0.25, FOR DIFFERENT SCALES: I) DISTRICT; II) CITY; AND III) REGIONAL LEVEL. 86
FIGURE 4-15. ILLUSTRATIVE CITY SCALE MAP OF THE SPATIAL DISTRIBUTION OF SS FOR VARIOUS DEMAND-SUPPLY PATHWAYS. 87
FIGURE 4-16. (A) SELF-SUFFICIENCY ANALYSIS OF COMMERCIAL BUILDING STOCK ACROSS DIFFERENT SCALES: I) BUILDING-BY-BUILDING; II) DISTRICT; AND III) CITY LEVEL; (B) AVERAGE DYNAMIC PERFORMANCE ASSESSMENT OF DIFFERENT DEMAND AND SUPPLY-SIDE STRATEGIES ACROSS DIFFERENT SCALES: I) DISTRICT; II) CITY; AND III) REGIONAL LEVEL. 88

Tables

TABLE 1-1. OVERVIEW OF STUDIES RELATED TO BOTTOM-UP BSEM METHODOLOGIES. 10
TABLE 1-2. OVERVIEW OF EXISTING PHYSICS-BASED BOTTOM-UP BSEMS. 12
TABLE 1-3. OVERVIEW OF EXISTING BSEM-BIPV COUPLED STUDIES. 14
TABLE 2-1. COMPARATIVE OVERVIEW OF CHARACTERIZATION TECHNIQUES FOR DIFFERENT APPROACHES. 23
TABLE 2-2. RAPD STATISTICS OF BUILDING STOCK APPROACHES. 26
TABLE 2-3. COMPOSITION OF ARCHETYPES FOR DIFFERENT BUILDING STOCK APPROACHES..... 27
TABLE 3-1. OVERVIEW OF SHAPE INDICES. 36
TABLE 3-2. DESCRIPTION OF STOCK LEVEL PARAMETER SETTINGS. 38
TABLE 3-3. TYPICAL CHARACTERISTICS OF THE UNIT BLOCK BUILDING MODEL. 40
TABLE 3-4. VALIDATION RESULTS FOR COMMERCIAL BSEM ACROSS DIFFERENT SCALES. 48
TABLE 4-1. DESCRIPTION OF DECARBONIZATION STRATEGIES AT DEMAND-SIDE. 72
TABLE 4-2. SENSITIVITY ANALYSIS OF KEY DESIGN AND PLANNING PARAMETERS OF BIPV..... 73
TABLE 4-3. SPECIFICATIONS OF BIPV MODULE. 73
TABLE 4-4. OVERVIEW OF CARBON EMISSION INTENSITIES (CEI) FOR DIFFERENT FUELS..... 73

Equations

2-1 24
3-1 35
3-2 35
3-3 35
3-4 35
3-5 40
3-6 40
4-1 74
4-2 74

Nomenclature

AUC	Area under curve
BIPV	Building integrated photovoltaics
BSEM	Building stock energy model
CDD	Cooling degree days
CEI	Carbon emission intensity
CMIP	Coupled model intercomparison project
CVRMSE	Coefficient of variation of the root mean square error
DER	Distributed energy resource
EI	Export index
ESM	Energy saving measure
EUI	Energy use intensity
GHG	Greenhouse gas
GIS	Geographic information system
HDD	Heating degree days
HVAC	Heating, ventilation and air-conditioning
II	Import index
OAT	One-at-time
PD	Population density
RBM	Reference building model
ROC	Receiver operating characteristics
SER	Sufficiency, Efficiency, Renewable
SS	Self-sufficiency
TFA	Total floor area
UBEM	Urban building energy model

This page is intentionally left blank

1 Introduction

1.1 Background

Building stock is one of the main sources of global final energy consumption and offers an enormous emissions reduction potential due to reliance on fossil fuel-based end-use equipments and lack of adoption of energy efficiency measures. In the building sector, commercial buildings are an energy intensive sub-segment, accounting for 15% of global greenhouse gas emissions (GHG) (IEA, 2019). As they possess significant energy-saving potential, this presents a unique challenge for accelerating the decarbonization of commercial buildings with existing technologies and practices. This requires an adequate understanding of the complex interactions between factors influencing energy usage for implementing energy-saving measures (ESMs) (Yoshino et al. (2017); Nägeli et al. (2022)). Therefore, there is a need to formulate regulations and strategies to perform the accurate assessment of energy demand patterns and emission reduction potential of commercial buildings.

At a stock level, the commercial building sub-sector is a source of enormous operational and embodied emissions due to diverse functionalities, non-renovated buildings and the use of carbon-intensive material stock for large-scale constructions. To analyze these emission reduction targets in the commercial building stock, it is important to develop a robust and comprehensive building stock energy model (BSEM) that allow to: (1) estimate the trends of energy demand and CO_2 emissions at multiscale level (Nutkiewicz et al. (2018); Ali et al. (2019)); (2) accurately consider the complexity in terms of building heterogeneity, typology and occupancy, even with limited data availability (Wang et al. (2022)); and (3) explore the influence of uncertain and external socio-technical factors on CO_2 emission reduction strategies and policies (Yu et al. (2021); Heidelberger et al. (2022)). To address these stock-level strategies, this chapter initially highlights a detailed description of the main drivers and processes for achieving carbon-neutral building stock and then, provides an overview of different modelling techniques for the development of BSEM and their use case.

1.2 Towards carbon-neutral building stock

As per the Intergovernmental Panel on Climate Change (IPCC) Sixth Assessment Report (AR6), Sufficiency, Efficiency, Renewable (SER) framework enables the identification of key drivers and determinants to consider for the decarbonization of building stock (Cabeza et al. (2022)). The implementation of the SER framework requires the deployment of a combination of technological and non-technological mitigation strategies, and renewable sources. The implementation of these transitional measures involves a combination of new technologies, enabling policies and regulations, resource planning, and socio-behaviour coherence as shown in Figure 1-1. In commercial building stock, realizing carbon neutral targets will be extremely challenging due to

diverse functionalities, large-scale buildings and longer lifetime of the buildings (Madhusanka et al. (2022)). Thus, the transitional pathway for commercial building stock requires adequately managing the degree of complexity by providing a coordinated effort with the implementation of non-technological mitigation strategies, improvement of efficiency measures, active and passive design strategies, and use of renewable distributed energy resources (DERs).

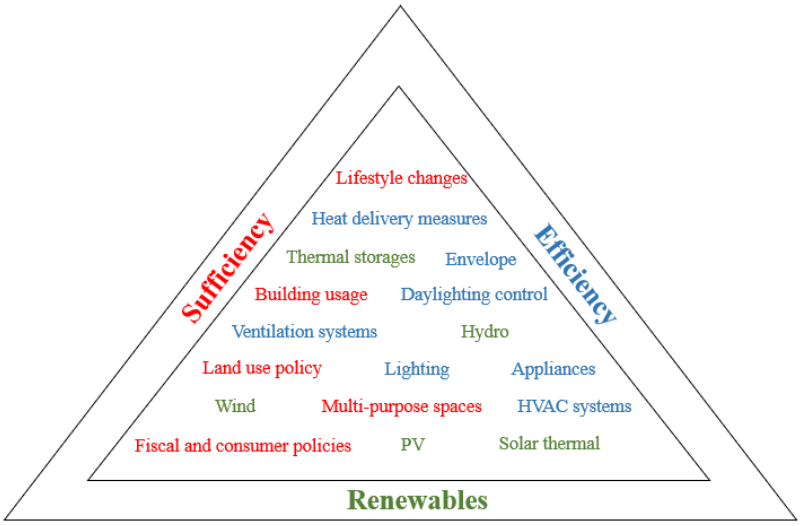

Figure 1-1. Overview of SER framework.

1.2.1 Sufficiency

The concept of sufficiency has recently gained focus due to the avoidance of cost and demand of energy by considering planetary boundaries. These are a set of non-technological options, such as land use management, use of buildings and appliances, and fiscal and consumer policies, that provide long-term non-energy use strategies to reduce the dependence of mitigation measures on technological aspects. The implementation of sufficiency measures in commercial building stock requires: (1) optimizing building usage to reduce land take and building waste; (2) lifestyle changes in terms of teleworking and conditioned set point temperature limits; (3) prioritizing multi-purpose commercial spaces; and (4) fiscal policies for the mandatory limit on building occupancy of commercial buildings. Gaspard et al. (2023) demonstrated that the volume and typology of buildings not only affect energy use but also reduce land take and building waste which has a significant impact on embodied emissions. Yang et al. (2022) considered lifestyle changes in the bottom-up simulation model to compare the decarbonization effect with other measures and found that green lifestyle strategies, teleworking and conditioned set point temperature limits, have similar carbon emission reduction potential to rooftop photovoltaics (PV). Ivanova and Büchs (2020) analyzed the impact of resource sharing by comparing the effect of shared and non-shared spaces on carbon footprints. Akenji et al. (2021) proposed a taxing and rationing concept to limit the per-capita floor area with legal and administrative procedures.

1.2.2 Efficiency

In the context of SER measures, efficiency is one of the conventional and widespread options to decarbonize building stock. These are set of mitigation options that provide a continuous short-term technological improvement which mainly consists of various active, heating, ventilation, and air-conditioning (HVAC) systems, lighting, appliances, daylighting control, and heat delivery measures, and passive design factors, type of buildings, building layout, envelope and geometry, that influence building energy use. To evaluate the correlation between building efficiency measures and energy use, various studies focused on optimizing parameters such as building geometry (Chen et al. (2019); D'Agostino et al. (2021)), insulations (Zhu et al. (2020)), opening or glazing (Zhang et al. (2017)), shading or overhang projection (Zhang et al. (2017); Chen et al. (2019)), and ventilation and HVAC (Kim et al. (2020); Yu et al. (2021)). In the context of passive strategies, Zhang et al. (2017) used passive design parameters, insulations, glazing, and shading, to estimate the thermal and daylight performance of school buildings. Chen et al. (2019) combined passive elements, building orientation, window-wall ratio (WWR), insulations, and shading, with BIPV to explore energy saving potential of high-rise commercial buildings. Zhu et al. (2020) optimized the energy use and daylighting of rural hotel buildings by varying building shapes and WWR. D'Agostino et al. (2021) proposed an automatic workflow to consider the influence of passive design parameters, building layout, insulations, and WWR, on the energy use of school buildings. Moreover, in the context of active strategies, Kim et al. (2020) developed a national scale model to evaluate the effect of heterogeneity of HVAC systems on the energy use of office building stock. Yu et al. (2021) evaluated multiple carbon-neutral tactics under climate change scenarios for a single office building and found that a feasible strategy will be to improve building system efficiency and reduce the carbon emission intensity factor on the supply side. Jokinen et al. (2022) analysed the co-influence of building retrofits, envelope insulations, ventilation, heat pumps and boilers, on the carbon emission reduction potential of building stock at a national scale. Lausselt et al. (2022) considered district heating and heat pumps to assess the decarbonization potential of building stock at a city scale.

1.2.3 Renewables

With the initiative to transition towards low carbon society, renewable technologies are gaining significance as an alternative pathway due to increasing prices of conventional fossil fuels and concerns related to climate change (Rasool et al. (2022)). The integration of these technological interventions in buildings has pushed the system boundaries towards distributed energy resources (DERs) that can further facilitate the large participation of prosumers. Recently, the ASHRAE Standard 90.1 (2022), a key benchmarking guideline for commercial building energy use,

incorporated a minimum requirement for the use of on-site renewables for commercial buildings to reduce the environmental impact of the use of energy. The implementation of on-site renewables in commercial buildings requires: (1) integration of solar technologies and storages; (2) phasing out of gas boilers, water and space heating systems; and (3) electrification of auxiliary and other building equipments. Kobashi et al. (2022) performed a techno-economic analysis of rooftop PV and electric vehicles (EV) to quantify the decarbonization potential of the commercial district of Kyoto, Japan. Borràs et al. (2023) assess energy-sharing strategies of rooftop PV and battery storage for buildings at a community level. Yamaguchi et al. (2022) developed a statistical-based commercial building stock model at a national level to consider multiple technological interventions and found that an increase in electricity demand can be avoided through electrification by improving the efficiency of building systems.

1.3 Overview of building stock energy modelling (BSEM)

BSEM is an approach which provides the assessment of building energy use and predicts the evolution of building stock performance over a specific time domain (Kavgic et al. (2010); Reinhart (2016)). These stock-level analyses provide information related to the group of building types and heterogeneity among buildings, which can address the regulations and strategies for assessing the aggregated energy demand and emission reduction potential of the stock (Geraldi et al. (2020)). Building stock can be further classified into geo-building and type-building stocks. Geo-building stock is the group of buildings which are disaggregated according to a geographically referenced description. Type-building stock is a group of buildings which are classified according to usage and characteristics in common.

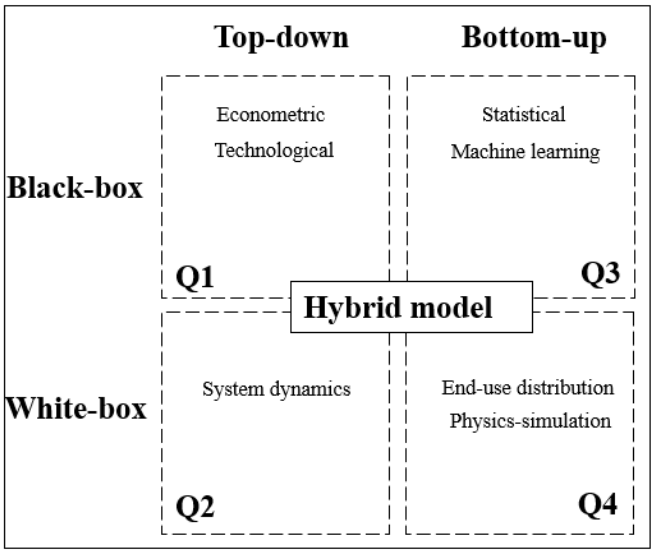

Figure 1-2. Quadrant-based classification of BSEM.

To classify the BSEMs, IEA-EBC Annex 70 (Langevin et al. (2020)) proposed a quadrant-based flexible framework employing a cross-over classification approach to classify them into two design approaches, top-down and bottom-up, and four quadrants, top-down/black-box (Q1), top-down/white-box (Q2), bottom-up/black-box (Q3), and bottom-up/white-box (Q4) as shown in Figure 1-2. The top-down models use technological-econometric indicators (Q1) or system dynamics (Q2) to determine the aggregated building energy use of building stock. With the availability of data at the disaggregated level, this recent advancement has allowed a greater focus on the bottom-up-based quadrant methodologies (Q3 and Q4) (Yang et al. (2020); Ali et al. (2020)). The bottom-up models use historical information or engineering estimates to determine the energy end-use of a representative building and aggregate that representative data to the entire stock level. Several existing bottom-up studies related to commercial buildings rely on the Q3 models owing to the low availability and quality of data to characterize building stocks and incorporate the complexity of system structure influencing building energy demand (Ma et al. (2016); Robinson et al. (2017); Abbasabadi et al. (2019)), whereas the Q4 models represent such complexities by explicitly dealing with the physical and technical attributes used in the stock level analysis. However, the model development requires detailed input data and granular-level information related to these attributes (Moazzen et al. (2020); Ye et al. (2021)).

1.3.1 Bottom-up/white-box (Q4) model

The bottom-up/white-box (Q4) models, also known as an engineering-based method, are based on the simulation of physics-based building dynamics to estimate the energy use of building stock (Reinhart et al. (2016)). These models commonly use representative buildings (or archetypes) to determine the energy end use (Österbring et al. 2016). Recently, with the availability of disaggregated data, a generalized data-driven approach has gained focus for the characterization of the archetypes in Q4 models that reduces inter-dependencies and further refine the quality of data. This approach has the potential to scale-up the flexibility and complexity of the model by incorporating technological interventions and long-term emission reduction strategies at the multiscale level. Moreover, these physics-based bottom-up stock models are further classified into urban building energy model (UBEM), synthetic-based and hybrid approaches (Ali et al. (2021); Dahlström et al. (2022)).

1) UBEM model: This methodology uses geographical information systems (GIS) to incorporate geo-referenced dataset within the model, and the energy demand of building stock is quantified by summing up the simulated energy demand of individual buildings (Davila et al. (2016)). This approach is mainly applied to smaller levels, typically district- to city-level, and the use of GIS data enables the consideration of the physical attributes of buildings within BSEM. Nageler

et al. (2017) developed a GIS-based UBEM for an urban district consisting of 1945 buildings, to predict the heating and domestic hot water demand of commercial and residential buildings. Chen et al. (2017) utilized a geo-database for developing a district-scale UBEM model, consisting of 940 buildings, for assessing the retrofit potential in commercial buildings. Zheng et al. (2019) integrated a GIS-based approach with the existing commercial building prototypes on a county scale to assess the impact of climate change on building energy use. Roth et al. (2020) proposed a GIS-based UBEM by combining physics-based simulation and machine learning methods to predict the hourly energy profiles of commercial and residential buildings at a city scale. Lausselet et al. (2022) constructed a dynamic GIS-based UBEM model at a city scale to assess the impact of various retrofit measures on the decarbonization potential of building stock.

2) Synthetic-based approach: This approach uses sample data of buildings related to physical and technical attributes as model input to calculate the energy consumption of building stock (Nägeli et al. (2018; 2020)). This approach consists of two main categories: (1) sample-free; and (2) sample-based synthetic models. The first synthetic approach uses aggregated data, such as census, due to the non-availability of micro-dataset, while the latter approach uses sample micro-dataset to generate disaggregated building stock. Moreover, the most commonly used techniques are either iterative proportional fitting (IPF) (Hermes et al. (2012)) or Monte Carlo random sampling (Lenormand et al. (2013)) which result in generating sample-based and sample-free datasets respectively.

3) Hybrid approach: This approach uses both deterministic and probabilistic characterization to integrate elements of one approach with other specific models that can bridge the gap within conventional bottom-up (Q4) models (Langevin et al. (2019); U.S. EIA, 2020). Fonseca and Schlueter (2015) developed a district-scale model by initially executing statistical Q3 and analytical Q4 models and then calculated the aggregated energy use by averaging both outputs. Nutkiewicz et al. (2018) adopted an inverse hybrid model for neighbourhood-scale by initially developing a baseline physics-based simulated bottom-up (Q4-based) model and then feeding its time series output into a machine learning (Q3-based) model to capture the influence of inter-building energy dynamics and microclimate on commercial building energy use. Huo et al. (2021a; 2021b) constructed an integrated dynamic simulation model by coupling a bottom-up end-use (Q4-based) model with system dynamics (Q2-based) model to consider the impact of various long-term dynamics parameters on the possible emission peaks and peaking times of building stock. Perwez et al. (2022) integrated a GIS-based approach with the synthetic UBEM model to evaluate the impact of uncertainty of physical and technical elements at multiple scales.

1.4 Methods to analyze carbon neutrality of building stock

Several methods have been developed to assess the carbon neutrality of building stock that differs on the basis of data availability, accounting principle, and scope of application. These methods are mainly divided into four classifications: (1) decomposition method (Zhang et al. (2022)); (2) input-output method (Zhu et al. (2020)); (3) statistical method (Geraldi et al. (2022); Vaisi et al. (2023)); and (4) simulation method (Reinhart et al. (2016); Langevin et al. (2020); Nägeli et al. (2022)). In terms of methodological characterization, decomposition and simulation methods use consumption-based accounting principles that mainly calculate operational carbon emissions, while input-output and statistical methods use production-based accounting principles that mainly calculate both embodied and operational carbon emissions (Cai et al. (2014); Zhang et al. (2016)). With the availability of data at a disaggregated level, this recent advancement has allowed greater focus on bottom-up simulation methods (Dahlström et al. (2022); Morewood (2023)). These methods use historical information or engineering estimates to determine the energy end-use of a representative building (or archetype) and aggregate that representative data to the entire stock level. Several existing bottom-up simulation studies related to commercial buildings rely on black-box (or machine learning) models owing to the low availability and quality of data to characterize building stocks (Robinson et al. (2017); Li and Yao (2021); Amasyali et al. (2022)). These models lack in analytical capability to conduct long-term studies and cannot identify the spatial distribution of energy use of building stock. Moreover, with the availability of GIS data, some of the studies have recently focused on GIS models to develop UBEM that bridge a gap within conventional bottom-up models by adding spatial dimension.

1.5 Methods for assessment of BIPV potential

The evaluation of BIPV potential has recently gained significance due to the focus towards low carbon cities and also for the integration of renewables in grids (Freitas et al. (2015)). However, the BIPV potential estimation at a large scale is highly challenging owing to computational and modelling complexities (Chatzipoulka et al. (2018)). Several estimation approaches are developed to assess the BIPV potential: (1) sampling approach (Groppi et al. (2018); Horan et al. (2020)); (2) geostatistical approach (Fathizad et al. (2017); Amjad and Shah (2020)); (3) machine learning approach (Yadav and Chandel (2015); Walch et al. (2020)); and (4) physical approach (Cheng et al. (2020); Liu et al. (2023)). The sampling approach uses key decision variables to extrapolate the potential estimation to the entire area, whereas the geostatistical approach uses spatial interpolation to determine the potential estimation of the entire area. Moreover, the machine learning approach uses data-driven predictive models to evaluate the potential estimation, whereas the physical approach uses a 3D model to consider the inter-building effect for the evaluation of BIPV potential. These approaches mainly use the GIS model to capture the urban

design factors and geographical constraints. Recently, the physical approach has gained a lot of focus because of its better accuracy, flexibility and granularity in comparison to other approaches (Gassar and Cha (2021)).

1.6 Literature review

This section mainly consists of three sub-sections. Section 1.6.1 outlines the studies related to different bottom-up BSEM methodologies and then summarizes those in terms of data acquisition and applications. Section 1.6.2 examines the studies related to physics-based BSEMs and then compares the analytical capability of those models in terms of granularity and integration of model components. Section 1.6.3 summarizes the physics-based bottom-up BSEM studies related to the assessment of carbon neutrality of building stock and then evaluated those on the basis of the SER framework.

1.6.1 Cross-over analysis of bottom-up BSEMs

In BSEM, several bottom-up methodologies have been developed to assess the energy demand and emission reduction potential of the stock. In this section, the most commonly used bottom-up BSEMs are reviewed and then summarizes the previous studies in terms of data acquisition and applications.

1) Sample-free synthetic method: This stock-level approach uses the known distribution of aggregated structure data to generate a synthetic population of buildings. A representative sample stock is constructed by iteratively performing Monte Carlo random sampling based on the known distribution of attributes, which represents the specified composition of an aggregated dataset (Lenormand et al. (2013)). Sample-free synthetic model is easy to develop even with limited availability of data but the major disadvantage is the randomness of input space due to the generation of de-correlated attributes within individual records. Nägeli et al. (2018) used a sample-free approach to transform aggregated building stock data into disaggregated one and then estimated the energy demand and carbon emissions of building stock at the national scale. Hietaharju et al. (2021) used Monte Carlo random sampling on building age classification to predict the renovation and demolition of each building within the stock at a district scale. Moreover, this approach is feasible to be used in those countries/regions or cities where the availability of micro-dataset is not possible.

2) Sample-based synthetic method: This approach is an extension of either synthetic reconstruction (SR) or combinatorial optimization techniques, which uses marginal distribution obtained from a survey-based sample to generate the representative individuals considering the various dimensions or elements of stock (Hermes et al. (2012)). Typically, iterative proportional fitting (IPF), a bi-proportional approach to estimate a k-way marginal table while still preserving

the correlation matrix, is the most common technique used in this method to fit the obtained disaggregated distributions. The general concept of the method is to apply multinominal logistic regression, a semiparametric classification approach which uses a logistic function to predict the probabilities of dependent variables, on the survey dataset to obtain the distribution probabilities and then uses the IPF technique to fit the obtained disaggregated distributions. Roth et al. (2021) used annual building energy data to develop synthetic hourly building energy estimates at a city scale by combining physics-based simulation and machine learning methods. Yamaguchi et al. (2022) developed a sample-based stock model to predict the distribution probabilities of building systems and energy saving measures of commercial building stock at a national scale. Moreover, this method is more flexible to be used at a specific level (from national to district scale) but can be very time-consuming due to sample collection, attainment of marginal distributions and complexity associated with fitting higher dimensional data.

3) Geo-referenced stock method: This approach utilizes geographical information systems (GIS) to retrieve a geo-referenced micro-dataset of building stock at a disaggregated level (Österbring et al. (2016)). The development of geo-referenced micro-dataset requires multiple acquisition techniques, such as drones, remote sensing, transformation of BIM data, and vectorizing existing drawings, to convert existing data into geo-database. Typically, a geo-database is characterized by five levels of details (LOD 0-4) which are differentiated based on a list of features, attributes, dimensionality, and complexity involved in the specified model (Biljecki et al. (2016)). This method facilitates data integration by coupling and merging multiple datasets to improve the quality of geo-building stock and provides better spatial dimensionality to consider urban environment settings and dynamic occupancy behaviour within the model (Dabirian et al. (2022)). Nageler et al. (2017) developed a GIS-based UBEM for an urban district consisting of 1945 buildings, to predict the heating and domestic hot water demand of commercial and residential buildings. Zheng et al. (2019) integrated a GIS-based approach with the existing commercial building prototypes on a county scale to assess the impact of climate change on building energy use. Lausselet et al. (2022) constructed a dynamic GIS-based UBEM model at a city scale to assess the impact of various retrofit measures on the decarbonization potential of building stock. Moreover, this method has gained greater attention in the field of urban building energy modelling (UBEM) due to facilitation in the development of a time-geo framework which can provide a realistic description of building details at multi-level temporal and spatial resolution.

In summary, the above review demonstrates several bottom-up BSEM methodologies for analysing commercial building stock. Table 1-1 compares the findings of existing bottom-up BSEMs in terms of approach and application. However, most of the previous studies focus on a specific approach depending on the availability of data, whereas there is a lack of comprehensive studies related to the comparison of different bottom-up BSEM methodologies for commercial

building stock. These comparative studies can provide the advantages and disadvantages of different bottom-up methodologies and can further assist in choosing the right approach depending on the availability and quality of data.

Table 1-1. Overview of studies related to bottom-up BSEM methodologies.

Studies	Approach	Scale	Application
Nageler et al. (2017)	Geo-referenced	District	Space heating
Nägeli et al. (2018)	Sample-free	National	Annual energy demand
Zheng et al. (2019)	Geo-referenced	City	Effect of climate change
Hietaharju et al. (2021)	Sample-free	District	Space heating
Roth et al. (2021)	Sample-based	City	Hourly load prediction
Lausselet et al. (2022)	Geo-referenced	City	Reduction potential

1.6.2 Development of multi-scale approach for bottom-up BSEM

In this section, physics-based bottom-up BSEM studies are reviewed and then summarizes in terms of model components, data integration and granularity as shown in Table 1-2. In the bottom-up/white-box (Q4) models, physics-based BSEM is the most established method to quantify the energy demand and the reduction potential of a building stock at the national and wider level. In the BSEM, the building stock is represented by reference building models (RBMs) having average features of a building stock segment (Buso et al. (2017); Pasichnyi et al. (2019); Perwez et al. (2020)). Many studies use the BSEMs to consider technological details (Kim et al. (2020); Yamaguchi et al. (2022)). Azar et al. (2014) proposed an operation-focused framework to quantify the energy-saving potential of non-technological drivers for commercial buildings. Mata et al. (2014) provided a guideline for developing RBM to signify the importance of diversity and heterogeneity within national building stocks. Hong et al. (2015) developed an energy retrofit tool for small- and medium-sized commercial buildings to provide a multi-step assessment of energy-saving potential. Fernandez et al. (2018) implemented building system control measures to estimate the reduction potential within commercial buildings. Happle et al. (2020) presented an occupant behaviour model for urban buildings at a district scale to assess the impact of occupancy diversity on energy demand in commercial buildings. Hirvonen et al. (2021) modelled an optimization-based retrofit approach to determine a feasible set of configurations to evaluate the energy-saving potential of commercial buildings. The BSEM studies demonstrate that this approach can deal with technological attributes to quantify the effect of these changes on energy demand and carbon emissions.

However, most previous studies employed a sample-based (or synthetic) approach (Nägeli et al. (2018); Perwez et al. (2021)) with a limited focus on spatial attributes except metrological conditions. Therefore, physical factors are not considered adequately in the existing BSEMs. Moreover, in terms of the urban environment, these models either ignored or have limited capabilities to involve the context of neighbourhood adjacency. Several methods (Reinhart et al. (2013); Chen et al, (2017)) involve city-scale energy simulation, resulting in computational constraints when performing analysis at multiple scales. Therefore, a rapid and substitutional mechanism for incorporating the urban environment within the BSEM needs to be developed.

Incorporating physical factors into the BSEMs can improve the capture value and accuracy of the models. However, the conventional approaches lack spatial information, hindering such incorporation within the model. Additionally, a review of GIS- and physics-based simulated bottom-up studies show that most of them related to commercial building stock either use a non-scalable framework or are implemented at a small (city or district) scale. These data limitations and context-specific issues can be overcome by integrating both approaches to develop a hybrid model incorporating physical and technical factors. Despite this advantage of a hybrid (or crossover) model, few studies have focused on bridging the gap within conventional bottom-up models by integrating elements of one approach with other specific models (Langevin et al. (2019); U.S. EIA, 2020). Fonseca and Schlueter (2015) developed a district-scale model by initially executing statistical Q3 and analytical Q4 models and then calculated the aggregated energy use by averaging both outputs. Nutkiewicz et al. (2018) adopted an inverse hybrid model for neighbourhood-scale by initially developing a baseline physics-based simulated bottom-up (Q4-based) model and then feeding its time series output into a machine learning (Q3-based) model to capture the influence of inter-building energy dynamics and microclimate on commercial building energy use. Huo et al. (2021a; 2021b) constructed an integrated dynamic simulation model by coupling a bottom-up end-use (Q4-based) model with system dynamics (Q2-based) model to consider the impact of various long-term dynamics parameters on the possible emission peaks and peaking times of building stock. The existing hybrid model studies have integrated various approaches without considering both physical and technical factors at the multi-scale level. This signifies the need to have a generalized geo-spatial hybrid (or crossover) model to predict the spatiotemporal patterns of the energy demand of commercial building stock across the scale.

Table 1-2. Overview of existing physics-based bottom-up BSEMs.

Studies	Scale	Approach	Physical			Urban context	Technical		Occupancy	Long-term dynamics
			Geometry	Shape	Envelope		Systems	ESM		
Fonseca et al. (2015)	D	G	✓		✓		✓			
Davila et al. (2016)	C	G	✓		✓	✓				
Nageler et al. (2017)	D	G	✓		✓		✓			
Nutkiewicz et al. (2018)	NH	G	✓			✓				
Chen and Hong (2018)	D	G	✓	✓	✓	✓				
Zheng et al. (2019)	C	G			✓					✓
Happle et al. (2020)	D	S	✓						✓	
Hietaharju et al. (2021)	D	S	✓							✓
Yamaguchi et al. (2022)	N	S			✓		✓	✓	✓	✓
Prataviera et al. (2022)	D	G	✓		✓				✓	

Notation: Scale: NH: Neighborhood; D: District; C: City; N: National; Approach: G: GIS; S: Synthetic; G-S: GIS-Synthetic.

1.6.3 Carbon neutrality assessment using bottom-up BSEM and BIPV model

In this section, the physics-based bottom-up BSEM studies related to the assessment of carbon neutrality of building stock are reviewed and then evaluated in terms of compliance with the SER framework. Table 1-3 compares the findings of existing bottom-up BSEM-BIPV coupled approaches in terms of modelling techniques, scale and temporal resolution.

With the availability of data at a disaggregated level, this recent advancement has allowed greater focus on bottom-up simulation methods. Some of the studies have recently focused on GIS models to develop UBEM that bridge a gap within conventional bottom-up models by adding spatial dimension. Nageler et al. (2017) developed a GIS-based UBEM model for an urban district consisting of 1945 buildings, to predict the heating and domestic hot water demand of commercial and residential buildings. Chen et al. (2017) utilized a geo-database for developing a district-scale UBEM model, consisting of 940 buildings, to assess the retrofit potential in commercial buildings. Jokinen et al. (2022) analysed the co-influence of building retrofits, envelope insulations, ventilation, heat pumps and boilers, on the carbon emission reduction potential of building stock at a national scale. Lausselet et al. (2022) constructed a dynamic GIS-based UBEM model to assess the decarbonization potential of building stock at a city scale. Therefore, the best approach to assess the decarbonization of building stock is the combination of GIS and bottom-up archetype

simulation method, a consumption-based accounting model that can integrate multiple building elements and transitional measures to not only improve the calculation accuracy but also capture the spatiotemporal dynamics of building energy use and carbon emissions.

The implementation of the SER framework requires the integration of a building energy model and BIPV potential estimation approach to consider a combination of efficiency measures, active and passive design strategies, and renewable distributed energy resources (DERs). To estimate BIPV potential, there are several approaches for the assessment of urban solar potential depending upon consideration of modelling comprehensiveness and level of temporal resolution (Gassar and Cha (2021)). However, the physical approach is considered to be a better approach in comparison to other approaches due to the incorporation of inter-building effects, varying meteorological conditions and urban morphological characteristics. Rodríguez et al. (2017) used a 3D-based physical approach to consider the uncertainties of the level of detail on the estimation of the PV rooftop potential at a regional scale. Cheng et al. (2020) developed a point-based sampling physical approach to estimate the PV rooftop and façade potential of multiple cities in China. Panagiotidou et al. (2021) utilized Rhinoceros 3D tool to examine the PV potential of building rooftops, façades and windows at a city scale, and further analysed the effect of urban morphology on BIPV potential. Liu et al. (2023) constructed an integrated physical approach to assess the city-scale BIPV potential at hourly temporal resolution. However, there is no evidence of studies capable to couple these approaches at a large scale either due to the infeasible choice of implementation method or the non-availability of a comprehensive database (Saretta et al. (2019); Chang et al. (2023)). Most of the previous studies mainly focused either on the energy-related characterization of building stock (Fonseca and Schlueter (2015); Mohammadiziazi et al. (2021); Zhang et al. (2022)) or the estimation of solar potential (Ghaleb and Asif (2022); Thebault et al. (2022)). Therefore, an integrated approach needs to be developed for the utilization of the SER framework for estimating the overall decarbonization potential of the commercial building stock.

In terms of granularity, the existing GIS-based bottom-up archetype simulation studies show that most of them related to commercial building stock either use a non-scalable framework (Nutkiewicz et al. (2018); Borràs et al. (2023)) or are carried out at an individual building (Liang et al. (2022); Hiyama and Srisamranrungruang (2023)) that lacks the differentiated perspective of transitional measures within the commercial building stock. Kim et al. (2020) developed a national scale model to evaluate the effect of various energy saving measures (ESMs) and different climate zones on the energy use of office building stock. It was found that the building system stock composition has a significant impact on energy reduction potential. Koutra et al. (2021) utilized a multi-criteria decision-making approach to realize the concept of net-zero energy districts. Yu et al. (2021) evaluated multiple carbon-neutral tactics under climate change scenarios for a single office building and found that a feasible strategy will be to improve building system

efficiency and reduce the carbon emission intensity factor on the supply side. Deng et al. (2023) constructed an automated UBEM model to analyse the co-influence of building retrofits, envelope insulations, lighting and cooling system, and rooftop photovoltaic (PV) on the carbon emission reduction potential of building stock at a city scale. Borràs et al. (2023) assess energy-sharing strategies of rooftop PV and battery storage for buildings at a community level. However, these models mainly lack the ability of spatiotemporal identification and assessment of carbon emission hot spots and decarbonization strategies, causing disparate coordination between local municipalities and regional-level stakeholders that further hinder the facilitation of carbon-neutral urban planning. Addressing this significant challenge, a geospatially explicit UBEM is needed to capture the dynamic changes and spatial constraints of these differentiated strategies to derive carbon emission inventories of commercial building stock at the multi-scale level.

Table 1-3. Overview of existing BSEM-BIPV coupled studies.

Studies	Scale	Temporal	Approach		BIPV
			BSEM	BIPV	type
Kim et al. (2020)	National	Hourly	S		
Yu et al. (2021)	Single building	Annual		Sample	R+F
Mohammadiziazi et al. (2021)	District	Annual	G		
Yamaguchi et al. (2022)	National	Hourly	S		
Lausselet et al. (2022)	City	Annual	G	Sample	R
Borràs et al. (2023)	Community	Annual	G	Sample	R
Deng et al. (2023)	City	Annual	G	Sample	R

Notation: Approach: G: GIS; S: Synthetic; BIPV type: R: Rooftop; F: Façade.

1.7 Research gap

Based on the literature review, BSEM has demonstrated the analytical capability to overcome the challenges associated with the stock-level analysis at a large scale, whereas there are still some limitations related to model functionalities and implementation. Moreover, most of the previous BSEM studies used a specific approach to quantitatively improve the robustness and accuracy of models but have not focused on identifying the impact of these approaches on the performance level of BSEMs. There is a lack of knowledge about the influence of data acquisition techniques on the model's accuracy. This signifies the importance of selecting a model based on the availability and quality of data as well as the relevant system features required to develop a discrete representation of building stock that can provide the transitional shift between aggregated and disaggregated boundary conditions. Hence, there is a need to focus on exploring the comparative performance of these approaches to further assess the evaluation of accuracy in predicting the energy demand and carbon emissions of the commercial building stock.

In terms of granularity and integration of model components in BSEM, the conventional bottom-up approaches cannot capture the spatial distribution of building stock and are also insufficient in concurrently mapping physical and technical factors at the building-by-building level. This can be attributed to the lack of information due to data availability and privacy issues related to commercial buildings, together with the need for detailed modelling of influential parameters. Moreover, most of the studies either established commercial BSEM at large (e.g., national level) or small (e.g., district level) spatial scales which shows that the proper method for modelling multi-scale framework still needs to be developed. As for uncertainty analysis, various parameters have been studied to investigate the effect on BSEM but most are explored at a specified scale instead of a multi-scale level. To overcome these research gaps, there is a need to address the limitations of existing commercial BSEMs, such as non-scalable framework and fragmented consideration of influencing factors (focusing on either physical or technological attributes), by establishing a multi-layer model across the scale.

In the context of carbon neutrality, the literature review provides us with evidence and methods for the feasibility assessment of carbon neutrality of commercial building stock. However, there is no evidence of studies capable to couple UBEM and BIPV approaches at a large scale either due to the infeasible choice of implementation method or the non-availability of a comprehensive database. This can be attributed to the lack of data coherence to facilitate the homogenous use of a comprehensive GIS dataset to provide the necessary coordination of building stock interventions with renewable DERs at high spatiotemporal resolution. Most of the previous studies mainly focused either on the energy-related characterization of building stock or the estimation of solar potential. Moreover, there is a granularity inconsistency in the scope of the existing decarbonization studies that are either established at an individual building or a specific scale. Therefore, an integrated approach needs to be developed for the consideration of the SER (Sufficiency, Efficiency, Renewable) framework in estimating the overall decarbonization potential of the commercial building stock at multiple scales.

1.8 Aim and objectives

The main aim of this thesis is to advance building stock analytics by understanding the impact of the quality of stock data on model functionality, accuracy and applicability, and to further improve the analytical capability of BSEM in terms of scalability and multiple building-oriented elements characterization that can assist in developing long-term energy efficiency monitoring strategies for commercial building stock. Additionally, this thesis also aims to develop a coupled scheme for the consideration of the SER framework that highlights the importance of coordination among different methodological characterizations to adequately manage the degree of complexity and modelling resolution for evaluating the feasibility of carbon neutrality of commercial building

stock at a multi-scale level. In order to address these aims, the following research objectives have been formulated:

1) How can the data acquisition influence the performance level and applicability of bottom-up BSEM in predicting the energy demand and carbon emissions of the commercial building stock.
2) How can bottom-up BSEM be modelled to incorporate scalability and integration of multiple building-oriented elements within the model.
3) How does the SER framework be considered for the evaluation of carbon neutrality of commercial building stock.

1.9 Contributions

This thesis resulted in three-fold contributions with the advancement of data acquisition and modelling techniques for commercial building stock. Firstly, to understand the transitional limitations of various BSEM approaches, a comparative study of three major bottom-up BSEMs was performed to evaluate the accuracy and added-value of these approaches for use in the bottom-up engineering model. This cross-over analysis will further provide a granular level framework to assist the city-level planners and policy makers in choosing the right BSEM approach for predicting the energy demand and carbon emissions of the commercial building stock.

Secondly, a hybrid BSEM is developed to facilitate the concurrent consideration of physical and technical elements and further extend the model to different spatial resolutions. This provided a multi-tier framework using spatial intelligence building stock approach to develop long-term energy efficiency monitoring strategies for commercial building stock at multiple scales. From a practical implementation perspective, this will further help address the data limitations and context-specific issues by overcoming the disparate coordination between the local and national level stakeholders, which could identify priority areas for implementing target-based energy efficiency strategies.

Thirdly, a UBEM-BIPV coupled approach is developed to consider the SER framework for the evaluation of carbon neutrality of commercial building stock. The coupled approach resulted in a purpose-driven perspective of the energy transition at multiple scales with reduced computational time. From a practical implementation process, it will further inform the stakeholders about the varying aspect of the adoption of BIPV technologies in the urban environment. Overall, this will provide a multi-level perspective to energy modelers and policymakers on how to achieve carbon neutrality in commercial building stock.

1.10 Thesis outline

This thesis mainly consists of an extensive literature review of the use and application of BSEM, a comparative analysis of modelling techniques, and a framework to perform BSEM and BIPV studies at multiple scales as shown in Figure 1-3. The thesis is comprised of six chapters whose summary is explained as follows:

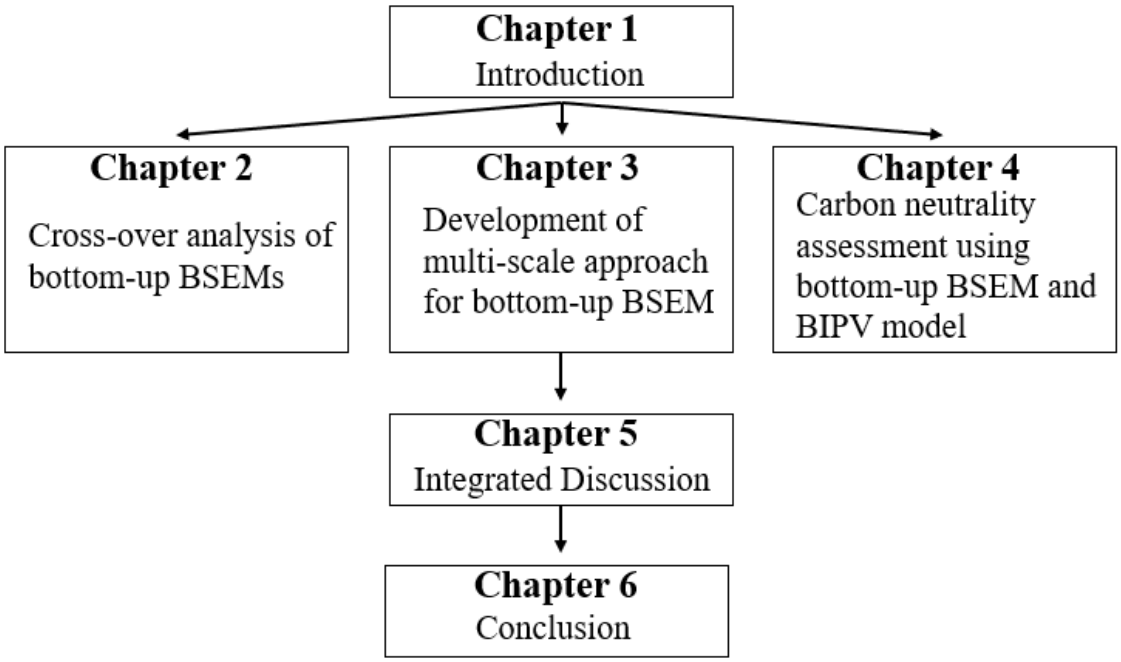

Figure 1-3. Thesis outline.

Chapter 1 initially identifies key drivers and determinants for achieving carbon-neutral building stock. This provides a comprehensive overview of transitional strategies and measures to decarbonize the commercial building stock. After this, a quadrant-based classification of BSEM is outlined and further review of methods related to carbon neutrality assessment and BIPV estimation are discussed. Finally, the literature review related to physics-based BSEMs is presented to illustrate various data acquisition techniques and their use cases.

Chapter 2 performs a comparative analysis of three major bottom-up BSEMs to evaluate the accuracy and added value of these approaches for use in bottom-up engineering models. A comprehensive comparative overview of these models will further assess the role of data availability and quality on the performance level of BSEMs.

Chapter 3 presents a novel GIS-synthetic hybrid model by integrating spatial and synthetic modelling approaches to facilitate the concurrent consideration of multiple building-oriented elements at multiple scales. In the study, building stock scenarios are developed to evaluate the analyticity of the proposed modelling method in assessing and examining the scale-bounded and

long-term dynamic uncertainties of BSEM simulations at the stock and element levels.

Chapter 4 proposes a GIS-synthetic hybrid UBEM model coupled with a physical-based approach of BIPV potential estimation for the consideration of the SER framework in the carbon neutrality assessment of commercial building stock. The decarbonization scenarios and strategies are further designed to demonstrate the applicability of the proposed coupled approach in estimating the emission reduction potential of commercial buildings under different stock interventions and penetration of renewable DERs across different scales.

Chapter 5 presents an integrated discussion to explain the contributions and practical perspective of the advancement of BSEM approaches. The chapter further highlights the importance of the role of data acquisition, multi-scale modelling and purpose-driven coupling for enhancing the model development process of BSEM.

Chapter 6 provides a summary of contributions related to formulated research objectives.

2 Cross-over analysis of bottom-up BSEMs

2.1 Purpose

In BSEM, several bottom-up methodologies have been developed to assess the energy demand and emission reduction potential of the stock but, often have transitional limitations to shift from aggregated to disaggregated stock boundary conditions. Therefore, there is a need to formulate regulations and strategies to perform an accurate assessment of energy demand patterns and emission reduction potential across the stock. However, these stock-level analyses can be challenging due to a lack of information corresponding to building characterization and quantification across various sectors. To provide a transitional framework between aggregated and disaggregated boundary conditions, it is important to select a model based on the availability and quality of data as well as the relevant system features required to develop a discrete representation of building stock. To further understand the limitations of various building-stock modelling approaches, this chapter presents a comparison of three major bottom-up building stock-level methodologies, GIS-based, sample-based and sample-free synthetic models, to evaluate the accuracy and added-value of these approaches for use in bottom-up engineering models. A comprehensive comparative overview of these models will further assess the role of data availability and quality on the performance level of BSEMs. Additionally, this study also points out the advantages and disadvantages of synthetic building stock approaches in comparison to a GIS-based building stock approach by using a detailed dynamic building simulation tool. Overall, this chapter aims to contribute to the literature development as follows: (1) quantification of the accuracy and added-value of these building stock modelling approaches for use in bottom-up engineering model; (2) development of a granular level framework in choosing the right building stock modelling approach by assessing the availability (or uncertainty) of data at either aggregated or disaggregated level; and (3) the use of these approaches in predicting the energy demand and carbon emissions of the commercial building stock.

2.2 Overview of bottom-up BSEMs

In this study, the most commonly used bottom-up BSEMs, as shown in Figure 2-1, are considered to evaluate the impact and limitations of data availability and various datasets on the performance level of BSEM. In terms of data acquisition, the sample-free synthetic model uses aggregated dataset, building census or tabular data, whereas the sample-based synthetic model uses a semi-disaggregated dataset, survey or reports, to generate the representative stock. The GIS-based model uses the disaggregated dataset to retrieve a geo-spatial representative stock. In terms of features, the sample-free synthetic model uses Montecarlo random sampling to obtain the multiple building features, whereas the sample-based synthetic model uses either statistical

techniques on the sample dataset to obtain distribution probabilities or deterministic values from reports or regulations. The GIS-based model uses a weighted average approach to obtain the building archetypes. In terms of applicability, the sample-free synthetic model is feasible to be used in those countries/regions or cities where the availability of micro-dataset is not possible, whereas the sample-based synthetic model is more flexible to be used at a specific level (from national to district scale) but can be very time-consuming due to sample collection, attainment of marginal distributions and complexity associated with the fitting of higher dimensional data. The GIS-based model provides a realistic description of building details at multi-level temporal and spatial resolution.

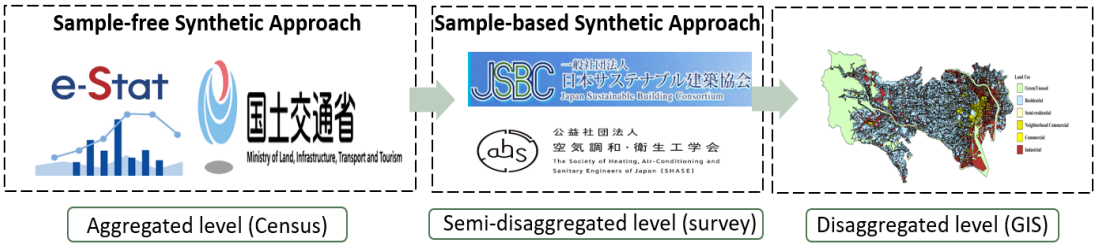

Figure 2-1. Overview of the transitional shift from aggregated to disaggregated boundary conditions.

2.3 Methodology

The following section provides a detailed overview of the cross-over framework of building stock-level approaches to develop a bottom-up engineering model and its application to the commercial building stock of Tokyo, Japan. In order to compare stock-level approaches, the three major building stock approaches are implemented with transitional shifts from aggregated to disaggregated boundary conditions, for quantifying the accuracy and added-value of each approach. The building stock-level cross-over methodology consists of the following steps (Figure 2-2):

1) The initial step is data collection. All the available information is gathered either through national (or city-level) census, sample surveys or GIS workflow to retrieve geo-referenced micro-dataset, depending on the preferred approach of building stock modelling.
2) The second step involves building stock initialization to generate either synthetic or geo-referenced stocks, which are further segmented on the basis of various criteria, such as building type, size, layout and age, according to the level of available information specified in each type of structural data.
3) After building stock initialization, the building stock characterization is performed to define all the possible attributes associated with the stock-level by using various techniques.
4) The fourth step involves building stock quantification and evaluation, during which the obtained proportion of basic block structure, such as building classification by size, total floor

area by building classification, floor composition and construction period, of buildings are compared with the existing structure of the stock.

5) In the last step, a detailed dynamic building simulation is performed to assess the accuracy implications of stock-level approaches in predicting the energy demand and carbon emissions.

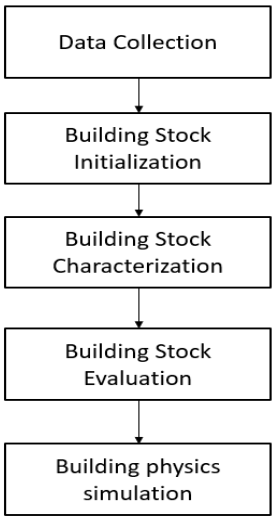

Figure 2-2. Cross-over framework to assess building stock-level approaches.

2.3.1 Data collection

As a case study for the application of these approaches, hotel buildings in Tokyo are selected to evaluate the accuracy and added-value of these building stock models. Moreover, the building stock of hotels is estimated to consist of 3320 buildings which nearly covers 13.61 million m^2 of the total floor area in Tokyo. In order to investigate the effect of various input factors on stock level, various input data sources, such as census, sample surveys and geo-database, are used to develop these approaches. To construct the sample-free synthetic stock, the most basic level of building stock aggregated data that comes from Statistical Bureau of Japan (SBJ, 2017) is considered, which only contains structural data of building type, building classification by size, total floor area by building classification and construction period. In a sample-based synthetic method, multiple survey datasets are obtained from Japan Sustainable Building Consortium (JSBC, 2017), Society of Heating, Air-Conditioning and Sanitary Engineers of Japan (SHASE-J, 2017) and Japanese Association of Building Mechanical and Electrical Engineering (JABMEE, 2010), that contains disaggregated building sample data such as total floor area, number of floors, construction period, insulation level and building systems (heating, ventilation, and cooling systems). To carry out the geo-referenced stock method, a geo-database is collated from Tokyo Metropolitan Government (TMG) which comprises approximately 150,000 commercial buildings in Tokyo. The geo-referenced micro-dataset contains key determinants and variables such as building geometric, non-geometric, typology and building-level morphological data.

2.3.2 Building stock initialization

In this step, all the methods use the same basic features of building structural data, such as building type, building classification by size, total floor area by building classification, floor composition and construction period, to initialize the building stock. Based on simplified structural data from Statistical Bureau of Japan (SBJ, 2017), sample-free stock is generated to initialize synthetic building stock for the hotel segment of Tokyo. In this method, correlation concept within building features, such as the relation between total floor area and number of buildings in each classification, are used to obtain the average total floor area and number of floors for each classification. Subsequently, the average footprint area for each classification is obtained by dividing the average total floor area by the average number of floors. The stock is segmented into 5 types based on building classification by size, CL1 to CL5 buildings are classified as those with sizes less than 300 m^2 for CL1, sizes between 300 and 2000 m^2 for CL2, sizes between 2000 m^2 and 10000 m^2 for CL3, size between 10000 m^2 and 30000 m^2 for CL4 and size greater than 30000 m^2 for CL5, as defined by Japan Sustainable Building Consortium (JSBC, 2017). From that extended simplified structural data, a representative stock is initialized which creates individual records of buildings.

In the sample-based synthetic approach, the data integration is performed to couple and merge multiple survey datasets, and then the distribution probabilities in terms of the number of floors and the construction period are obtained from an integrated dataset. After this step, iterative proportional fitting (IPF) is used to initialize synthetic building stock by constraining obtained distributions through marginal data table schemes. Moreover, in the geo-referenced stock method, the retrieval workflow of GIS is applied to extract the geo-referenced micro-dataset which contains the main attributes of buildings incorporated with spatial characteristics. Overall, this step results in the basic block structure of building stock that represents aggregated/disaggregated level data which can be further characterized in terms of other attributes.

2.3.3 Building stock characterization

This step involves further characterization of attributes associated with initialized building stock. Table 2-1 provides a detailed description of techniques used to characterize building attributes for different approaches. In the sample-free synthetic approach, the initialized building stock is further characterized depending on the availability of specified data by using either a deterministic approach or Monte Carlo sampling from distribution. In case of the non-availability of empirical data related to any building attribute, the maximum and minimum range value of the distribution is used to run the Monte Carlo simulation. In this method, truncated log-normal distribution is

used to characterize continuous variables such as building height, window-wall ratio and aspect ratio, for incorporation of skewed distribution associated with these variables within stock. Those attributes, such as building orientation, that show equal chances of outcomes are characterized by uniform distribution. The proportion of HVAC (Heating, Ventilation and Air-Conditioning) systems are obtained from Society of Heating, Air-Conditioning and Sanitary Engineers of Japan (SHASE-J, 2017) data, which is considered within the stock by using a normal distribution. In terms of the building envelope, all methods use building age-band classification to define the thermal properties of windows and walls.

By using multiple survey datasets in a sample-based synthetic method, the proportion of building attributes is obtained in terms of distribution probabilities and then characterization is performed by using iterative proportional fitting (IPF) to fit the specified distribution probabilities. In this method, the distribution probabilities of building attributes, such as building height and aspect ratio, are obtained from the sample dataset of Tokyo metropolitan government report and property tax data. To model the shading effect of neighbourhood, Ministry of Land, Infrastructure and Tourism (MILT) regulations are used to consider the typical conditions for each classification. Moreover, the HVAC stock model is structured and calibrated after the model of logistic regression to quantify HVAC probabilities by Yamaguchi et al. (2017), in which several predictors such as total floor area, demographic factors and building age are considered.

Table 2-1. Comparative overview of characterization techniques for different approaches.

Attributes	Sample-free	Sample-based	Geo-referenced
Total floor area			
Number of floors	Census	Multiple surveys	
Building age			TMG geo-database
Building height	Log-normal distribution	TMG report	
Aspect ratio	Log-normal distribution	Property tax data	
Orientation	Uniform distribution	×	
Neighborhood adjacency	×	MLIT land use	✓
HVAC systems	Normal distribution	Logistic regression	Logistic regression
Building shape	Rectangular parallelepiped (R)		L, U and R
Building envelope	Age-band classification		

The geo-referenced stock method involves an enriched dataset which contains key determinants and variables, such as building height, orientation, aspect ratio, shape coefficient and urban

morphological attributes, for individual buildings in the stock. Moreover, to further enrich the geo-referenced micro-dataset, logistic regression is used to incorporate heating and cooling systems within the stock, to achieve better comparability with other synthetic building stock approaches. In order to show the significance of the geo-referenced model, we also developed a neighbourhood adjacency model (NAM) to simplify the analysis of the shading effect made by adjacent buildings (Sun et al. (2021)). NAM consists of the following four steps: 1) Search for neighbourhood buildings adjacent to the target building; 2) Calculate solar altitude angle (δ) for a specific location; 3) Extract potential shading buildings ($n_{Dj} \leq n_{SH}$; where n_{Dj} and n_{SH} are the distance of neighbourhood from target building and the shading length of neighbourhood building); and 4) Shadow pre-processing to determine effective shading neighbourhood building ((Min(nDj), Max(nHj)); where nHj is the height of neighbourhood building). Based on the analysis, we obtained the distance and height of the neighbourhood adjacent to each target building, which was considered to calculate the ranges of these key parameters for each archetype.

2.3.4 Building stock evaluation

To further evaluate the accuracy of synthetic stock approaches, the relative absolute percentage difference (rAPD) measure is considered. rAPD is the performance measure to assess the initialization accuracy by determining the absolute percentage difference between estimated and generated stocks. rAPD is mathematically defined as follows:

$$rAPD_i = \frac{\overline{T}_{ij} - T_{ij}}{T_{ij}} \qquad 2\text{-}1$$

where, T and $\overline{T}$ are the estimated and generated stock respectively. Thus, an APD value close to 0 suggests a better generation accuracy of that approach.

2.3.5 Building stock energy simulations

In order to perform the building energy simulations at the stock level, the segmentation process is performed based on various criteria, such as building classification by size, age and HVAC systems. In the initialization step, the stock is segmented into 5 types based on building classification by size and then to further improve the granular level details, building age and HVAC systems which consists of 6 age-bands and 44 systems respectively, are considered after the characterization step to segment the stock into heterogeneous archetypes.

The baseline building energy models are developed for each archetype by using EnergyPlus 8.6 interface and then simulated models to further assess the energy demand and carbon emissions of the hotel building stock. The simulated model also requires climate data, occupancy schedule, internal and external equipment loads and HVAC operational data, which are set based on

Japanese building regulations and some previous studies (Kim et al. (2020)). The simulated results are further validated by comparing them with national-level database estimates, which are obtained by calculating the weighted average values of each building classification by size and then aggregating those to get estimates in terms of primary energy demand and carbon emissions.

2.4 Results and discussion

This section presents the results of the cross-over analysis of building stock-level approaches. First, the structure of building stocks obtained from different approaches is presented. After that, the evaluation process to quantify the structure quality of building stock is described. Finally, the results of dynamic building simulations to assess the accuracy of each approach are presented.

Figure 2-3 shows the structure of building stock in terms of building classification, floors and total floor area using different approaches. The structure of modelled stock using a sample-free approach deviates majorly in all aspects in comparison to other approaches. This is because the building stock is randomly initialized, using only census data, on the basis of the number of buildings within each classification. In this study, the geo-referenced stock is assumed to be the reference case for the evaluation of the structure of building stock using synthetic approaches due to the better granular capability of this method to represent realistic descriptions of building details at multi-level temporal and spatial resolution. Table 2-2 shows the statistical overview of rAPD for different building stock approaches. As it is evident, the sample-free synthetic approach produces maximum rAPD values across all the aspects, while sample-based synthetic and GIS-based stock approaches show a very good agreement in terms of rAPD. At a more disaggregated aspect level, it is observed that at a lower level (CL1 or 1 to 5 floors), the sample-free synthetic approach shows reasonable generation accuracy, while at a higher level (CL5 or 20+ floors), it results in overestimation in comparison to other approaches. Overall, the comparison shows that in order to achieve better generation accuracy from a sample-free synthetic approach, it is important to consider a minimum level of building classifications to minimize distortion within the share of stock.

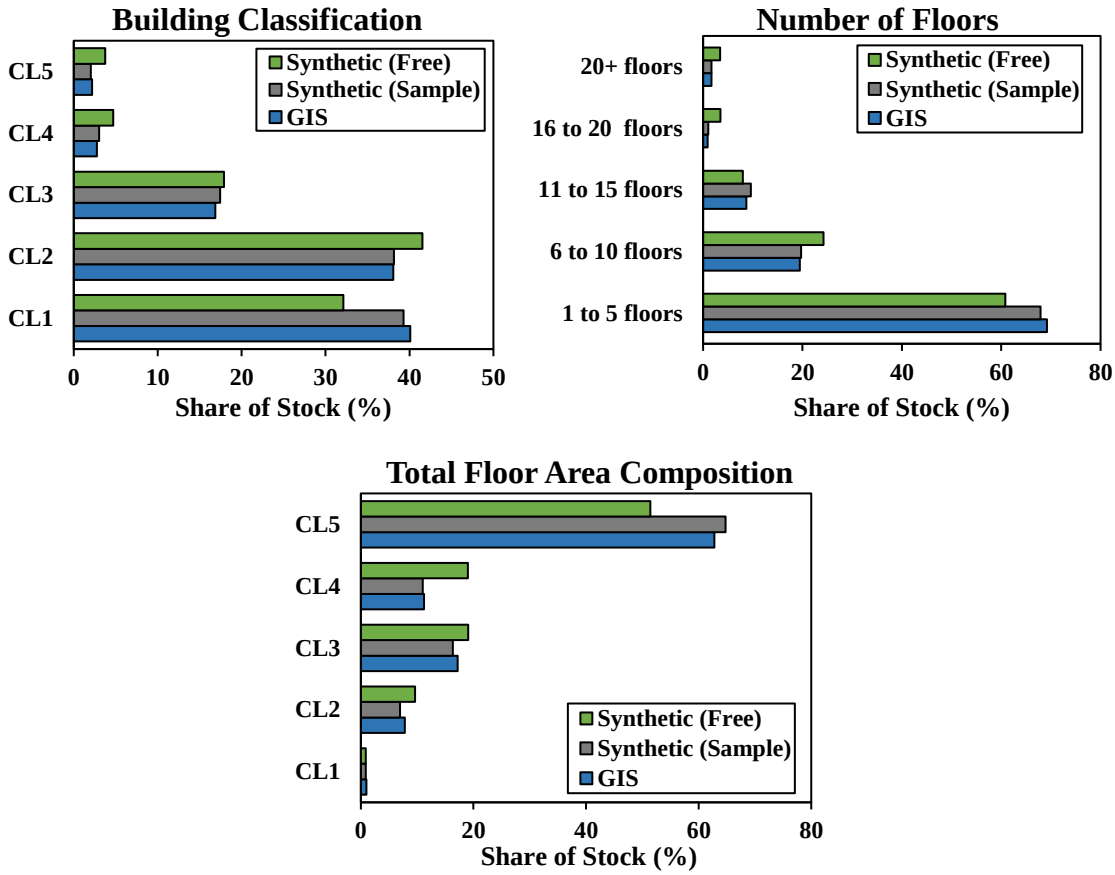

Figure 2-3. Structure of building stock using different approaches.

Table 2-2. rAPD Statistics of building stock approaches.

Distribution	Approach	Min	Max	STD	Mean
Building classification	Sample-free	0.06	0.71	0.37	0.27
	Sample-based	0.00	0.10	0.06	0.01
Number of floors	Sample-free	0.08	0.74	0.35	0.24
	Sample-based	0.00	0.13	0.06	0.05
Total floor area	Sample-free	0.11	0.74	0.32	0.17
	Sample-based	0.00	0.15	0.06	0.06

Table 2-3 shows the composition of building archetypes for different approaches in terms of basic attributes. As a result of the segmentation process, 1320 archetypes are constructed for each method to represent the entire stock of hotels in Tokyo. To reduce the number of archetypes for each case, dynamic threshold criteria are used for each building classification by size to consider 90% of the total floor area composition for each classification. The dynamic threshold criteria

resulted in the reduction of archetypes to 600, 532 and 412 archetypes for geo-referenced, sample-based and sample-free methods respectively. This implies that the sample-free method provides less heterogeneity in terms of the number of archetypes, with is majorly due to the simplistic approach adopted for HVAC stock modelling.

Table 2-3. Composition of archetypes for different building stock approaches.

Classification	Approach	TFA (m^2)	GFA (m^2)	Floors
CL1	Sample-free	68	34	2
	Sample-based	104	52	2
	Geo-referenced	103	51	2
CL2	Sample-free	700	175	4
	Sample-based	830	138	6
	Geo-referenced	838	167	5
CL3	Sample-free	3273	409	8
	Sample-based	4283	535	8
	Geo-referenced	4179	418	10
CL4	Sample-free	10870	836	13
	Sample-based	16562	1380	12
	Geo-referenced	16579	1184	14
CL5	Sample-free	46752	1979	22
	Sample-based	144638	6288	23
	Geo-referenced	117083	3902	30

Figure 2-4 shows the share of HVAC (Heating, Ventilation and Air-Conditioning) stock using different stock-level approaches in terms of cooling and heating sources, and fuel types for 5 building size classifications. In terms of cooling systems, the proportion of OHU-FCU (fan coil with outdoor handling unit) system is overestimated for small-size buildings in sample-free method, whereas VRF (variable refrigerant flow) system has a higher proportion of stock in logistic regression-based methods. Moreover, the sample-free method underestimated the proportion of decentralized heating systems (Ele-VRF), whereas the proportion of gas-driven

centralized systems (Gas-AbCH and Gas-AbCB) is larger in other methods. The composition of fuel type for HVAC systems shows that the sample-free method underestimated gas/oil-driven systems, whereas electricity-driven systems have a lower proportion of stock in other methods. The results show a major deviation between sample-free and sample-based approaches, which show the differences rising due to the usage of normal distribution of stratified samples and non-consideration of various predictors to model the stock. In other methods, it is also observed that the application of logistic regression results in the better distinction of centralized and decentralized HVAC systems across small and large size buildings due to the consideration of various predictors, such as total floor area, population density (PD), heating degree days (HDD) and building age. This result implies that the consideration of building attributes and other demographic factors to model the HVAC stock provides better heterogeneity of the system across different building classifications by size.

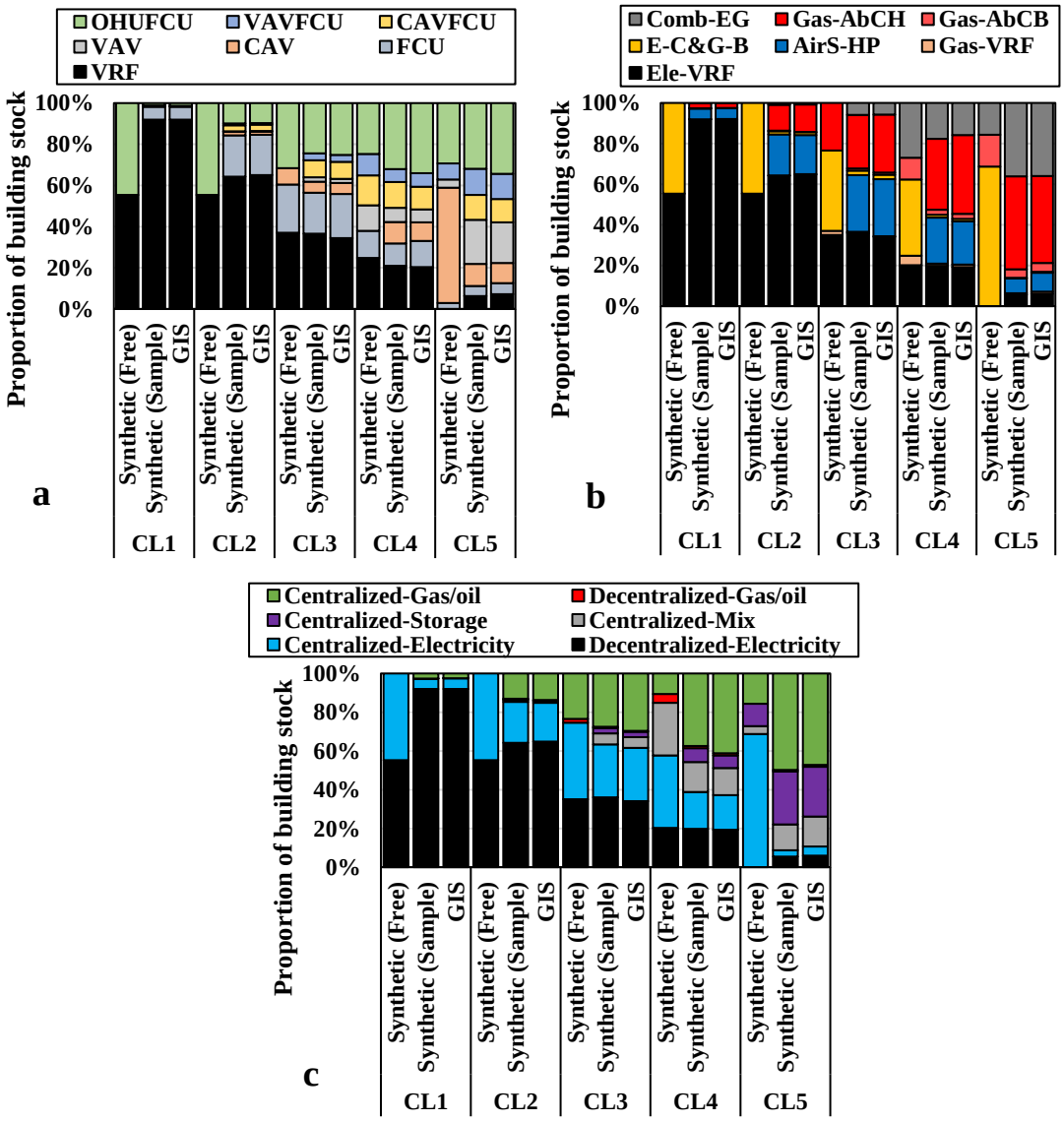

Figure 2-4. Distribution of HVAC stock using different building stock approaches: (a) cooling systems; (b) heating systems; and (c) fuel type.

Following the procedure described in the methods section, a detailed dynamic building simulation is performed to assess these modelled building stocks in terms of energy demand and carbon emissions. The aggregated results of three building stock approaches are shown in Figure 2-5 and further compared with national-level database estimates (JSBC, 2017). The results show that the total primary energy demand is underestimated by 8.3%, 18.4% and 20.6% for sample-based, geo-referenced and sample-free stock approaches respectively. This also demonstrates the added-value of sample-based modelled stock to accurately reproduce the estimated energy demand of the stock. The main reason is the cross-sectional and longitudinal enrichment associated with the sample-based approach, which increases data dimensionality and non-linear interactions within the stock.

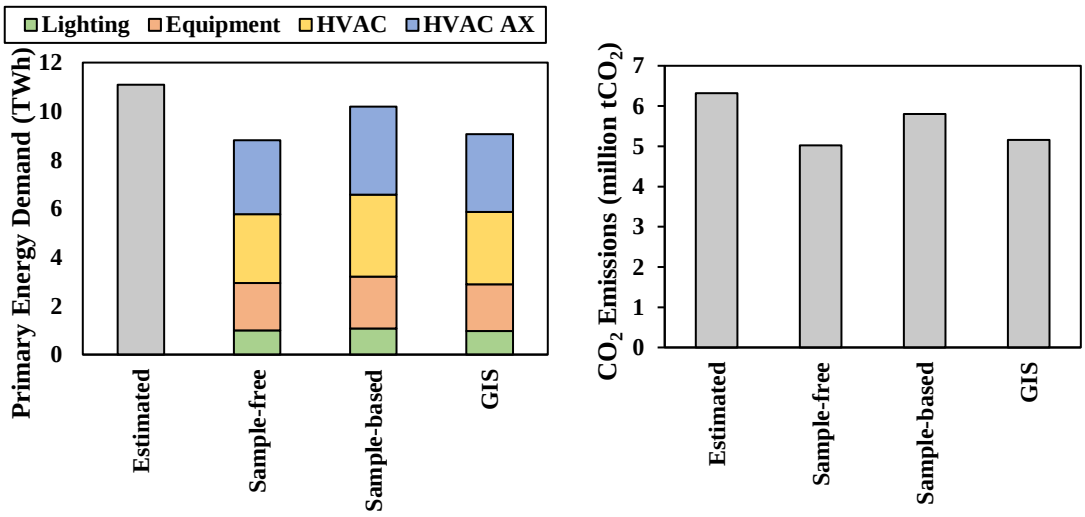

Figure 2-5. Comparison of aggregated energy demand and carbon emissions across the stock for different bottom-up BSEMs.

2.5 Conclusion

This study has focused to determine the accuracy and added value of the building stock modelling approaches, in terms of heterogeneity, data dimensionality, integration and non-linear interactions within the stock, for use in the bottom-up engineering model. The proposed analysis uses four main steps, such as building stock initialization (or geo-referenced dataset collection), building characterization, quantification and building energy simulations, to assess the data needs and performance gap of each approach. The building stock modelling methodologies are implemented on the commercial building stocks (hotel segments) of Tokyo, to evaluate the cross-sectional and longitudinal enrichment of building attributes and heating, ventilation, and air-

conditioning (HVAC) stock. The preliminary results show that the sample-based synthetic method can incorporate multiple input distributions using a survey micro-dataset, while the geo-referenced method provides additional key determinants such as building typology (shape coefficient, aspect ratio and orientation) and morphological attributes. This implies that these are data-enriched methods which resulted in better performance in terms of building stock development and simulated building energy use that signifies the accuracy and added-value of these methods. However, the sample-based synthetic method provides a better compromise between data availability and simulation accuracy in comparison to other methods. This shows that the synthetic approach can be extended to commercial building stock, which mostly has a poorer data availability than residential building stock, which further allows to encompass modelling of a typical mixed-use urban environment. Moreover, this cross-over analysis will provide a granular level framework to assist the city-level planners and policy makers in choosing the right BSEM approach for predicting the energy demand and carbon emissions of the commercial building stock.

3 Development of multi-scale approach for bottom-up BSEM

3.1 Purpose

The conventional bottom-up BSEMs mainly use a non-scalable stock-level framework due to modelling coherence and context-specific limitations. These scalability issues lead to granular level uncertainties depending upon the selection and description of scale, availability and quality of data, and use case. To address these uncertainties within conventional approaches, multi-scale modelling is one of the possible techniques that can incorporate granularity and multi-dimensionality within BSEM. Such implementation needs intensive information at the granular level to identify the target areas where the energy policymakers can conduct target-based planning and decision-making (Yoshino et al. (2017); Nägeli et al. (2022)). However, the available data are limited and provide incomplete coverage, causing disparate coordination between local and national level stakeholders, further hindering the implementation of a target-based approach. A differentiated description of strategies is needed across the scale to integrate an appropriate level of detail for promoting the ESMs within the commercial building stock.

Moreover, the existing BSEMs are insufficient in concurrently mapping physical and technical factors at the building-by-building level. These studies mainly focused on either physical (Nageler et al. (2017); Chen and Hong (2018)) or technical factors (Mata et al. (2014); Hirvonen et al. (2021)) due to a lack of modelling capabilities. The concurrent consideration of physical and technical factors within the BSEMs can improve the capture value and accuracy of the models. However, the conventional approaches lack spatial information, hindering such incorporation within the model. These data limitations and context-specific issues can be overcome by integrating both approaches to develop a hybrid model incorporating physical and technical factors. Despite this advantage of a hybrid (or crossover) model, few studies have focused on bridging the gap within conventional bottom-up models by integrating elements of one approach with other specific models (Nutkiewicz et al. (2018); Langevin et al. (2019)). The existing hybrid model studies have integrated various approaches without considering both physical and technical factors at the multi-scale level. Therefore, a generalized geo-spatial hybrid (or crossover) model is needed that predicts the energy performance of commercial building stock across the scale.

To address these limitations, this chapter presents a novel hybrid model by integrating spatial and synthetic modelling approaches to facilitate the concurrent consideration of multiple building-oriented elements at multiple scales. The main research objective is to illustrate a hybrid workflow that facilitated the concurrent consideration of multiple building-oriented elements at the multi-scale level, leading to further improvement in the analytical performance of the BSEM. The proposed approach is developed to demonstrate the transferability and applicability of the model to three different scales. These scales are modelled based on geometry, system, adjacency context,

typology, and socio-behavior responses to examine and identify various drivers and determinants for a better understanding of mechanisms and conditions leading to different demand levels for commercial building stock across the scale. The building stock scenarios are further designed to evaluate the proposed modelling method: (1) to determine what happened if RBMs of non-representative scale were applied to the other scales and (2) to concurrently quantify the influence of physical and technical factors on the model across different scales.

3.2 Methodology

Figure 3-1 illustrates the conceptual scheme of our GIS-synthetic hybrid model consisting of four steps: (1) GIS building stock analysis, (2) synthetic building stock analysis, (3) building stock energy modelling and simulation, and (4) building stock scenarios.

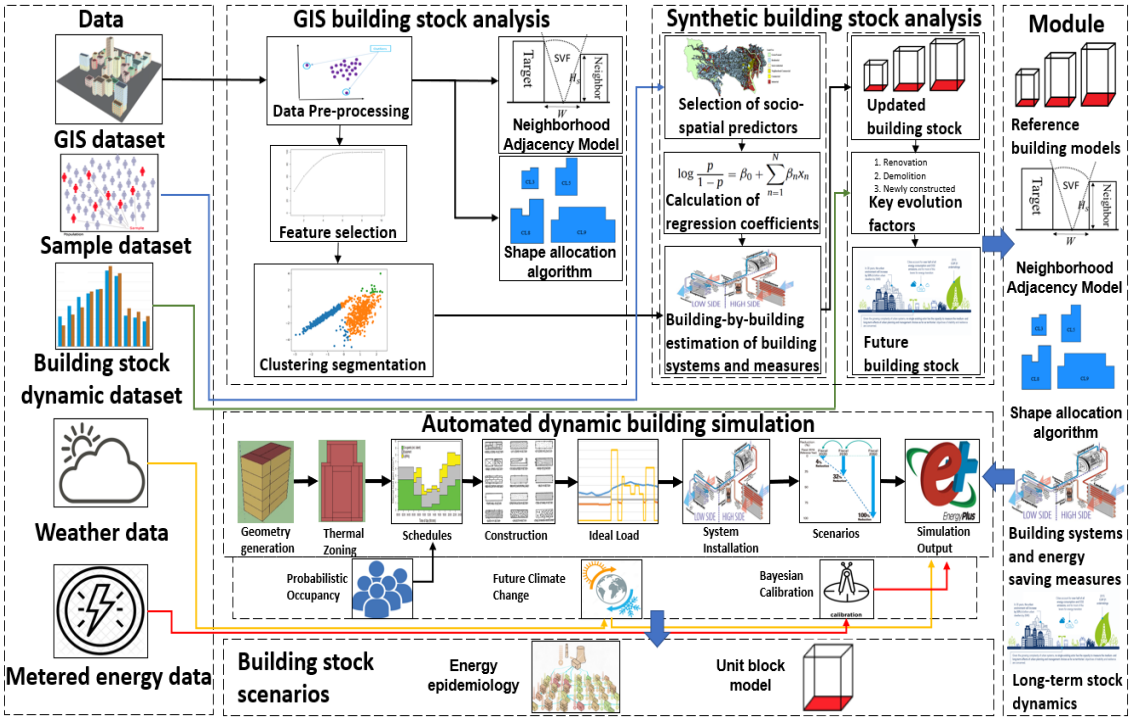

Figure 3-1. Schematic overview of GIS-synthetic hybrid approach.

1) The GIS building stock analysis used a data-driven formulation process to characterize all the buildings in a target area by using physical factors associated with the stock. This process used a geo-referenced dataset consisting of physical factors, such as geometric, non-geometric, and typology data of buildings, representing the building stock composition, thermo-physical properties, and shape features, respectively (see Section 3.2.1).
2) The synthetic building stock analysis constructed the synthetic elements using a two-stage process to predict the probabilities of technical factors and stock turnover. This step involved those elements that were unavailable in the geo-referenced dataset. In the first stage, the

socio-spatial predictors were assigned to each building within the stock. Subsequently, the statistical (or machine learning) model was developed using sample data comprising technical factors. The most probable alternative was selected based on the best possible probability of each alternative for a specific building. In the second stage, the long-term stock dynamics were modelled by using key evolution factors obtained from the census.

3) RBMs were developed by performing a characterization process using physical and technological building attributes. The RBMs were validated considering metered energy data by using a multivariate calibration technique, and then the annual energy use intensity (EUI) was calculated for each RBM.

3.2.1 Data

The proposed method was applied to three different Japanese commercial building stocks, namely national, Tokyo, and Chuo, to provide a comprehensive understanding of the model's overall extent and accuracy across various scales. Figure 3-2 illustrates the data types used in the model. For the city scale, Tokyo is considered, which consisted of wards and sub-urban areas; whereas, Chuo ward is one of the ward areas in Tokyo. Japanese commercial building stocks, involving office, hotel, hospital, and school segments, consisted of 440, 87, and 6 thousand buildings, which approximately covered 1005, 195, and 16 million m^2 of total floor area (TFA) for national, Tokyo, and Chuo scales, respectively. Moreover, Appendix A lists the data sources and conversion process used in this study.

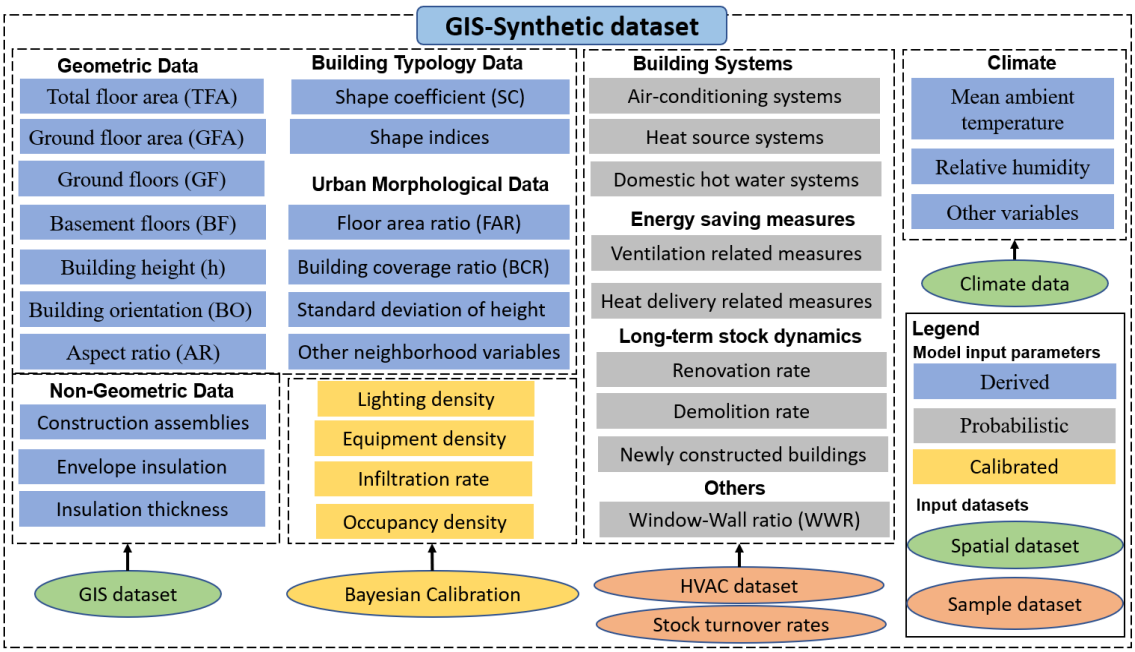

Figure 3-2. Simplified workflow of datasets used in GIS-Synthetic hybrid framework.

3.2.2 Hybrid stock modelling

1) GIS building stock analysis

In GIS building stock analysis, the stock was initially classified by using clustering segmentation to obtain the optimum number of RBMs for each segment. Finally, the building shape allocation algorithm and neighborhood adjacency model were developed by performing an additional process on the geo-referenced micro-dataset.

i) Clustering segmentation

After dataset collection, data pre-processing was performed to remove anomalies and select features from the specified dataset by considering ± 3σ threshold. Additionally, various outlier detection techniques, namely Mahalanobis distance (MD), local outlier factor (LOF), isolation forest (IF), and extended isolation forest (EIF), were compared in terms of the performance metric of area under curve (AUC) based on receiver operating characteristics (ROC) to select the best suitable method for the specified integrated building dataset (Goldstein and Uchida (2016)). The final phase in data pre-processing was feature selection, which optimally extracts the most feasible and influential variables from the integrated dataset to improve the quality and dimensionality of model input. In this study, PCA was applied on the geo-referenced building stock dataset, consisting of key physical factors and urban morphological data related to building stock, as shown in Figure 3-2, to identify features that showed significant covariance within the model. The selected features were then used to perform the clustering segmentation of the building stock.

Building stock clustering segmentation used a multi-variate k-means algorithm to provide a guideline for selecting the best possible similarity measure and a further improvement in the clustering partition by applying different similarity (or distance-metric) measures to each cluster validation index as compared to previous studies (Ali et al. (2019); Ledesma et al. (2021)). Then a unified clustering validity measure was proposed to evaluate the clustering scheme in terms of the best possible similarity measure and maximum interaction of validity indices. Three internal validation indices namely Silhouette (SI), Davies-Bouldin (DBI), and Dunn (DI) indices, which interact among themselves, were unified to produce the cohesion-dispersion index (CDI) to overcome the noticeable gaps in finding a single optimal cluster value (see internal validation indices explanation in Supplementary Appendix S1). For the distance-metric combination, we considered four different measures of distance and clustering metrics (Euclidean, Manhattan, Correlation, and Spearman). Therefore, this distance-metric cross-over analysis resulted in a comparison of 16 combinations (λ) for each internal validation index. The CDI for each cluster

was calculated using the probabilities (p_{SI}, p_{DBI}, and p_{DI}) of the three internal validation indices and their respective weight contributions (w_{SI}, w_{DBI}, and w_{DI}).

$$CDI = w_{SI} \times p_{SI} + w_{DBI} \times p_{DBI} + w_{DI} \times p_{DI} \quad \text{3-1}$$

$$p_{SI}(\lambda) = \frac{SI(\lambda) - min\ (SI)}{max(SI) - min(SI)} \quad \text{3-2}$$

$$\mathrm{p}_{DBI}(\lambda) = \frac{DBI(\lambda) - \max\ (DBI)}{\min(DBI) - \max(DBI)} \quad \text{3-3}$$

$$\mathrm{p}_{DI}(\lambda) = \frac{DI(\lambda) - \min\ (DI)}{\max(DI) - \min(DI)} \quad \text{3-4}$$

To obtain the normalized index range of CDI, the values of internal validation indices were homogenized. Thus, a CDI value close to one suggested the maximum interaction of the three internal validation indices, implying optimum clustering in terms of cohesion and dispersion. To ensure homogeneity across the specific study, the same number of classifiers were used to perform segmentation, resulting in an equal number of clusters at different scales.

ii) Building shape allocation algorithm

This algorithm developed a characterization process that allocated a true unifying shape to RBMs across the stock. The building shape allocation algorithm consisted of three steps as follows:

1) Shape indices calculation: The initial step involved the computation of shape indices of each building polygon. GIS-based shape indices are geometrically derived values representing a particular building polygon shape that varies between 0 and 1 (see Table 3-1) (Basaraner and Cetinkaya (2017)).
2) Weighted average of shape indices: In this step, weighted average shape indices for each RBM were computed.
3) Matching indices: The obtained average values of shape indices were utilized to match a specific shape with RBMs by using the geo-referenced dataset.

Table 3-1. Overview of shape indices.

S. No	Shape Index	Equation	Description
1	Circularity (CI)	$\mathrm{CI} = \frac{A_{PN}}{A_{EPC}} = \frac{4\pi A_{PN}}{P_{PN}^2}$	Polygon's degree of circular compactness.
2	Convexity (CNV)	$\mathrm{CNV} = \frac{A_{PN}}{A_{CH}}$	Polygon's degree of being curved inward or outward.
3	Fractality (FR)	$\mathrm{FR} = 1 - \frac{\log(A_{PN})}{2 \times \log(P_{PN})}$	Edge roughness or smoothness of polygon.
4	Rectangularity (REC)	$\mathrm{REC} = \frac{A_{PN}}{A_{MABR}}$	Polygon's degree of being rectangular.
5	Squareness (SQN)	$\mathrm{SQN} = \frac{P_{EAS}}{P_{PN}} = \frac{4\sqrt{A_{PN}}}{P_{PN}}$	Polygon's degree of being square.

Notation: A_{PN}= Polygon area; P_{PN}= Polygon perimeter; A_{CH}= Convex hull area; A_{MABR}= Minimum area bounding rectangle; A_{EPC}= Equal-perimeter circle area; and P_{EAS}= Polygon equal area square

iii) Neighborhood adjacency model

The neighborhood adjacency model was proposed to develop a rapid and efficient mechanism to consider the neighborhood adjacency conditions. This model consisted of four steps:

1) Geo-referenced building stock decomposition: The proposed method decomposed the building blocks into multiple individual target buildings and extracted their relevant adjacent environment in a pre-defined radius of 50 m to search for surrounding buildings adjacent to target buildings (see Appendix B.1).
2) Neighborhood adjacency criteria: This step determined the necessary adjacency criteria required to remove irrelevant surrounding buildings by focusing on shading impact instead of other inter-building effects.
3) Potential shading planes: To determine the effective shading direction and length, solar azimuth and altitude angles were utilized to filter out the surrounding buildings with no shading impact on the target building.
4) Effective shading planes: The final step involved pre-processing of potential shading planes to filter out overlapping planes (see Appendix B.2). The effective shading planes were determined by comparing the shadow height of a nearby shading plane with that of a distant one.

2) Synthetic building stock analysis

In synthetic building stock analysis, statistical techniques were applied to sample datasets to assign the synthetic elements to the building stock.

i) Long-term stock dynamics

This study modelled the long-term stock dynamics by considering the data interpolation (ex-post) and probabilistic function (ex-ante) techniques as explained in Sartori et al. (2016) and Hietaharju et al. (2021) (see detailed explanation in Supplementary Appendix S2). The long-term commercial building stock dynamics model was constructed for the study period from 2016 to 2030 by using key evolution factors, as shown in Appendix C (SBJ, 2017; Tokyo Statistical Yearbook, 2019). Moreover, the weighted random probability was assumed based on age band classification to predict the long-term stock turnover at the building-by-building level.

ii) System stock modelling

In this study, the developed logit model by Yamaguchi et al. (2017) was further modified to extend its applicability at the building-by-building level. The model considered the socio-spatial predictors based on building characteristics ($\log_{10}$ TFA and building size), demographics (Population density (PD) and HDD), and age band classifications (6 bands from 1980 to 2030). The initial step involved the assignment of socio-spatial predictors to the sample dataset and then, the regression analysis was performed to obtain the coefficients of these predictors. The probability of each system classification for a specific building within the stock was quantified by multiplying the obtained regression coefficients with real predictors of buildings. For selecting the HVAC systems, the joint probability was calculated to select the pair of air-conditioning and heat sources for each building. The ESMs were selected depending on the most probable alternative for a specific building. Furthermore, this method was extended to different spatial boundaries, namely national, Tokyo, and Chuo, by initially obtaining the building stock data for the specific area type. Then the social-spatial predictors were allocated at the building-by-building level to distinguish between area types. This resulted in the varying estimated probability of system alternatives between area types.

3.2.3 Building stock energy modelling and simulation

After developing the hybrid stock model, the RBMs were further segmented based on multi-stage criteria using physical and technical attributes. As a result of the multi-stage segmentation process, the development of 0.21 million (clusters x 3 construction types x 6 vintages x 5 system

age-band x 16 ESMs x 44 HVAC systems) RBMs was possible which represented the entire commercial building stock at the specified scale. To reduce the number of RBMs for each scale, aggregated criteria combined buildings that exhibited the same classification in terms of the building size, construction type, age-band, ESMs, and HVAC systems. For example, the aggregated criteria reduced 440,846 actual buildings to 30,688 RBMs at the national scale. In the case of other scales, this specified criterion reduced models to 7,145 and 2,115 RBMs for Tokyo and Chuo, respectively.

Subsequently, the characterization was performed by using a deterministic approach involving computation of the weighted average of characteristics associated with each RBM (see detailed geometric characterization results in Supplementary Table S2). Moreover, the RBMs were developed by using an automated dynamic building simulation platform, which executed modelling stages through Python and R scripts to generate input files for EnergyPlus. Those models were then simulated to estimate the energy demand of the commercial building stock. The simulation model also required the climate data, occupancy schedule, internal and external equipment loads, and HVAC operational data (see detailed explanation in Appendix D), which were either calibrated or set based on Japanese building regulations (ECKDIC, 2000; IEIJ, 2006; METI, 2011; Kondo et al. (2011)) and some previous studies (Kim et al. (2020); Yamaguchi et al. (2022)). The description of stock-level parameter settings for different cases is illustrated in Table 3-2.

Table 3-2. Description of stock level parameter settings.

Parameter	2016	2030	Electric/Potential
Building stock composition	As per base year	Projected as per long-term stock dynamics (see Section 3.2.2(2))	
Lighting	Conventional lighting devices (fluorescent and incandescent lamps)	All lighting devices are replaced with LED	
Plug load	Calibrated as per metered data (see Section 3.2.3(1))	40% reduction from the 2016 level	
System stock composition	Estimated as per socio-spatial predictors and age band classification (see Section 3.2.2(2))		All the systems are either replaced with those driven by electricity or installation of all possible ESMs.

1) Model Calibration and Validation

In this study, a multivariate (or Bayesian) calibration technique was utilized to obtain the representative value of uncertain parameters for specific RBMs. Most of the uncertain parameters in this study are related to operational data and the input range of these parameters was determined from the literature (see Supplementary Table S3) (Sokol et al. (2017); Chong et al. (2017); Chong et al. (2018)). The calibrated parameters were selected based on their impact on model sensitivity (see Supplementary Figure S1). Based on the parameter screening, four high uncertainty parameters were chosen in this study: lighting density (LD), plug load (EE), occupant density (OD) and space infiltration (INF). This calibration process minimized the error between simulated output and metered data. At the aggregated level, the model was validated in terms of secondary energy consumption by comparing it with estimates from Energy Data and Modeling Center of Japan (EDMC, 2017).

3.2.4 Building stock scenarios

Building stock scenarios were developed to evaluate the analyticity of the proposed modelling method in assessing and examining the process of model development. In this study, two scenarios, energy epidemiology analysis and unit block concept, were developed to understand better the model development process of the commercial building stock.

The first scenario aimed to understand better the selection and description of appropriate scales for developing commercial BSEMs and estimate the error uncertainty when a non-representative scale was applied to other scales. For this purpose, we applied three different ranges of scales, namely national, Tokyo, and Chuo, on a reference (or Chuo) scale to assess the scale-bounded and long-term dynamic uncertainties across the stock. Furthermore, we proposed a concept of a unit block model to quantify the influence of building-oriented elements on the model across different scales. The unit block building model is a simplistic model consisting of typical building characteristic assumptions related to geometry, systems, retrofits, and operating conditions, as shown in Table 3-3. In this scenario, model elements were replaced by the typical ones to quantify the impact of these characteristics on the extent and accuracy of the model. This proposed concept also provided an initialization point for the development of BSEM to examine the trade-off between the model's complexity and reliability.

Table 3-3. Typical characteristics of the unit block building model.

Parameter	Assumption	Description
Aspect ratio	40	Most of the studies use these assumptions for geometric characteristics in building stock model.
Building orientation	0^0	
Building shape	Rectangular	
Window-to-wall ratio	-	Neglected due to unit block concept.
Neighborhood adjacency	-	Neglected due to model simplification.
Building age	1990	Selected based on average value.
HVAC	EHP-MUL	Assumption of simplified heating and cooling system.
Building system age	Base year	Considered based on the study period.
ESM	-	Neglected due to simplified HVAC system.
Occupancy strategy	Typical	Considered based on a simplified strategy.

The performance assessment of these scenarios was performed by designing a one-at-time (OAT) and combined effect evaluations. The former assessed the model's output corresponding to omitting a single building element, while the latter examined the non-linear interaction (or added one by one) of these elements on the model output. These analyses were evaluated by using two predictive performance indicators, impact factor (IF) and relative coefficient of variance of the root mean square error (CV RMSE), at building element and stock levels. The element-level predictive performance was assessed by using IF indicator (Kim et al. (2020)).

$$IF = \frac{\hat{y}_i - y_r}{y_r} \qquad 3\text{-}5$$

where $\hat{y}_i$ and y_r are the annual predicted and referenced (or validated) values, respectively. The relative index of CV RMSE evaluated the predictive performance across the stock.

$$CV\ RMSE_r = \frac{\sqrt{\sum_{i=1}^{n}(y_r - \hat{y}_i)^2 / (n-1)}}{\overline{y_r}} \qquad 3\text{-}6$$

where $\overline{y_r}$ is the referenced (or validated) mean annual value of n observations.

3.3 Results

This section presents the results of a multi-scale framework using a GIS-synthetic hybrid approach. First, the structure of building stocks obtained from a multi-stage segmentation process, using geo-referenced and sample datasets, is presented. After that, the results of building stock energy model validation and calibration using automated dynamic building simulations are

illustrated. Finally, the building scenarios are analyzed to explore the influence of various parameters on energy epidemiology across the scale and stock.

3.3.1 GIS building stock analysis

This analysis presents the results related to the development of RBMs based on the geo-referenced dataset for multiple scales. After comparing outlier detection methods, the EIF detection technique was selected as it showed better robustness and accuracy in identifying the outliers, evident from the performance metric of AUC based on the ROC. Supplementary Table S4 shows the performance evaluation of different outlier detection techniques. The PCA method revealed that GFA, floors, height, and shape coefficient represent more than 80% of variability within the model; therefore, these four features were used as the input for building stock clustering. This also suggests that fewer input features would produce similar segmentation results since they represent the most influencing classifiers of the stock.

Figure 3-3 shows the optimum number of clusters obtained by evaluating the CDI index (as discussed in Section 3.2.2). The clustering scheme showed the significance of this criteria in determining the maximal cohesion-dispersion of the clustering, as the resulting number of clusters varied with different distance-metric combinations. The unified validity index, CDI, identified 17 RBMs (five clusters each for office and hotel, four and three clusters for hospital and school, respectively) to represent the entire commercial building stock. For instance, the segment-wise analysis of clustering showed a significant amount of inter-cluster heterogeneity within school building stock due to similar inter-distances between them. Moreover, the school building stock segmentation showed that the Cosine-Manhattan distance-metric combination (Cosine vs Manhattan) provided the highest value of CDI for school buildings, if k equaled three. Therefore, schools needed to be segmented into three types of RBMs at the national scale to obtain the optimum number of clusters in terms of compactness and separation. To further illustrate the specified clustering segmentation scheme, the development of RBMs is explained in Supplementary Figure S2. Overall, the results show a two-fold reduction in the number of RBMs in comparison to one of the previous studies (Kim et al. (2020)) using an individual classifier, which implies a useful reduction strategy to increase the complexity (level of details) of building stock model and maintain a reduced computational time.

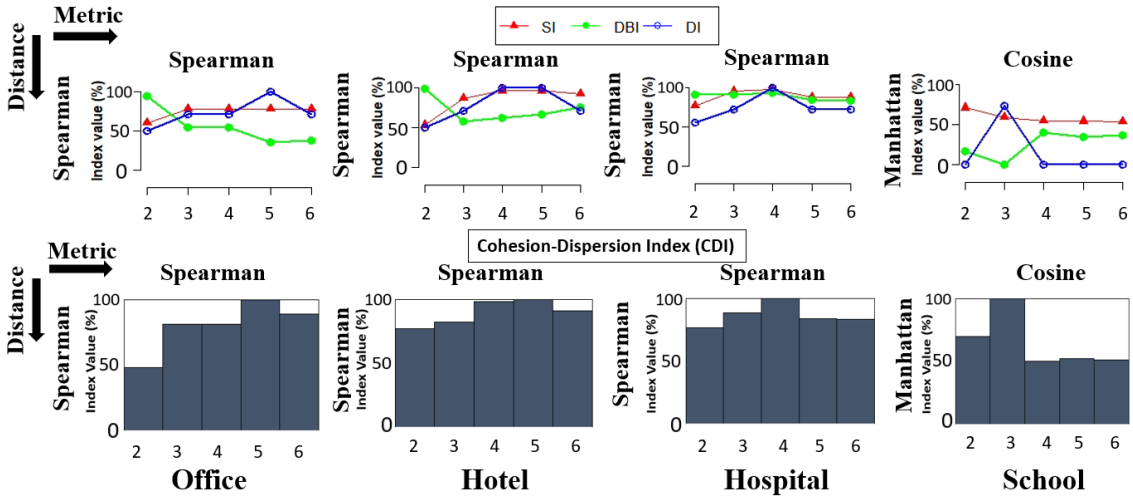

Figure 3-3. K-means optimum clustering using distance-metric measurement criteria. (Where x- and y-axis present K (or cluster) value and normalized index respectively; top and bottom figures show the variation of internal validation indices and unified validation index respectively, for four different measures of distance and clustering metrics (Euclidean, Manhattan, Correlation, and Spearman).)

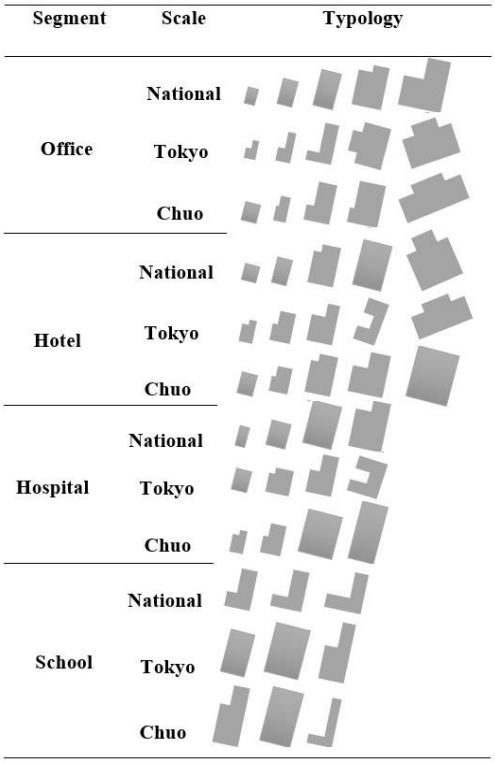

Figure 3-4. Overview of building typologies of commercial building stock across different scales.

1) Building shape allocation algorithm

The proposed algorithm was applied to the commercial building stock to extract the true shape representation of RBMs. Figure 3-4 illustrates the overview of building shape allocation of

commercial building stock across different scales. As the building composition varied in size and geometric terms, the shape indices fluctuated to respond to the shape complexity and diversity associated with large-size building stock. Moreover, this provided heterogeneity within building shape by capturing rectangular, square, slab, U- (or C-), L-, and T-typologies for RBMs. For hotel building stock, a rectangular shape was allocated due to the predominance of REC index for the specified cluster within the national stock (see Appendix E), while the specified cluster associated with Tokyo stock was assigned a more complex shape (or U-shape) due to a lower value of CNV index. Overall, this analysis showed no significant proportion of CI within the stock, while a major proportion was skewed towards one for REC and SQN.

2) Neighborhood adjacency model

Figure 3-5 shows the segment-wise composition of the neighborhood context for different scales. We observed that built-up density varied significantly across the scales, and Chuo (or district scale) possessed high built-up density with the taller neighborhood than other scales. In terms of TB, Chuo and other scales were significantly different, with the average height being twice higher in the hotel segment case compared to other scales.

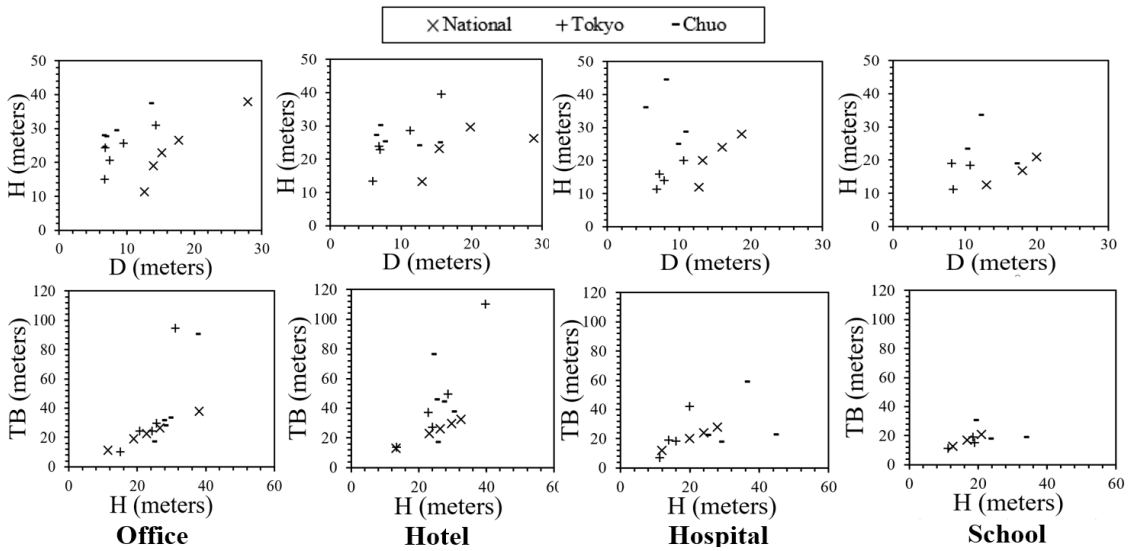

Figure 3-5. Segment-wise composition of neighbourhood context for different scales (Notation: D is the adjacent average distance between target building and neighbourhood; H is the average neighbourhood height; and TB is the average height of target building).

3.3.2 Synthetic building stock analysis

1) Long-term stock dynamics

Figure 3-6 shows the long-term stock distribution of building vintage for commercial buildings across different scales. For building vintage, the composition of existing building stock showed

higher aging stock in Chuo compared to other scales, whereas the average age-band of existing stock was 1990. For long-term stock dynamics, the commercial building stock floor area increased from 2016 to 2030 by 24.3%, 23%, and 12.5% for national, Tokyo, and Chuo, respectively. This difference is attributable to the varying percentage of newly constructed buildings across the scale. The addition of new buildings and replacing aging buildings by 2030 would result in a transition of the average age-band from 1990 to 2010. Moreover, the system stock dynamics showed higher stock turnover in Chuo compared to other scales, whereas the systems installed after 2010 nearly doubled by 2030. Overall, this implied the significance of considering both stock dynamics within the model due to their distinctive frequency distribution.

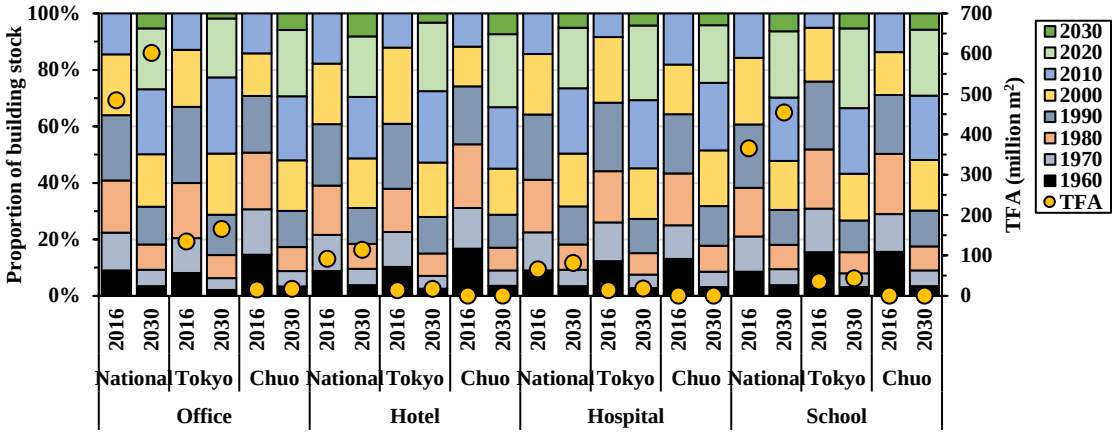

Figure 3-6. Long-term stock distribution of building vintage for commercial buildings across different scales.

2) System stock modelling

Figure 3-7 shows the share of HVAC systems for different scales in terms of cooling and heating sources. For air-conditioning systems, the proportion of fan coil unit (FCU) and outdoor handling unit (OHU) systems was lower in Chuo, while constant and variable air volume (CAV and VAV) systems had higher proportions at larger scales (national and Tokyo). The long-term projection of air-conditioning systems showed an increased proportion of variable refrigerant flow (VRF) systems and a decreased proportion of FCU and OHU systems. For heat sources, the proportion of centralized-gas/oil source was larger in Tokyo, while the centralized-storage source had a lower proportion at national and district scales. The long-term projection of heat sources showed a decreased proportion of centralized-gas/oil source and an increased proportion of decentralized-electricity source.

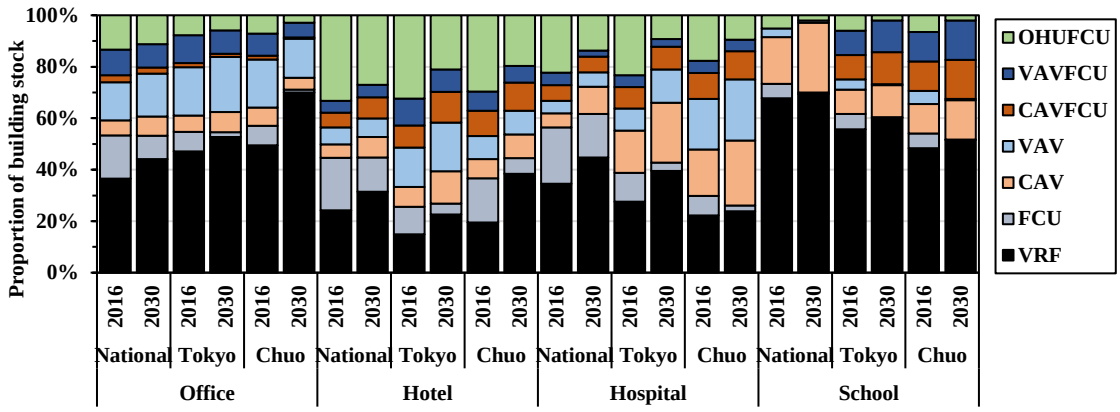

(a) Air-conditioning systems.

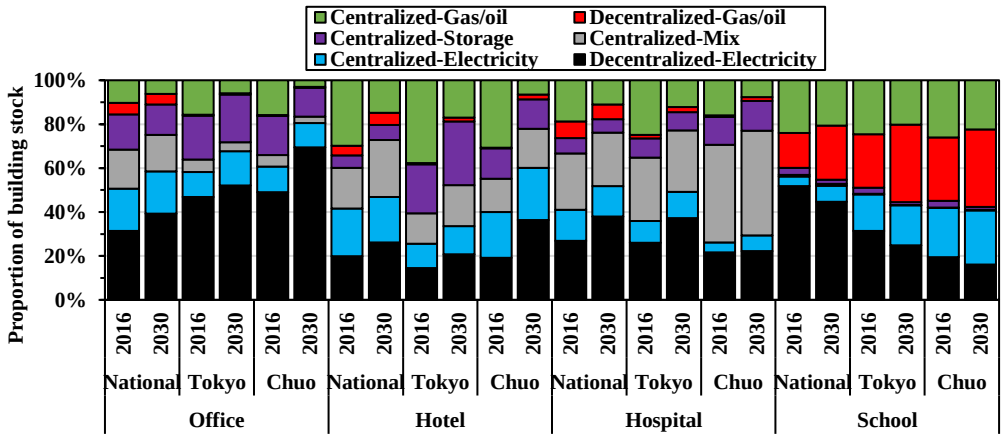

(b) Heat sources.

Figure 3-7. Distribution of HVAC systems in the commercial building stock for different scales.

Figure 3-8 shows the distribution of energy saving measures (ESMs) for different scales based on ventilation- and heat-delivery-related measures. For ventilation-related measures, the incorporation of outside-air-based (OA) measures was higher and the incorporation of heat-exchanger-based measures in Tokyo and Chuo decreased. The long-term projection of ventilation-related measures showed an increased proportion of combined measures (All) and a decreased overall composition of ventilation-related measures in Tokyo and Chuo due to a faster transition towards VRF systems. For heat-delivery-related measures, the proportion of VAV and variable water volume (VWV) control measures was higher at other scales compared to the national scale. The long-term projection of heat-delivery-related measures showed an increased proportion of VWV control measures (except the school segment). However, for the socio-spatial predictors, these factors significantly influenced the adoption probability of system alternatives for a specified building. For example, HDD, which accounts for the variation of climatic effect, resulted in higher adoption of gas-driven HVAC systems in the colder region (as evident at the

national scale). Overall, the application of logistic regression resulted in a better distinction between the centralized and decentralized HVAC systems across small and large size buildings by considering various predictors, such as TFA, PD, HDD, and building age.

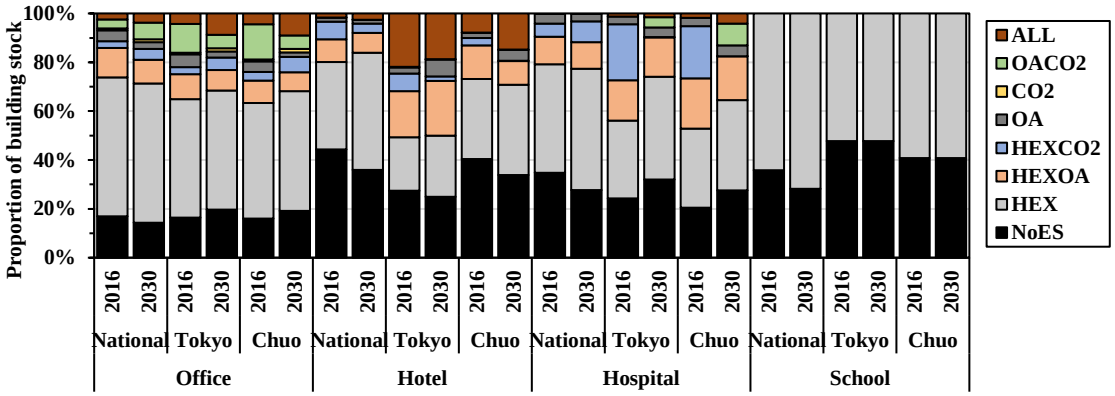

(a) Ventilation-related measures.

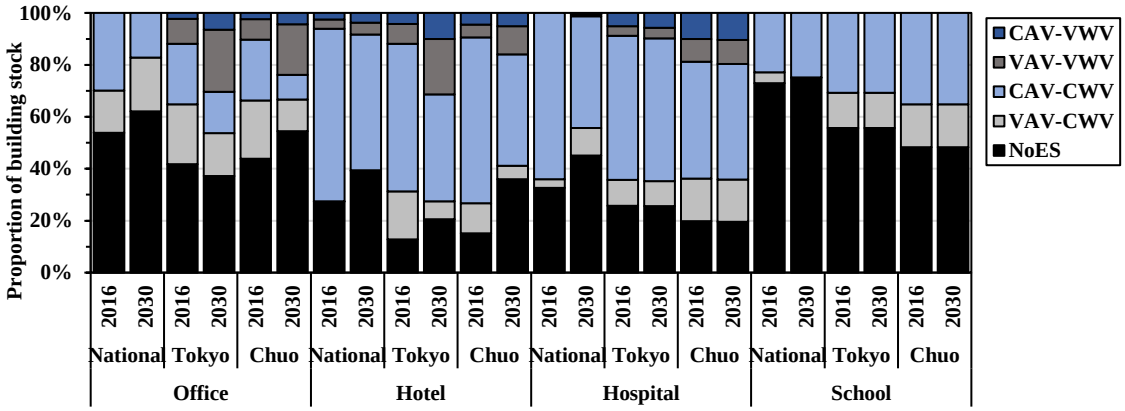

(b) Heat delivery-related measures.

Figure 3-8. Distribution of ESMs in the commercial building stock for different scales.

3.3.3 Building stock energy modelling and simulation

1) Model validation

Figure 3-9(a) shows the validation results of the RBMs for different scales by comparing metered and simulated values in terms of the EUI, a primary energy metric. It is observed that the proposed model provided better EUI agreement for all the RBMs across different scales. For stock-wise analysis (Figure 3-9(b)), our model accurately followed a long-tail distribution but was underestimated at a low EUI level, which can be attributed to the differences in building operating conditions due to the assumption of typical floor usage within the model.

To further evaluate the model, the aggregated-level validation was performed by comparing the specified model output with EDMC and TMG metered data, as shown in Figure 3-9(c). At the

national scale, the model underestimated the total secondary energy consumption by 10% due to the omission of educational institutes other than schools; whereas, the model estimate agreed well with a difference of 4% and less than 1% from metered data for Tokyo and Chuo scales, respectively.

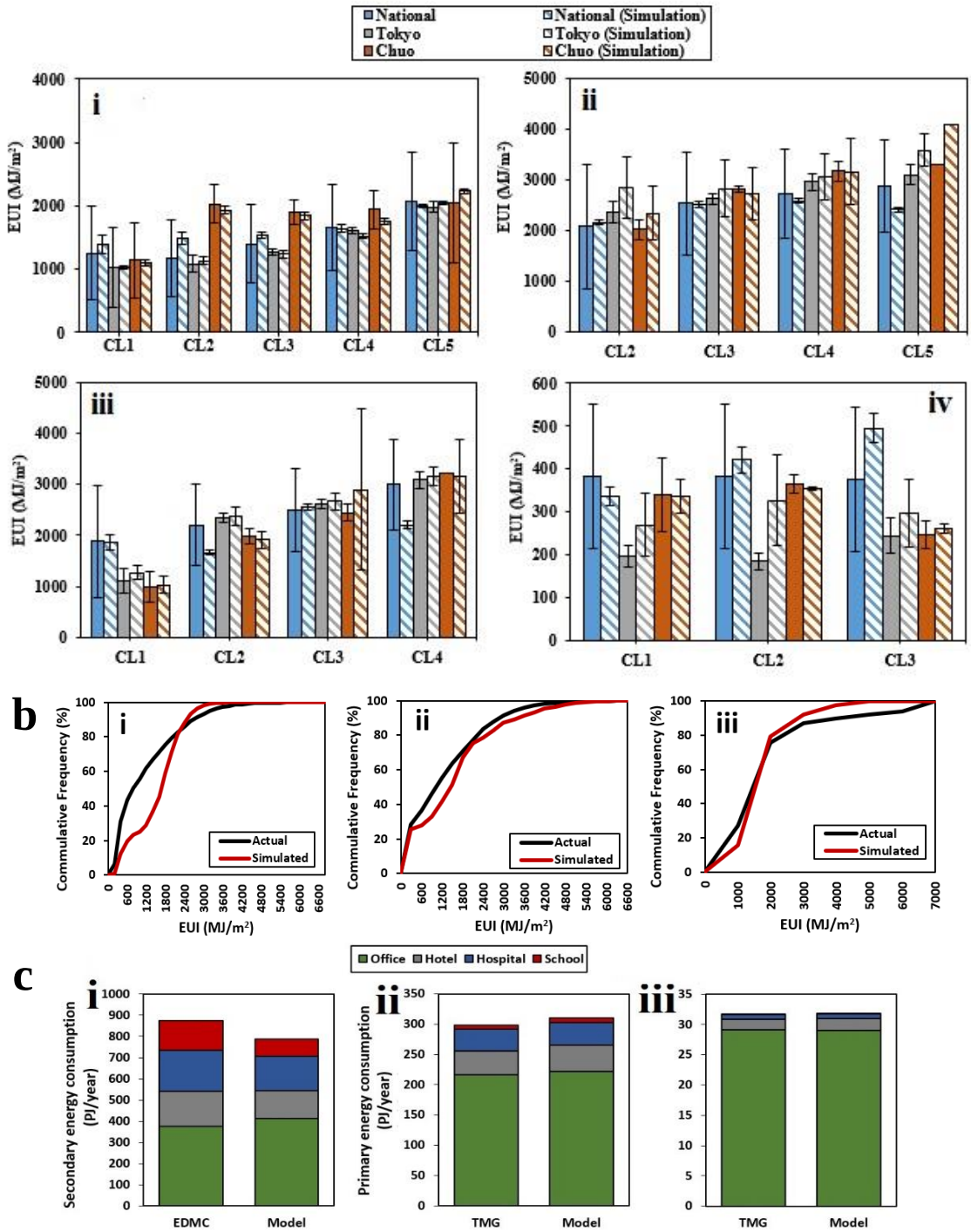

Figure 3-9. (a) Validation of RBMs for different scales: i) office; ii) hotel; iii) hospital and iv) school.; (b) Cumulative frequency distribution of EUI across the stock for different scales: i) national; ii) Tokyo; and iii) Chuo; (c) Aggregated-level evaluation of the model for different scales: i) national; ii) Tokyo; and iii) Chuo.

Table 3-4 shows the deviation of key error indicators, absolute percentage (%), coefficient of determination (R^2), coefficient of variation of root mean square error (CV RMSE), and normalized mean bias error (NMBE), for commercial BSEM across different scales. The results show that all the error indicators are higher at larger scale in comparison to smaller scales. For instance, when looking at R^2, the standard deviation (σ) goes from 0.09 at the district scale to 0.24 at the national scale.

Table 3-4. Validation results for commercial BSEM across different scales.

Scale	(%)	R^2	CV RMSE	NMBE
Chuo	0.3	0.95 (σ=0.09)	5.6 (σ=2.56)	1.6 (σ=4.21)
Tokyo	4.1	0.85 (σ=0.11)	10.2 (σ=3.16)	-1.9 (σ=4.86)
National	10.1	0.77 (σ=0.24)	13.2 (σ=3.29)	-5.3 (σ=9.32)

2) Multi-scale modelling results

The analysis of the multi-scale model evaluated the annual energy consumption patterns across the scale for end-uses and fuel types, as illustrated in Figure 3-10. The energy consumption patterns of the RBMs across the stock showed higher usage for HVAC and others in hotel and hospital stocks, whereas office and school stocks were more electricity-centric compared to other segments. The multi-scale analysis of end-use energy consumption patterns showed higher plug load patterns in Chuo than large scales, attributable to its higher occupancy density as a major commercial district of Tokyo. For plug load patterns, lighting and equipment usage showed a correlation with the building classification size. For example, a large-size office building (or CL5) exhibited a higher plug load pattern than a small-size office building (or CL1). This was because of varying floor composition, as large-size buildings have more multi-purpose facilities than small-size buildings. However, large-scale stock exhibited a relatively higher proportion of HVAC usage (except hotels) than other end-uses, because of the degree of balance between heating and cooling demand due to metrological variations. For fuel type, the large scale seemed more electricity-centric, whereas higher gas usage was observed at other scales. These differences in the energy end-uses were due to the varying structural and stock composition (as explained in Sections 3.3.1 and 3.3.2) across different scales, which were mostly neglected by non-scalable models.

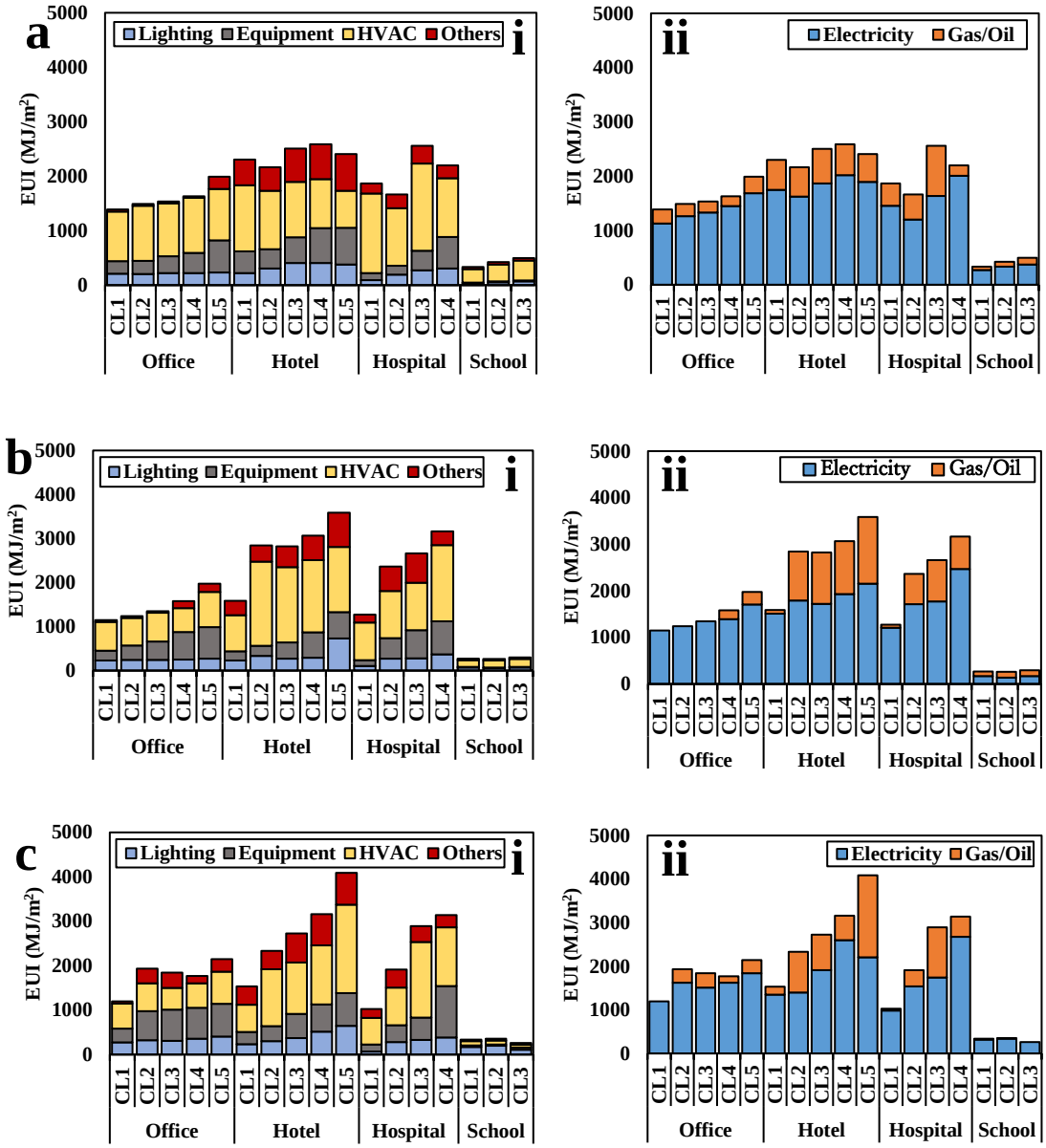

Figure 3-10. Annual EUI of RBMs for national (a), Tokyo (b), and Chuo (c) in terms of; i) end-use and ii) fuel type.

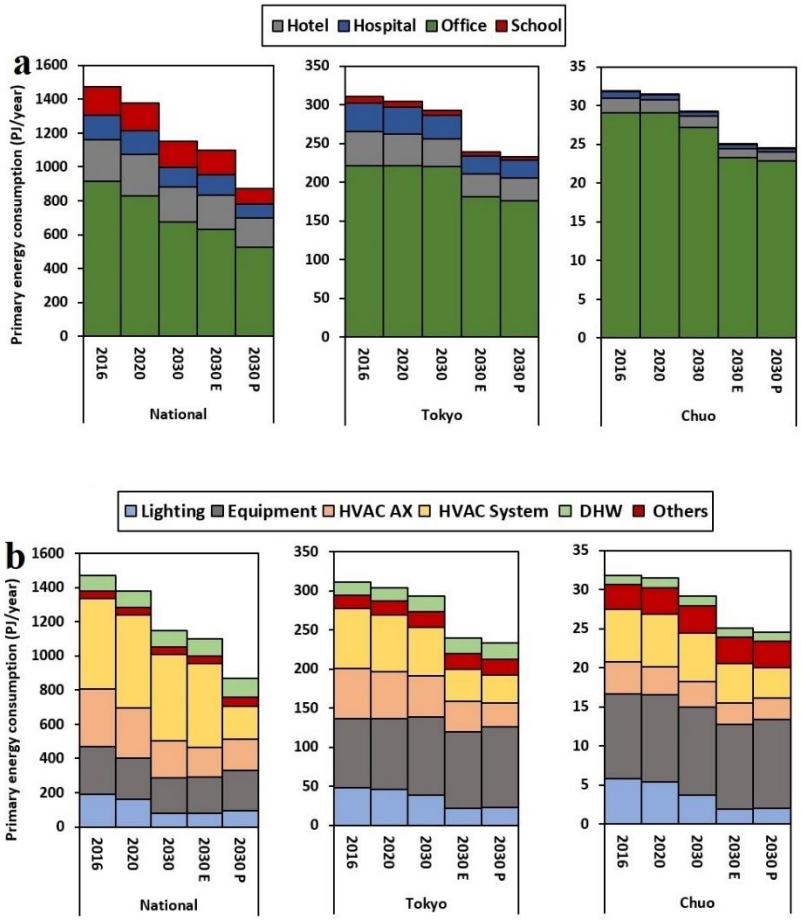

Figure 3-11. Long-term primary energy consumption across different scales; a) segment-wise and b) end-use (where 2030E and 2030P represent electrification and potential scenarios for the 2030 year respectively).

3) Long-term energy demand

Figure 3-11 shows the long-term primary energy consumption across different scales up to 2030. The annual primary energy consumption of commercial building stock was projected to be 1372, 307, and 29 PJ/year by 2030 for national, Tokyo and Chuo scales, respectively. In terms of energy end-uses, different equipment usage was noticed, which is attributable to varying building operation conditions from large to small scale. Whereas higher thermal load at a large (or national) scale is attributable to climatic variation. The adoption of ESMs as per the baseline scenario would result in the avoidance of 7, 3, and 5% of primary energy consumption by 2030 at national, Tokyo, and Chuo scales, respectively. Incorporating electrification and retrofit measures, the maximum reduction potential was estimated to be 39, 26, and 23% of primary energy consumption by 2030 at the national, Tokyo, and Chuo scales, respectively. This difference in the reduction potential across different scales highlighted the significance of using target-based planning and decision-making to implement ESMs within building stock.

3.3.4 Building stock scenarios

1) Energy epidemiology

Figure 3-12(a) shows the varying energy consumption by implementing different models (national and Tokyo) on a reference scale (Chuo). A significant difference in energy consumption patterns was observed when the models developed for national and Tokyo scales were applied to the Chuo scale. The adoption of the models resulted in the annual energy consumption being 26.6, 28.8, and 31.8 PJ/year for national, Tokyo, and Chuo scales, respectively. This indicated that the annual energy consumption was underestimated by 10–17% when different models were applied to Chuo building stock. Moreover, the differences in carbon emissions varied from 479 to 819 ktCO_2, which would be neglected if an appropriate scale was not considered. For energy end-uses, an absolute difference existed in energy usage processes, such as lighting, equipment usage, and building systems. As discussed in Section 3.3.3(2), the major difference in energy consumption patterns occurred due to lighting and equipment usage related to higher occupancy density in Chuo.

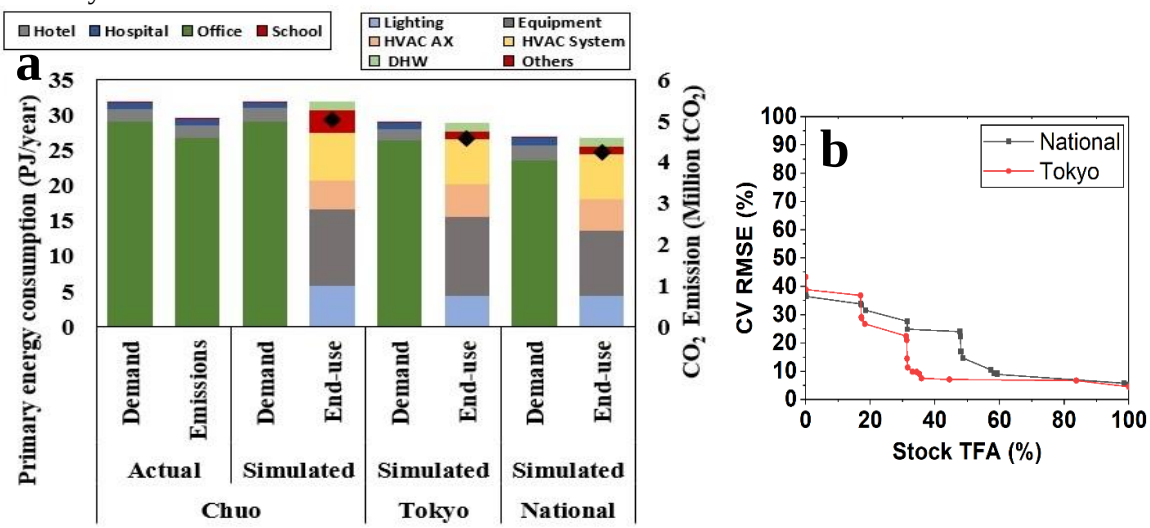

Figure 3-12. Variation of energy consumption by the implementation of different scales (national and Tokyo) on a reference scale (or Chuo): a) Annual primary energy consumption and carbon emissions; b) scale uncertainty relative to Chuo scale (where each dot represents a specific RBM cluster which is sorted from highest to lowest CVRMSE value).

Figure 3-12(b) shows the stock-wise uncertainty induced by implementing different models (national and Tokyo) on a reference scale (Chuo). We observed that using national- and city-level representative RBMs resulted in 60 and 35% of the stock having CVRMSE of 10% or higher, respectively. This indicated that the larger the description of a scale, the higher the error uncertainty when applied to a smaller representative scale. The comparison of energy mapping,

as shown in Figure 3-13, exhibits the spatial deviation of the primary energy metric at the building-by-building level when a non-representative scale is applied to other scales.

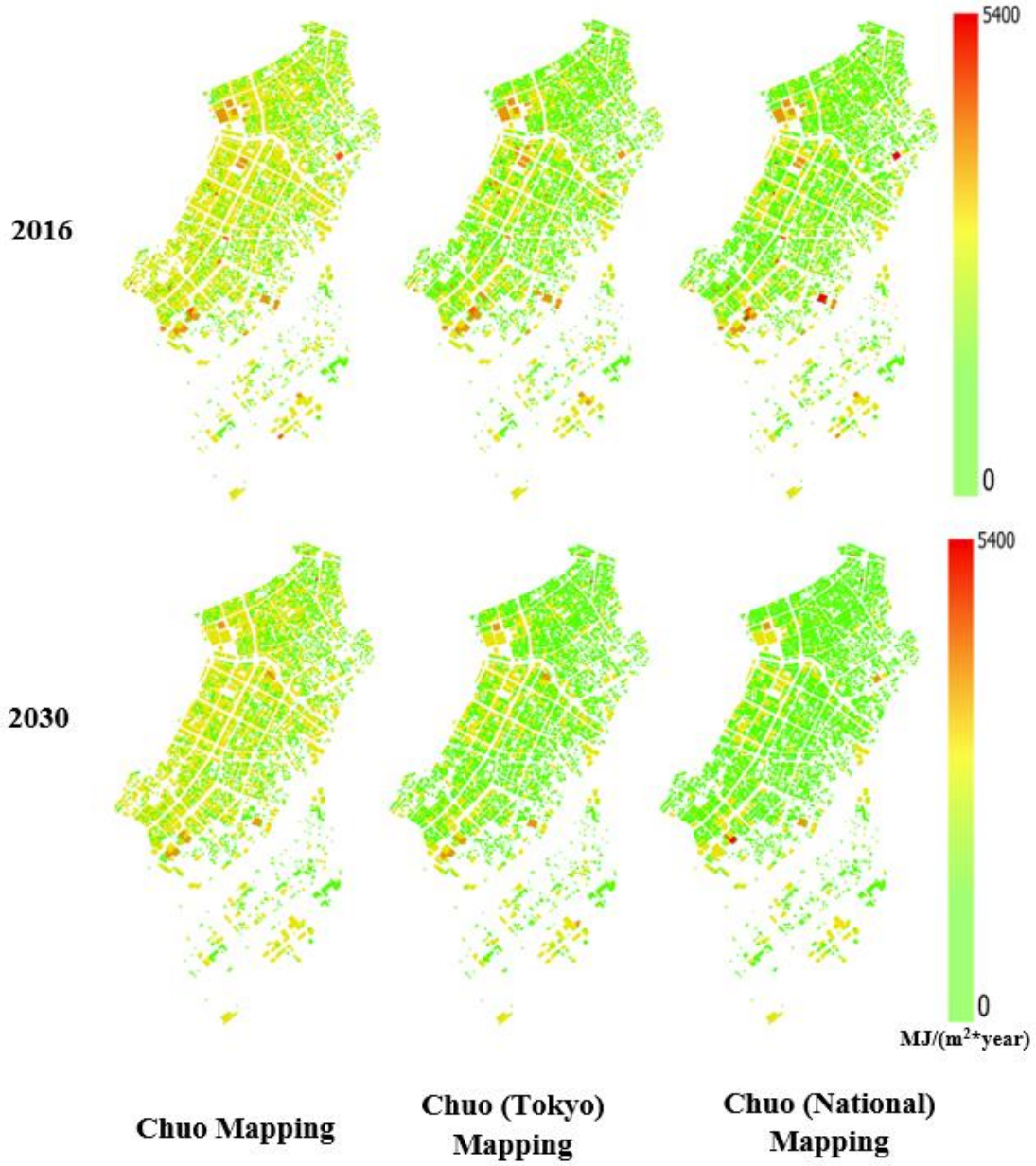

Figure 3-13. Illustrative building-by-building mapping of the spatial distribution of primary energy consumption by the implementation of different scales (national and Tokyo) on a reference scale (or Chuo).

i) OAT analysis

This analysis quantified energy epidemiology considering the structure and conditions of systems and practices by applying relative parameters of other scales on a reference (Chuo) scale, as shown in Figure 3-14 (see detailed results in Supplementary Figure S3). The OAT analysis showed a significant scale-bounded impact of building geometry and plug loads on primary

energy consumption, attributable to variations in stock structural (building size, aspect ratio, and typology) and end usage patterns across the scale. For other significant influencing parameters, the occupancy density exhibited a negative impact similar to plug loads, which showed a strong correlation between them. The structural composition of HVAC systems obtained by using other models resulted in a positive impact, depicting a higher thermal dynamic system stock than the reference scale, but the overall impact was not as significant as building geometry and plug loads. Additionally, this implied that the HVAC systems had a significant scale-bounded impact on large-size buildings, indicating a higher sensitivity of socio-spatial predictors, such as HDD and PD, with building size. However, the scale-bounded impact of the neighborhood urban context was very similar and negligible across the scale. This analysis examined and identified various drivers and determinants to understand better the mechanisms and conditions leading to demand levels when a non-representative scale was applied to other scales.

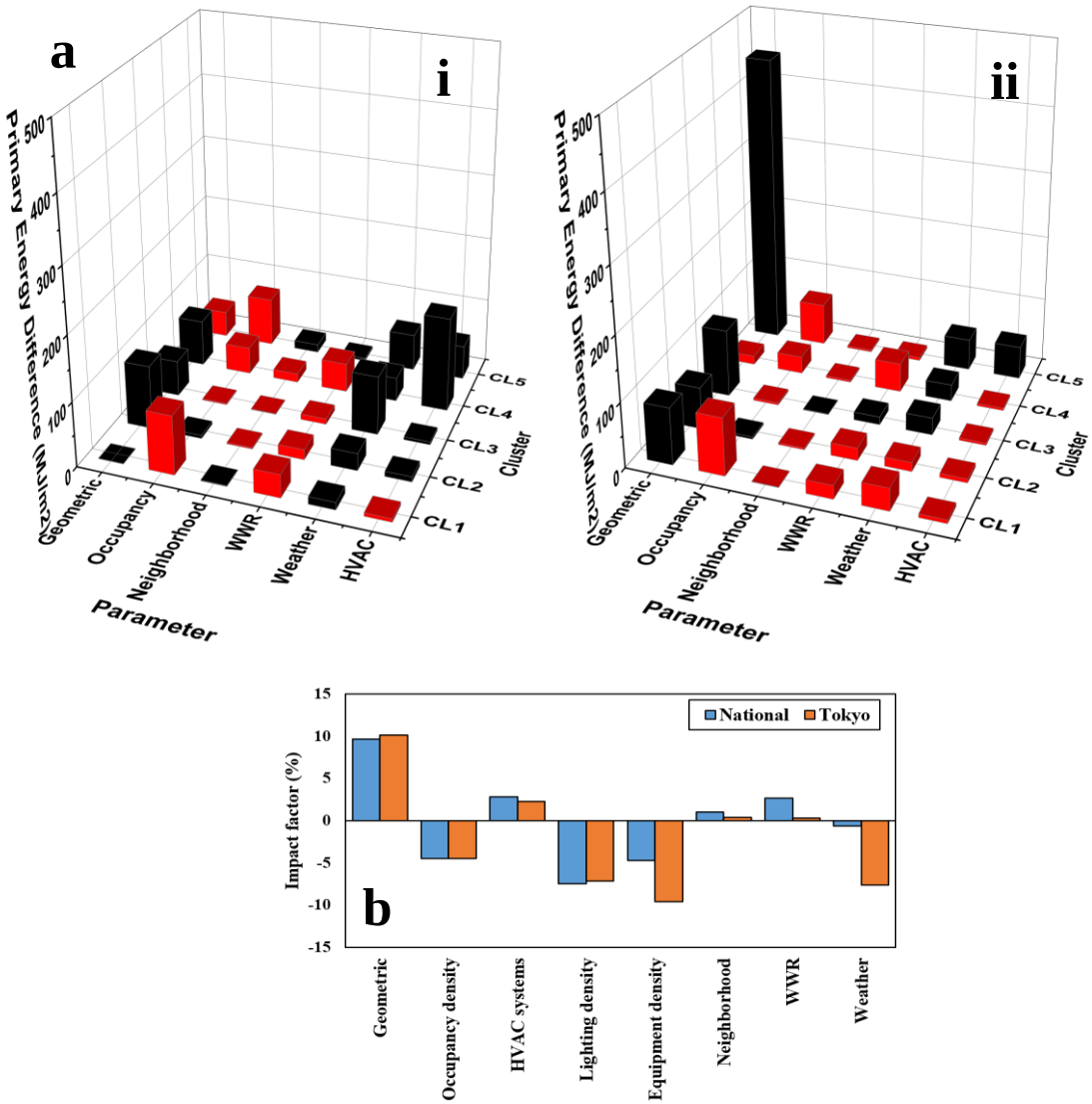

Figure 3-14. OAT analysis for quantifying energy epidemiology (with Chuo as reference scale): a) cluster-wise primary energy difference due to various parameters by implementing national (i) and Tokyo (ii) office building stock (Notation: black as positive and red as negative); b) average impact factors of various parameters.

ii) Long-term energy epidemiology effects

Figure 3-15(a) shows the long-term variation of energy consumption by implementing different models (national and Tokyo) on a reference scale (Chuo). The results showed a significantly different reduction potential when different scales were applied to the Chuo scale (also see Figure 3-13). The annual energy reduction potential in 2030 was 7.8, 4.9, and 2.2 PJ/year at the national, Tokyo, and Chuo scales, respectively. Moreover, the carbon emissions avoided in 2030 were 52, 46, and 40% at the national, Tokyo, and Chuo scales, respectively. Thus, the difference in energy and emissions reduction potential varied by 2–3 times and 6–12%, respectively, when different scales were applied to the Chuo scale. The significant deviation between the reduction potential of energy consumption and carbon emissions was due to the assumption of a reduction in carbon emission intensity by 2030 (from 0.57 to 0.25 kg-CO_2/kWh). This implied that in the long-term scenario, the scale-bounded uncertainty seemed higher in estimating energy consumption than carbon emissions. For energy end-uses, the lighting and HVAC systems accounted for a significant reduction potential that was overestimated by up to 10 and 5%, respectively, compared to the reference scale. This implied that the long-term stock structure changes were inaccurately captured when a non-representative scale was applied at other scales. Figure 3-15(b) shows the stock-wise uncertainty induced for long-term aspects by implementing different models (national and Tokyo) on a reference scale (Chuo). The long-term stock-wise analysis showed highly varying error terms, with 95% and 45% of the stock having CVRMSE of 10% or higher, compared to the base year analysis, which illustrated more necessity for an appropriate selection of scale for the long-term studies than the base year analysis.

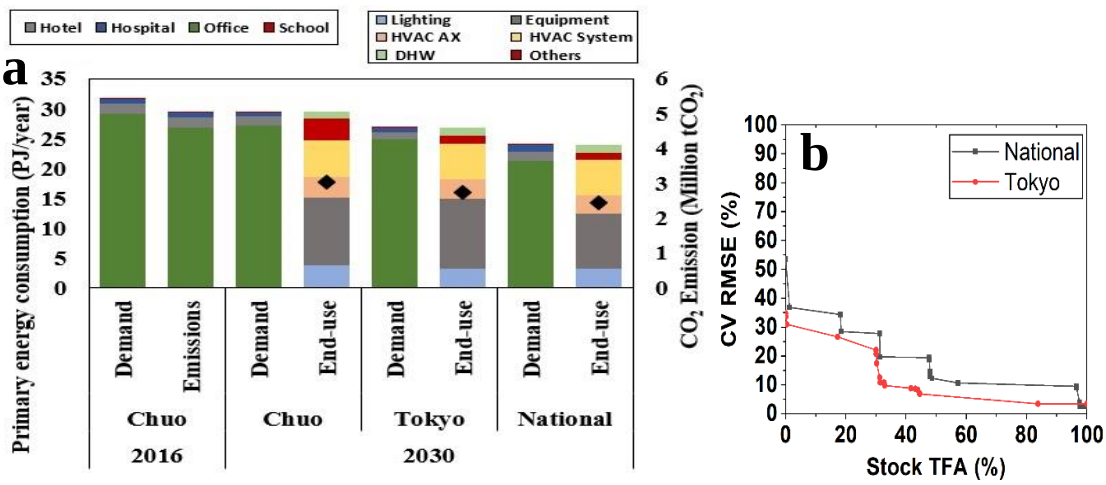

Figure 3-15. Long-term energy epidemiology effects: a) annual primary energy consumption and carbon emissions; and b) scale uncertainty relative to Chuo scale (where each dot represents a specific cluster which is sorted from highest to lowest CVRMSE value).

2) Unit block concept

i) OAT analysis

To determine the influence of physical and technical parameters, the OAT analysis assessed the accuracy and extent of the model across the scale and stock. Figure 3-16 shows the stock-wise uncertainty in model prediction across the stock for the different scales. The percentage of building stock within 10% CVRMSE represented 5, 50, and 55% of the stock TFA with varying technical parameters, which increased up to 20, 70, and 80% of the stock TFA with varying physical parameters for national, Tokyo, and Chuo scales, respectively. This demonstrated more skewness of error terms as we transitioned from larger to smaller scale, signifying the need for developing minimum viable guidelines classified depending upon the scale of that specific study. Moreover, considering the influence of parameters, the results showed a stagnant response of building orientation and neighborhood modelling on the accuracy and extent of the model at all scales. Thus, these parameters could be neglected if the objective is to perform the modelling with minimum viable concept criteria. The multi-scale analysis showed a need for a more integrated model at a large scale than other scales due to a modular and diversified distribution of building stock that levers out the variability within the model output.

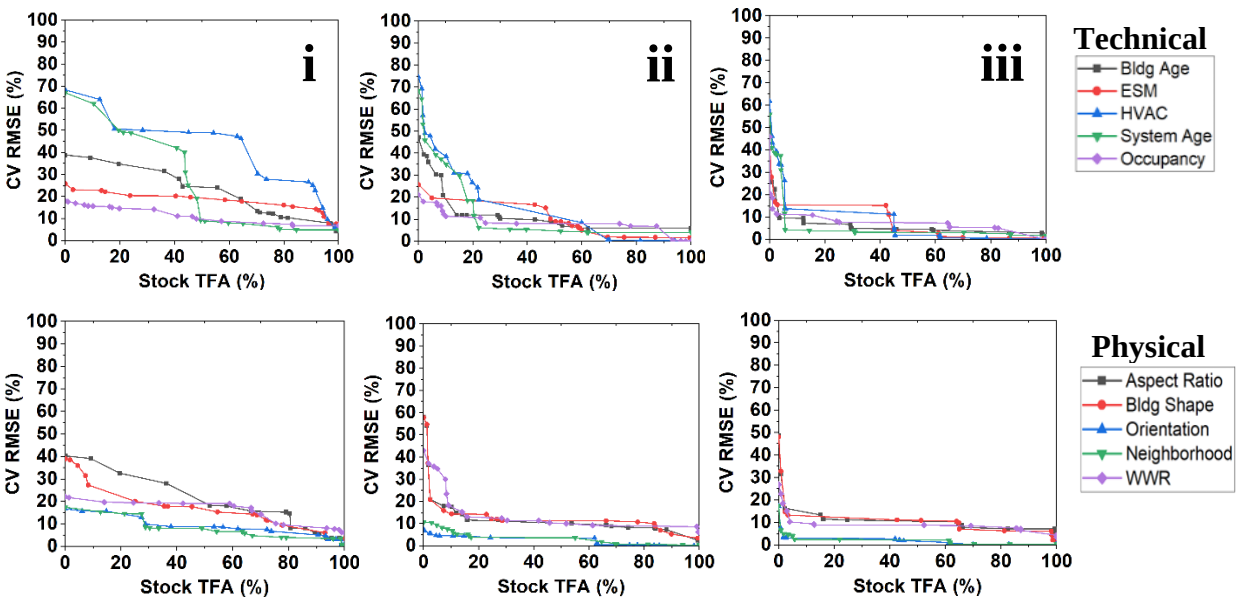

Figure 3-16. OAT effect on the stock-wise uncertainty for national (i), Tokyo (ii) and Chuo (iii) (where each dot represents a specific cluster which is sorted from highest to lowest CV RMSE value).

Figure 3-17 shows the impact of various parameters on model prediction across different scales. The sensitivity analysis results showed that building system age and the HVAC systems were the fundamental technical factors that needed consideration while performing building stock energy modelling at any scale. Thus, due to the high thermal dynamics associated with these parameters, considering stock dynamics and the heterogeneity of HVAC systems was significant within any specified BSEM. For physical factors, building shape and aspect ratio were more sensitive to the accuracy and extent of the model across the scale. However, the variability of model error due to geometric parameters was notably lower than that caused by technical factors.

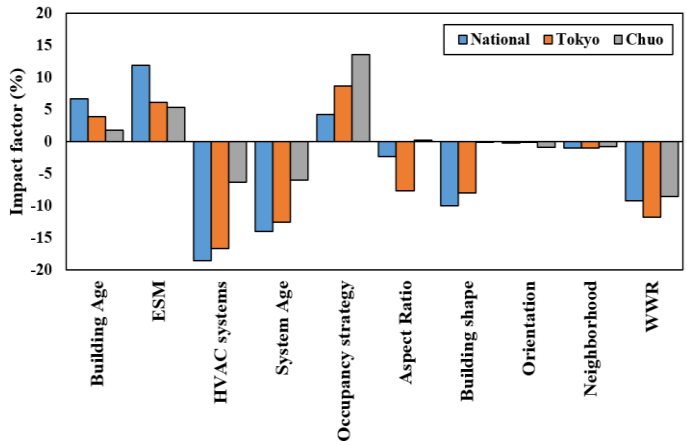

Figure 3-17. OAT effect on the element-wise uncertainty across the scale.

ii) Combined effect

This analysis was performed by adding the building-oriented elements one by one within the unit block model to study the non-linear interaction of various influencing parameters in the BSEM. Figure 3-18(a) shows the stock-wise combined effect of various parameters on the EUI for different scales. The element-wise analysis of RBMs showed a non-linear increase (positive or negative) in the parameters' response to the EUI as the size of the building increased. For segment-wise, hotel RBMs produced higher variability by omitting influencing parameters, attributable to the need for detailed modelling for capturing multiple end-use activities, such as equipment usage and the heterogeneity of building systems, within the segment (see details in Section 3.3.2 and 3.3.3(2)). The stock-wise results revealed that omitting the probabilistic occupancy model and ESMs resulted in the overestimation of primary energy consumption across the stock. Whereas, primary energy consumption was underestimated by omitting the HVAC systems and system age within the model

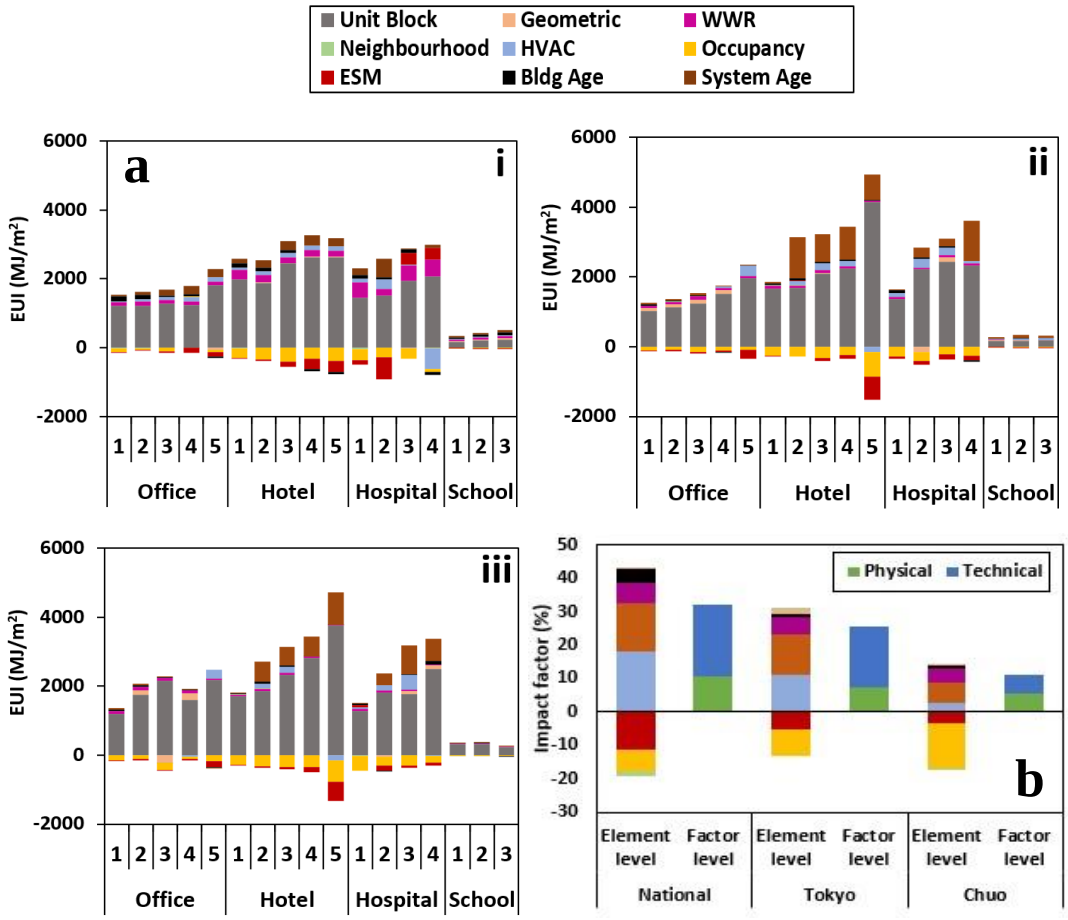

Figure 3-18. Combined effect on the model prediction: a) stock-wise uncertainty for national (i), Tokyo (ii) and Chuo (iii); and b) element-wise uncertainty across the scale.

Figure 3-18(b) shows the element-wise combined effect of various parameters on the EUI for different scales. The results obtained by considering the combined effects of various parameters within the BSEM indicated a positive correlation of the building and system age, HVAC systems, geometric, and window-wall ratio (WWR) factors. In contrast, the occupancy and ESMs factors negatively correlated to primary energy consumption. Moreover, a higher order of variability was induced by considering the typical occupancy model, signifying the importance of considering a probabilistic occupancy model instead of a typical one to capture these non-linearities within the BSEM.

3.4 Discussion

With the development of the proposed hybrid workflow, the model facilitates the concurrent consideration of physical and technical factors and extends the capability to different spatial resolutions. As shown in Section 3.3.3(2), the results indicate that the differences in the energy end usages and reduction potential exist due to varying structural and stock composition across

different scales. This implies that the hybrid models capture these variations, which a conventional non-scalable model could not distinguish. From a practical implementation perspective, this further helps address the data limitations and context-specific issues to overcome the disparate coordination between the local and national level stakeholders, which could identify priority areas for implementing target-based energy efficiency strategies. Moreover, this multi-stage process also resulted in the enhancement of the analytical capability of the model by concurrently incorporating physical, technical, and socio-behavioral factors within a commercial BSEM across different scales. Additionally, the proposed scheme can be used as an assessment tool to identify various drivers and determinants to understand better the mechanisms and conditions leading to different demand levels for commercial building stock across the scale. From a practical implementation perspective, this paper provides insight to energy modelers about the sources of uncertainties within commercial BSEM.

Considering evaluation capabilities, the hybrid approach improves the existing assessment framework of the BSEM by providing a better understanding of the model development process in terms of end-use energy processes (function and boundary of the systems), practices (socio-behavioral interaction, such as occupancy patterns and resource usage), and context (structure and conditions of systems) across a range of scales and sectors. This assessment gap exists in the previous multi-scale studies that either established models for a different scope (like residential building stock) or focused on urban morphological and metrological conditions (Nutkiewicz et al. (2018); Ali et al. (2019)). According to the energy epidemiology analysis (Section 3.3.4(1)), the selection and description of the appropriate spatial boundary are critical for the base year and long-term studies related to building stock energy modelling. The long-term studies are more sensitive to an adequate spatial boundary than the base year studies and show significantly different energy consumption patterns, 10–17%, and reduction potential, 2–3 times, when a non-representative scale is applied to other scales. This implies a need to develop multi-tier long-term building stock strategies to promote the adoption of ESMs and alternative technologies for achieving net-zero emissions in the building sector. Recently, most of the studies related to commercial buildings have relied upon black-box (or machine learning) models using advanced techniques to predict and identify the building energy consumption and critical building-oriented features (Li and Yao (2021); Yu et al. (2021)). However, they lack the analytical capability to conduct long-term studies for estimating the energy reduction potential. As discussed above, this approach also demonstrates the ability to regularly update based on new data streams and provide the capture value to evolve long-term changes within the commercial BSEM. In addition, the two most critical building-oriented elements are geometry and plug loads when the non-representative scale is applied to other scales. This suggests that these elements lead to higher scale-bounded

uncertainties, induced due to structural heterogeneity, typological complexities, and diverse functionalities associated with the stock composition of commercial buildings.

Considering the modelling capabilities, Section 3.3.4(2) shows that the physical and technical factors result in a performance gap of up to 11 and 21%, respectively, with the cumulative gap varying from 11–32% for different scales. Moreover, previous studies revealed that disregarding the physical and technical factors results in energy use differences of 10–19% (Heidarinejad et al. (2017); Chen and Hong (2018)) and 15% (Kim et al. (2020)), respectively. This implies that the BSEM needs to be modelled with the concurrent consideration of building-oriented elements. Otherwise, a fragmented consideration of these factors may lead to a performance gap within the model. The quantitative analysis of building-oriented elements indicates that the building system age and HVAC system composition are the two most critical building-oriented elements because of their higher thermal dynamic effect on the model. Moreover, the physical factors cannot influence as much as the above factors. This implies that the unit block model identifies the critical building-oriented elements for providing in-depth details about the influence and the order of magnitude of these elements within the BSEM across the scale and stock. From a practical implementation perspective, the energy modelers need to pay more attention to system stock and turnover dynamics when developing BSEM for a specific scale, because omitting system heterogeneity might lead to the prediction of different energy consumption patterns.

Additionally, a unit block concept also provides an initialization point for developing a stock-level model at any demographic landscape or spatial resolution. Thus, the focus has recently been on developing minimum viable model guidelines depending on the application category of building energy models (Ang et al. (2020)). A minimum viable model requires a minimum level of detail to provide transparency and capture value with the least cost and effort. Analyzing the unit block model, the influence of building-oriented elements on the energy modelling gap reduces as we transition from larger to smaller scale, which is an opportunity for the energy modelers and planners to develop minimum viable guidelines to fasten the development cycle with minimum cost constraint as per the specific scale.

Although the developed approach demonstrated improved adequacy at the multi-scale level and could be further applied to different regions, there are still some limitations that need to be addressed. To ensure homogeneity across the specific study, the same number of classifiers are used to perform the segmentation, resulting in an equal number of clusters at different scales. This scheme needs further improvement by implementing it at a specific granular level to obtain the optimum number of classifiers as per the specifications. Moreover, a multi-nominal statistical approach is applied to a large sample dataset to fill the energy modelling gap due to a lack of

information related to the technical factors. This requires further effort to conduct a multi-scale field survey for validating the probabilistic building systems stock model by comparing it with actual stock. Furthermore, an auto-calibration framework needs to be developed that can transform the existing multi-scale model into a scalable model, ensuring transparency at a granular level by providing a comprehensive insight into uncertainties at the spatial level.

3.5 Conclusions

This paper presents a novel hybrid framework that integrates geo-referenced and sampled-based synthetic stock models to facilitate the concurrent consideration of multiple building-oriented elements within commercial BSEMs at a multi-scale level. The proposed framework enhances the capability of the bottom-up engineering models to be further extended to any demographic landscape or spatial resolution and evolve into a long-term transitional workflow. Thus, enabling long-term spatial energy resource planning and decision-making for commercial building stock across various scales. Moreover, when implemented on the commercial building stock of Japan, the developed model provides a comprehensive understanding of selecting and describing the minimum viable requirements for a specific scale by considering the effect of various influencing parameters on scale-bounded uncertainties. Additionally, multi-level validation is performed to ensure transparency and capture value that exhibits an acceptable level of adequacy and accuracy of the model at multiple scales. The main findings of this hybrid framework at multiple scales are:

1. The proposed multi-scale model identifies various drivers and determinants of energy end-uses and resource usages to provide a better understanding of mechanisms and conditions that lead to different levels of demand for commercial building stock across the scale. This addresses the underlying complexity associated with the BSEMs by examining influencing factors that cause different levels of outcomes at different scales.
2. The scale-bounded comparative approach indicates that the larger the description of the scale, the higher the error uncertainty when applied to a smaller representative scale. This scale variability seems significant due to relatively higher thermal dynamics induced by the building typology and functional composition of the commercial building stock.
3. The long-term perspective of scale-bounded uncertainties shows an overestimation of reduction potential by 2–3 times when a non-representative scale is applied to a smaller representative scale. Therefore, an accurate description of scale is necessary in BSEM for long-term studies.
4. As per the quantitative analysis, disregarding the physical and technical factors drops cumulative performance by up to 32%. This signifies the need for a concurrent consideration of these factors within BSEM.

5. For model complexity, a more integrated model is needed at a large scale than other scales because of the modular and diversified distribution of large-scale building stock, which leverages variability within the model output. The results imply that the performance gap increases significantly up to 21% when the description of a scale shifts from a smaller to a larger one.
6. The unit block model concept provides a simplified value proposition by using a bottom-up engineering model for developing minimum viable model guidelines. This establishes the correlation effect of various parameters to gauge the non-linearities within the model that highlight the trade-off between the model's complexity and reliability.

Overall, this model provides a granular-level framework using the spatial intelligence building stock approach to assist city-level planners and policymakers in developing long-term energy efficiency monitoring strategies at multiple scales. This also provides a new dimensional aspect by considering alternative technologies and measures within the GIS-based building stock modelling. Future work will be extending this model to develop multi-scalable reduced-order models for commercial building stocks, which could speed up the development cycle by minimizing computational resources.

3.6 Appendix

3.6.1 Appendix A

The geo-databases of Tokyo and Chuo were provided by Tokyo Urban Development Bureau (TUDB, 2017), whereas ArcGIS Geo Suite (Esri Japan, 2015) was used to develop a national-scale model. In synthetic stock modelling, sample datasets collected from Society of Heating, Air-Conditioning, Sanitary Engineers of Japan (SHASE-J, 2017), and Japanese Association of Building Mechanical and Electrical Engineering (JABMEE, 2010), were used to estimate the composition of building system stock and ESMs at different scales. Supplementary Table S1 lists the types of Heating, Ventilation, and Air-Conditioning (HVAC) systems and ESMs considered in the study. Furthermore, the long-term stock dynamics were modelled by using key evolution factors obtained from Building Construction Survey Data (BCSD) (SBJ, 2017) and Tokyo Statistical Yearbook (TSY, 2019) to consider building vintages and system stock dynamics within the model. To validate and calibrate the developed models, we used metered data obtained from Tokyo Metropolitan Government (TMG) and Database of Energy Consumption for Commercial Buildings (DECC) (JSBC, 2017; TMG, 2020).

Table A.1. Description of building stock data.

Category	Data	Source	Conversion
Physical	Geometric	GIS dataset (Esri Japan, 2015; TUDB, 2017)	Derived
	Non-geometric		
	Typology		Multiple operations in ArcGIS
	Others (WWR)	Survey	
Technical	Building systems	Sample dataset (JABMEE, 2010; SHASE-J, 2017)	Logistic regression
	ESMs		
Urban context	Urban morphological	GIS dataset (Esri Japan, 2015)	Merged using ArcGIS
Climate	Weather	AMEDAS (JMA, 2014)	Morphed
	Climate change	CMIP6 (Karl-Hermann et al. (2019))	
Long-term dynamics	Key evolution factors	Census dataset (SBJ, 2017; TSY, 2019)	Statistical techniques

3.6.2 Appendix B

B.1 Determine the spatial effect of neighborhood-level urban form

In this study, spatial regression analysis was performed to assess the spatial effect of neighborhood-level urban form on building energy use. The main purpose of this analysis was to determine a buffer (or radius) limit, which showed the correlation between the building energy use and neighborhood adjacency environment. To investigate this correlation, five neighborhood-level urban form measures, namely lot coverage ratio, floor area ratio, green area, average shape factor, aspect ratio, and standard deviation (STD) of the building heights were considered up to a radius of 200 m with a step of 50 m. Moreover, the building energy data was obtained from TMG (2020), and then the samples (n=580) belonging to the Chuo ward were geocoded within the GIS dataset. The model results revealed that four of the seven urban form measures (the average building coverage ratio, average building height, STD of building height, and average shape coefficient) were significantly associated with the EUI of the commercial building for the

neighborhood of the 50 m buffer. Based on these results, a pre-defined radius of 50 m was used to search for the surrounding buildings adjacent to the target buildings.

Table B.1. Results of spatial regression analysis

Variable	Model 1 (50-m buffer)		Model 2 (100-m buffer)		Model 3 (150-m buffer)		Model 4 (200-m buffer)	
	Coefficient	z-statistics	Coefficient	z-statistics	Coefficient	z-statistics	Coefficient	z-statistics
Average green area	-0.004	-1.150	-0.001	-0.485	-0.001	-1.316	-0.001	-1.121
Average floor area ratio	0.199	1.005	0.102	0.505	0.211	0.978	0.284	1.241
Average building coverage ratio	15.213*	2.490	3.730	0.627	6.166	1.025	6.088	0.917
Average building height	5.688*	2.118	4.094	0.991	-0.032	-0.005	-2.299	-0.383
STD of building height	2.321*	2.486	-4.775*	-2.146	-3.732	-1.478	-3.595	-1.336
Average shape coefficient	366.383*	2.475	-67.916	-0.304	-208.892	-0.710	-179.092	-0.556
Average aspect ratio	181.954	1.286	-235.739	-1.105	-501.201	-1.736	-661.760	-1.872
R-squared	0.462		0.449		0.454		0.455	
Log likelihood	-2327.4		-2330.6		-2329.2		-2328.9	

n = 580

** $p < 0.01$

* $p < 0.05$

B.2 Selection of effective shading planes

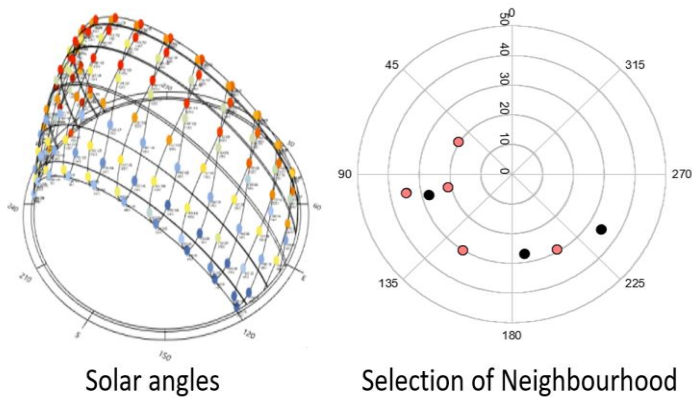

Figure B.1. Selection of effective shading planes using solar angles (where black dots are the effective neighbourhood buildings out of all the adjacent buildings).

Table B.2. Pre-processing of potential shading planes.

Algorithm: Construction and analysis of effective shading neighbourhood buildings.

1. Search for neighbourhood buildings adjacent to target archetypes (i); s and n represent the size of the data set for target and neighbourhood buildings, respectively.

   Loop:

   For i: = 1 to s do

   For j: = 1 to n do

   $$\left.\begin{array}{l} n_{\text{A-area}} \\ n_{\text{BU-building usage}} \\ n_{\text{D-distance}} \\ n_{\text{F-floors}} \\ n_{\text{G-angle}} \\ n_{\text{H-height}} \\ n_{\text{O-orientation}} \end{array}\right\} f\,(i, s_{BUi}, s_{Ai}, s_{Oi})$$

   done

2. Calculate solar altitude angle (δ) for specific location

   δ — *f (declination angle, latitude, hour angle)*

3. Extracted potential shading buildings

   Loop:

   For j: = 1 to n do

   $n_{\text{SH-shadow length}}$ — $f\,(j, \delta, n_{Hj})$

   P_n — extract $(n_{Dj} \leq n_{SH})$

   done

4. Shadow pre-processing to determine effective shading neighbourhood building

   Loop:

   For i: = 1 to s do

   For j: = 1 to n do

   M_n — extract $\{P_n\,(\text{Min}(n_{Dj}), \text{Max}(n_{Hj}))\}$

   Done

3.6.3 Appendix C

Table C.1. Overview of key evolution factors for different scales (SBJ, 2017; TSY, 2019).

Factors	National	Tokyo	Chuo
Mean lifetime (years)	30	26.7	29.5
Shape parameter (k)	1.1-1.6	1.1-1.65	1.1-1.5
Newly constructed buildings (%)	1.57	1.49	0.85
Renovation time cycle (τ_{REN})		30 years	

3.6.4 Appendix D. Settings for building stock energy simulation

D.1. Stochastic occupant behavior model

In this study, a stochastic occupant behavior model was used based on a person-based occupancy approach (Yamaguchi et al. (2022)). This occupancy approach consisted of three main features: 1) determination of nominal building area capacities for each RBM; 2) implementation of different occupancy modes for building system operations, such as unoccupied building, stand-by zone, and occupied zone; and 3) consideration of main occurrences. This method initially determined the number of building users and nominal building area capacities (or typical per capita area) for each RBM. Subsequently, the occurrence of events, arrival time, duration of stay, and out-of-building activities was determined stochastically by assigning a uniform random number to cumulative probability distributions.

D.2. Climate change

Climate models provide a better understanding of how climate change will happen in the near future. These models are constantly updated and expanded based on future emissions scenarios and different sets of assumptions. This study used the sixth Coupled Model Intercomparison Project (CMIP6) to generate future weather files for building stock energy simulations (Karl-Hermann et al. (2019)). To obtain these future weather datasets, a statistical downscaling method, and morphing were used to stretch and derive different climate variables, such as dry-bulb and dew-point temperatures, relative humidity, atmospheric pressure, wind speed, and solar radiation. This process consisted of the following steps: 1) selection of scenarios and other output settings; 2) mapping of CMIP6 output file and output settings; and 3) creation of future weather file from the morphed variables.

3.6.5 Appendix E

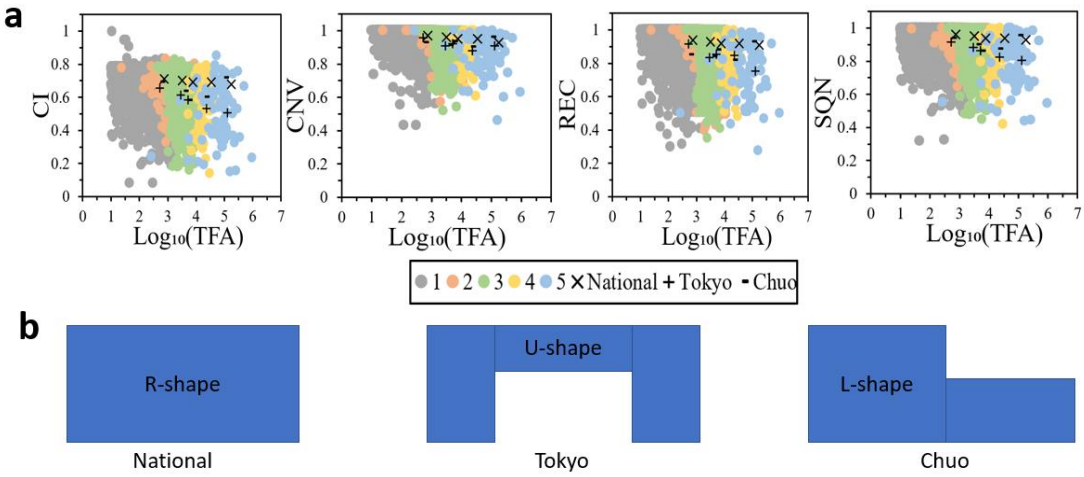

Figure E.1. Classification of building typologies for hotel stock across different scales: a) shape indices and (b) shape extraction of cluster 4 (Each dot represents the specified value of shape indices for each building, while different colors represent the representative cluster of stock).

3.7 Supplementary data

Supplementary data to this chapter can be found online at:
https://doi.org/10.1016/j.apenergy.2022.119536

4 Carbon neutrality assessment using bottom-up BSEM and BIPV model

4.1 Purpose

As per the Intergovernmental Panel on Climate Change (IPCC) Sixth Assessment Report (AR6), Sufficiency, Efficiency, Renewable (SER) framework enables the identification of key drivers and determinants to consider for the decarbonization of building stock (Cabeza et al. (2022)). The implementation of the SER framework requires the integration of a building energy model and BIPV potential estimation approach to consider a combination of efficiency measures, active and passive design strategies, and renewable distributed energy resources (DERs). Moreover, with the availability of geographic information system (GIS) data, some of the studies have recently focused on GIS models to develop UBEM that bridge a gap within conventional bottom-up models by adding spatial dimension (Ali et al. (2021); Dahlström et al. (2022)). This approach can integrate multiple building elements and transitional measures to not only improve the calculation accuracy but also capture the spatiotemporal dynamics of building energy use and carbon emissions. In terms of BIPV potential estimation, the solar potential assessment at high spatiotemporal resolution is highly challenging owing to computational and modelling complexities (Gassar and Cha (2021)). However, there is no evidence of studies capable to couple these approaches at a large scale either due to the infeasible choice of implementation method or the non-availability of a comprehensive database (Saretta et al. (2019); Chang et al. (2023)). Most of the previous studies mainly focused either on the energy-related characterization of building stock (Fonseca and Schlueter (2015); Mohammadiziazi et al. (2021); Zhang et al. (2022)) or the estimation of solar potential (Ghaleb and Asif (2022); Thebault et al. (2022)). Therefore, an integrated approach needs to be developed for the consideration of the SER framework for estimating the overall decarbonization potential of the commercial building stock.

To address these limitations, this chapter proposes a GIS-synthetic hybrid bottom-up simulation model coupled with a physical-based approach of BIPV potential estimation to consider the demand-supply synergy of commercial building stock at multiple scales. The main aim is to illustrate a coupled workflow that facilitated the homogenous use of a comprehensive GIS dataset to provide the necessary coordination of building stock interventions with renewable DERs at the multi-scale level, leading to further improvement in the methodological characterization to evaluate the carbon neutrality of commercial building stock. The decarbonization scenarios and strategies are further designed to demonstrate the applicability of the proposed coupled approach: (1) to determine the emission reduction potential of commercial buildings under different stock interventions and penetration of renewable DERs; and (2) to quantify the spatiotemporal evolution of energy demand and decarbonization potential across different scales.

4.2 Methodology

This study proposed a GIS-synthetic hybrid UBEM model (Perwez et al. (2022)) coupled with a physical-based approach of BIPV potential estimation (Cheng et al. (2020); Shono et al. (2023)) to incorporate a building-level energy model at a large scale that could evaluate the feasibility of carbon neutrality of commercial building stock at a multi-scale level. The proposed scheme is applied to the commercial building stock of the Tokyo region that involves 1593 postcode districts and 54 cities with a total floor area (TFA) of 195 million m^2. As illustrated in Figure 4-1, the framework utilized multiple steps to model the energy demand and supply of commercial building stock.

1. The UBEM model used a data-driven formulation to integrate geo-referenced and synthetic stock models. The building stock was initially segmented by using a GIS dataset that mainly consists of physical elements (geometric and non-geometric data). Thereafter, statistical technique (or machine learning) was applied to the sample dataset to assign technical elements, building systems and ESMs, to the building stock. After the development of a hybrid stock model, reference building models (RBMs) were developed and then dynamic building simulations were performed to obtain the energy demand patterns at the building-by-building level.
2. The BIPV potential estimation approach used a physical-based technique to develop a roof-façade framework that utilized an identical GIS dataset for calculating the point-based irradiance while considering the shading and sky view factor and then converted those irradiances to estimate solar energy potential at the building-by-building level.
3. After the development of the UBEM-BIPV coupled approach, decarbonization scenarios and strategies were constructed to consider active, HVAC systems, lighting and equipment retrofits, and passive, building envelopes and storages, design measures, and renewables.
4. The carbon neutrality assessment of demand-supply scenarios and strategies was performed at the spatiotemporal level by considering specified performance metrics.

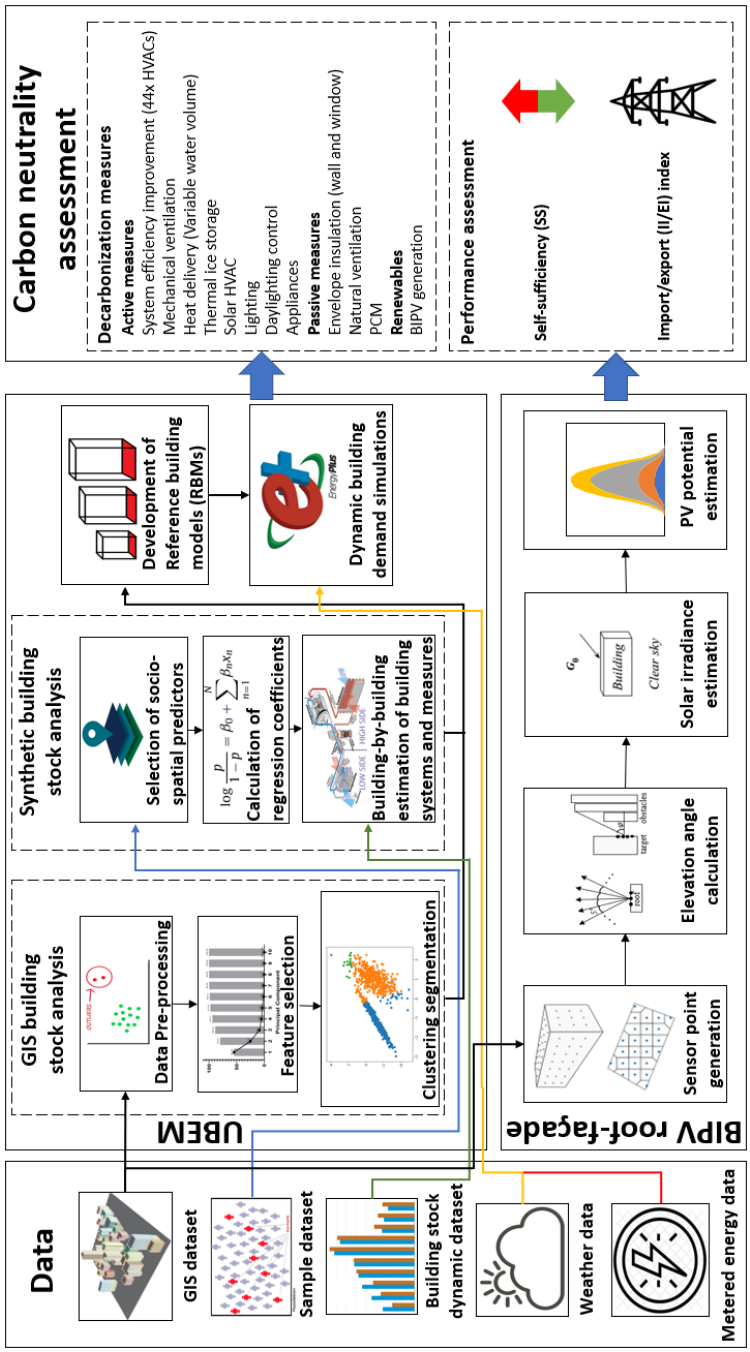

Figure 4-1. Schematic overview of UBEM-BIPV coupled approach.

4.2.1 UBEM model

A model for the estimation of building energy demand was developed based on the GIS-synthetic hybrid approach as explained in detail in Perwez et al. (2022). In the initial stage, a geo-referenced dataset consisting of physical elements was obtained and then, outlier detection and feature selection techniques were applied to the dataset to remove anomalies and obtain the most feasible

variables. After this, clustering segmentation was performed by using a multi-variate K-means algorithm. This process was further improved by applying different similarity (or distance-metric) measures to each cluster validation index and then, a unified clustering validity measure, cohesion-dispersion index (CDI), was proposed to find out the optimum number of clusters. Subsequently, the characterization of physical elements was performed by using a deterministic approach involving the computation of the weighted average of characteristics associated with each RBM.

Synthetic element modelling was performed to consider technical elements in the UBEM model. Initially, the socio-spatial predictors, building characteristics, demographics, heating degree days (HDD), and age-band classifications, are assigned to the sample dataset and then, the logit model is applied to obtain the coefficients of these predictors. The probability of each system classification (or ESMs) for a specific building within the stock was quantified by multiplying the obtained regression coefficients with real predictors of buildings. After obtaining the probabilities, the system alternatives were selected depending on the most probable alternative for a specific building. This resulted in the concurrent consideration of physical and technical elements for the development of RBMs. Moreover, the RBMs were developed by using an automated dynamic building simulation platform, which executed modelling stages through Python and R scripts to generate input files for EnergyPlus. The RBMs were validated considering metered energy data by using multivariate (or Bayesian) calibration technique and then further simulated to estimate the energy demand patterns of the commercial building stock.

4.2.2 BIPV potential estimation approach

A physical-based BIPV roof-façade framework is developed by extending a point-based sampling approach (Cheng et al. (2020)) to a higher spatiotemporal level and further validated with a simulation engine (Shono et al. (2023)), which consists of five steps that involve: (1) Data collection and transformation, (2) sensor point generation, (3) elevation angle calculation, (4) solar irradiance estimation, and (5) PV potential estimation.

1) Data collection and transformation: The data retrieval workflow included a collection of datasets related to 2D building footprints (TUDB, 2017), horizontal solar irradiance, and meteorological conditions (JMA, 2022). In data transformation, the 2D polygons obtained from the Tokyo City Planning Geographic Information System (2017) were extruded into 3D models by using Tokyo survey sample data (Ashie and Kagiya (2010)) that contains average floor height as per building type and usage.

2) Sensor point generation: The building rooftop and façade were discretized into point arrays by using a pre-defined sampling distance of 3 meters. Voronoi division was performed to obtain the representative area (3m x 3m) of the sensor point.
3) Elevation angle calculation: The surrounding region of each sensor point was divided into 72 directions by setting an angular interval of 5° and then, the maximum elevation angle was calculated for each angular interval. Moreover, to consider the effects of shadow, the maximum shaded angle θ_{max} was determined by obtaining the elevation of senor point z_p, distance and height of surrounding buildings.
4) Solar irradiance estimation: Solar irradiation, which mainly consists of direct and diffuse irradiance, was calculated while considering the effect of shading and sky view factor (see Appendix A). The solar constants and angles were calculated based on Mghouchi et al. (2016). For direct irradiance, the direct normal radiation obtained from the weather data and incidence angle were used to calculate the irradiance for each sensor point. For diffuse irradiance, the anisotropic diffuse model proposed by Perez et al. (1986, 1987) was used to calculate three diffuse components: (i) circumsolar, (ii) sky dome, and (iii) horizontal diffuse irradiances.
5) PV potential estimation: The equivalent power capacity was calculated by considering the conversion efficiency and nominal operating cell temperature (NOCT) model (Duffie and Beckman (2013)) to estimate the solar potential.

4.2.3 Decarbonization scenarios and strategies

The scenario analysis was performed to demonstrate the applicability of the proposed coupled approach to quantify the spatiotemporal evolution of energy demand and decarbonization potential across different scales. The scenarios considered the effect of building energy efficiency measures, penetration of renewable DERs, and carbon emission intensity (CEI) factors. To investigate the demand-supply synergy of commercial building stock at a multi-scale level, this study constructed three demand-side, base, potential, and electric scenarios that involve several decarbonization strategies, and multiple supply-side scenarios were selected based on key design and planning parameters of BIPV as shown in Table 4-1 and Table 4-2 respectively. In terms of demand-side scenarios, the base scenario was assumed to follow the current policy pattern with the non-adoption of new reduction measures. All the available decarbonization strategies, active and passive design measures, except electrification were adopted to estimate the maximum reduction potential in the potential scenario, whereas the electric scenario assumed electrification of heating and cooling source systems. On the supply-side, sensitivity analysis was performed based on the BIPV generation threshold, cell efficiency, and utilization factor to select the most feasible scenario in terms of the level of the penetration

rate of BIPV. The generation threshold is a criterion to determine the suitability of the BIPV installation area on the basis of annual incident solar radiation. The utilization factor is the ratio of the available rooftop area for PV installation to the total rooftop area of the building. For sensitivity analysis, nominal values of key design and planning parameters of BIPV were considered to estimate the variance in terms of yearly BIPV potential output on the basis of an individual parameter. This study employed a mono-crystalline PERC cell type with an efficiency of 20.43% whose specifications are listed in Table 4-3 (Jinko Solar, 2021). The range of cell efficiency is considered between 20% to 30% in order to consider the futuristic improvement of PV technology. Moreover, the different levels of CEI factors were used as per Tokyo Electric Power Company (TEPCO, 2016) and Tokyo Gas (TG, 2021) to quantify the carbon emissions of commercial building stock across different demand-supply scenarios as shown in Table 4-4.

Table 4-1. Description of decarbonization strategies at the demand-side.

Parameter	Base	Potential/Electric	
Envelope (Supplementary Table S1.1)	Current envelope standards remain unchanged	Additionally insulated to improve building performance standards	
Lighting (Supplementary Table S1.2)	Conventional lighting devices (fluorescent and incandescent lamps)	1. All lighting devices are replaced with LED. 2. Daylighting control is considered with indoor illuminance and limiting glare of 500 lux and 22 index respectively.	
Appliance (Supplementary Table S1.2)	Calibrated as per metered data	40% reduction from the base level	
System stock composition (Appendix Table B1 and B2)	Current system types remain unchanged	In Potential scenario, Absorption chillers are replaced with Solar heating and cooling.	In Electric scenario, all the systems are electrified by considering Elect-VRF and AHP for decentralized and centralized systems.
System efficiency improvement (Appendix Table B3)	Same as base level	Improvement in COP standards	
Ventilation and heat delivery measures (Appendix Table B4)	Same as base level	All possible combinations of these measures are considered	
Thermal Storages		For passive thermal storage, Phase change material (PCM) is considered, whereas in terms of active thermal storage, thermal ice storage is coupled either with an air-source heat pump (AirS-HP) or Comb-EG.	

Table 4-2. Sensitivity analysis of key design and planning parameters of BIPV.

Parameter	Units	Roof	Façade
Cell efficiency (%)	0-1	**20**, 25, 30	
Generation threshold (kWh/(m^2·year))	1-0	**No**, 400, 600, 800, 1000	
Utilization factor	0-1	0.1, 0.3, 0.5, 0.75, **1**	**1**

Note: Bold values indicate nominal values.

Table 4-3. Specifications of BIPV module.

Parameter	Description
Cell type	Mono-crystalline PERC
Dimensions (mm)	1855 x 1029 x 30
Maximum power (W)	390
Cell efficiency (%)	20.43
Temperature coefficient of maximum power (%/˚C)	-0.35
NOCT (˚C)	45 ± 2

Table 4-4. Overview of carbon emission intensities (CEI) for different fuels.

Fuel	Baseline	2030
Electricity (kgCO_2/kWh)	0.47 (TEPCO, 2016)	0.25 (MOE, 2016)
Gas (kgCO_2/Nm^3)	2.21 (TG, 2021)	

4.2.4 Carbon neutrality assessment

In this study, the performance assessment of these scenarios was performed at the static and dynamic temporal level by using two metrics: self-sufficiency (SS) and import/export index (II/EI) (Sartori et al. (2012); Ala-Juusela et al. (2016)). These metrics were selected that fit the scope to be utilized with the further consideration of more physical energy infrastructures, electric vehicles and storages, which lead to load shifting and flexibility. The SS is formulated to estimate the percentage of energy demand met by renewable energy at annual temporal resolution. SS varies between 0 and 1, with a value equal to 0 and 1 depicting all annual energy demand needs

to be imported and all annual energy demand is met by local renewable energy supply respectively. The II/EI index is developed to assess how well the energy demand and supply are balanced at an hourly temporal resolution that provides quantification of excess or deficit local renewable supply relative to energy demand. II/EI index equal to 0 indicates that energy demand is met by local renewable energy at a particular hour, whereas a positive (or export index (EI) value of the index (greater than 0) indicates the amount of hourly surplus of local renewable supply to the energy demand at that particular hour and a negative value (or import index (II)) of the index (varies between -1 and 0) indicates the amount of hourly deficit of energy demand to the local renewable supply at that particular hour. The SS and II/EI indices were expressed as:

$$SS = \frac{E_{s,a}}{E_{d,a}} \qquad 4\text{-}1$$

$$II/EI = \frac{E_{s,hr} - E_{d,hr}}{E_{d,hr}} \qquad 4\text{-}2$$

where $E_{s,a}$ and $E_{s,hr}$ are the BIPV supply at annual and hourly temporal resolution respectively, and $E_{d,a}$ and $E_{d,hr}$ is the total energy demand of the building stock at annual and hourly temporal resolution respectively (whereas the annual aggregated units are specified in terms of MJ (or TJ or PJ) and the hourly units are specified in terms of MW). Hence, larger SS and EI are both desired.

4.3 Results

4.3.1 Building stock analysis

This analysis presents the results related to the development of RBMs based on the geo-referenced and sample datasets. The data-driven approach involving data pre-processing and segmentation was performed on the geo-referenced dataset resulting in 17 RBMs on the basis of physical elements (see Appendix C). Furthermore, the logistic regression technique was applied to the sample dataset to assign technical elements to each building within the stock. As a result of the hybrid approach, the development of 17.2 million (17 clusters × 3 construction types × 6 vintages × 5 system age-band × 256 ESMs combination × 44 HVAC systems) RBMs was possible. To reduce the number of RBMs, aggregated criteria combined buildings that exhibited the same classification in terms of the building size, construction type, age band, ESMs, and HVAC systems. For example, the aggregated criteria reduced 91,299 actual buildings in the Tokyo region to 7,145 RBMs for the base scenario. In the case of other scenarios, this specified criterion reduced models to 1,280 and 440 RBMs for potential and electric cases, respectively.

Figure 4-2 shows the composition of commercial building stock for different scenarios. In terms of building usage and vintage, it is observed that the office segment constitutes a major proportion of floor area with higher built-up density, whereas the average age-band of existing stock is 1990 that estimated to transition to 100% highest insulation level (or 2010 level) for potential and electric scenarios. The composition of the heat source of HVAC systems showed that the proportion of AHP increased from 6% in the base case to 31% in the electric scenario, whereas the potential scenario constitutes 10% of solar heating and cooling systems with the replacement of absorption chillers. The adoption of ventilation measures showed the aggressive deployment of ESMs in potential and electric scenarios as compared to the base case.

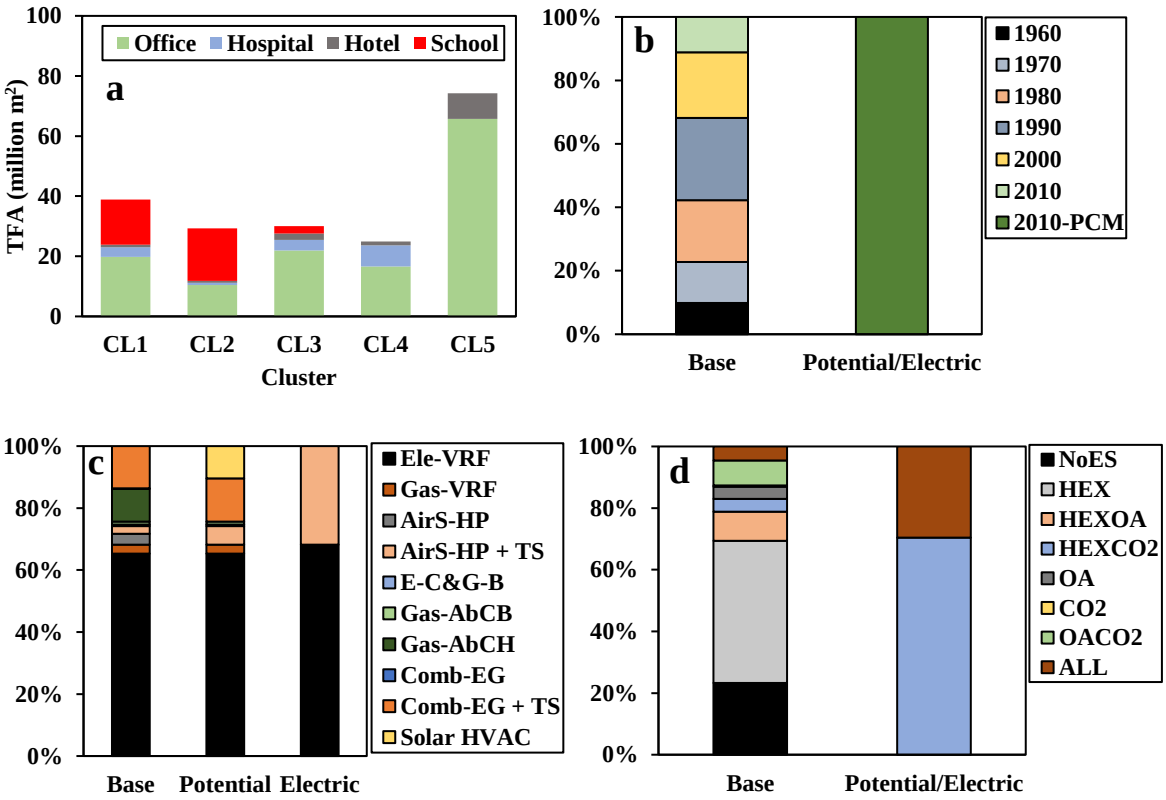

Figure 4-2. Composition of commercial building stock for different scenarios: (a) building usage (Appendix C); (b) envelope; (c) HVAC system heat source (Appendix Table B1); and (d) ventilation measures (Appendix Table B4).

4.3.2 Aggregated evaluation

1) Energy demand

To validate the UBEM model, the archetype and aggregated-level validations were performed, as explained in detail in Perwez et al. (2022), that showed the model estimate agreed well with a difference of 10.2% and -1.9% in terms of the coefficients of variation for the root mean square

error (CV(RMSE)) and normalized mean bias error (NMBE) respectively. Figure 4-3(a) shows the cumulative frequency distribution of energy use intensity (EUI) across the commercial building stock. The EUI range varied from 126 to 6321 MJ/(m²·year) with a mean value of 1558 MJ/(m²·year). In terms of segment-wise, the EUI pattern shows left-side skewness due to school buildings, whereas long-tail distribution representing higher EUI levels was mainly due to the hotel and hospital buildings. Figure 4-3(b) shows the average hourly energy demand of commercial building stock at the regional level and to compare load profiles, the daily load factor is calculated as the ratio between the average daily demand and daily peak demand. As observed, the peak demand occurred in the summer month for electricity[1], whereas gas peak demand happened in the winter month. In terms of peak demand analysis, it is observed that a higher load factor is observed in spring which depicts a better utilization rate, whereas a lower load factor is observed in winter due to higher maximum peak demand for heating.

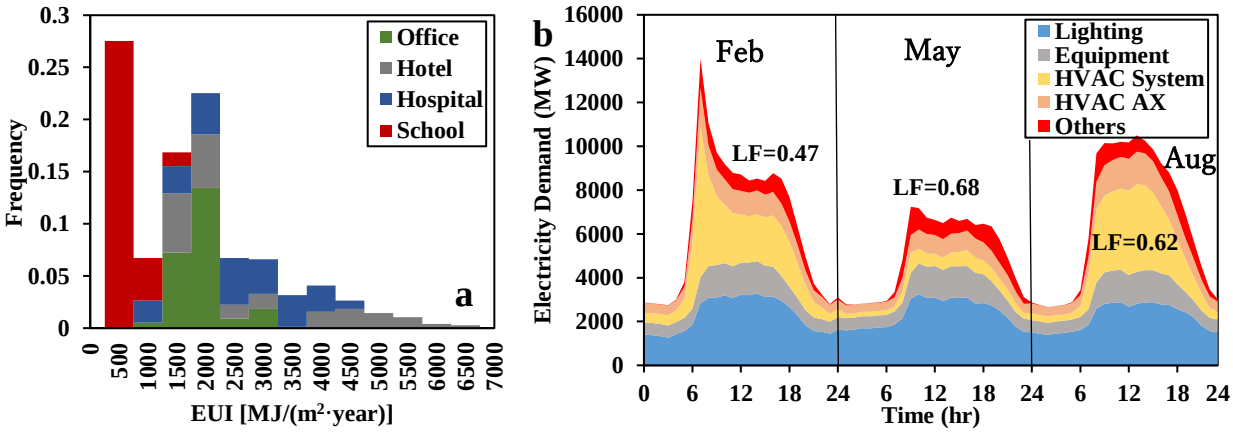

Figure 4-3. (a) Cumulative frequency distribution of EUI across the commercial building stock; (b) Average hourly regional electricity demand of commercial building stock.

2) Reduction potential

At a regional level, the primary energy consumption of commercial building stock is estimated to be 316 PJ/year in the base case. The incorporation of multiple measures resulted in a reduction potential of 49% with a significant decrease in gas consumption by 68% to 78% as shown in Figure 4-4. In terms of end-use, space heating and cooling demand were reduced by 68% which implied the potential impact of active design strategies on the demand side. Figure 4-5 shows the average hourly regional electricity and gas demand considering seasonal changes and the impact of various measures on commercial building stock. The incorporation of multiple measures also resulted in a peak average ratio to decrease by 18% and 65% for electricity and gas respectively.

[1] An unnatural peak observed in the winter month due to stochastic synchronization of occurrence of occupancy events with the HVAC system operation schedule (Yamaguchi et al. (2022)).

The scale of the change of gas demand in the electric scenario was not significant in comparison to the potential scenario due to a large portion of heat sources using gas boilers being shifted to solar HVAC in the potential scenario. Consequently, the dissemination of electrification of exterior equipment (or for cooking purposes) was not considered in the electric scenario. Moreover, the monthly values during winter months were significantly reduced when system efficiency improvement and highly insulated envelopes were implemented, whereas the upgradation of lighting and appliances resulted in the reduction of energy demand during summer months.

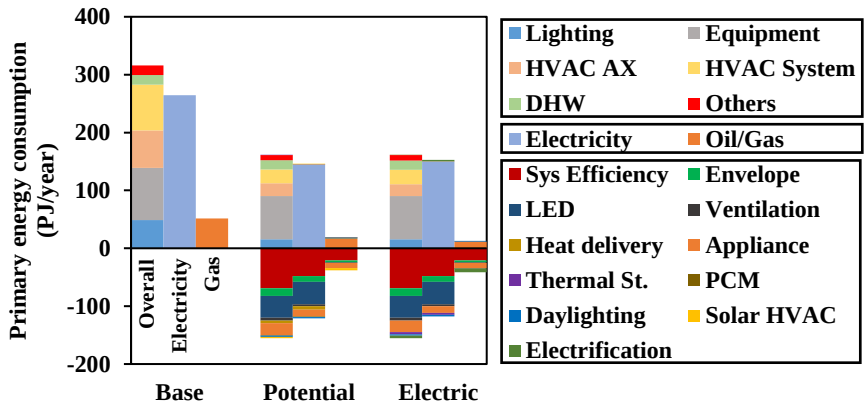

Figure 4-4. (a) Annual primary energy consumption of commercial building stock across different pathways (Note: negative values indicate the reduction induced by each measure between the transition of pathway).

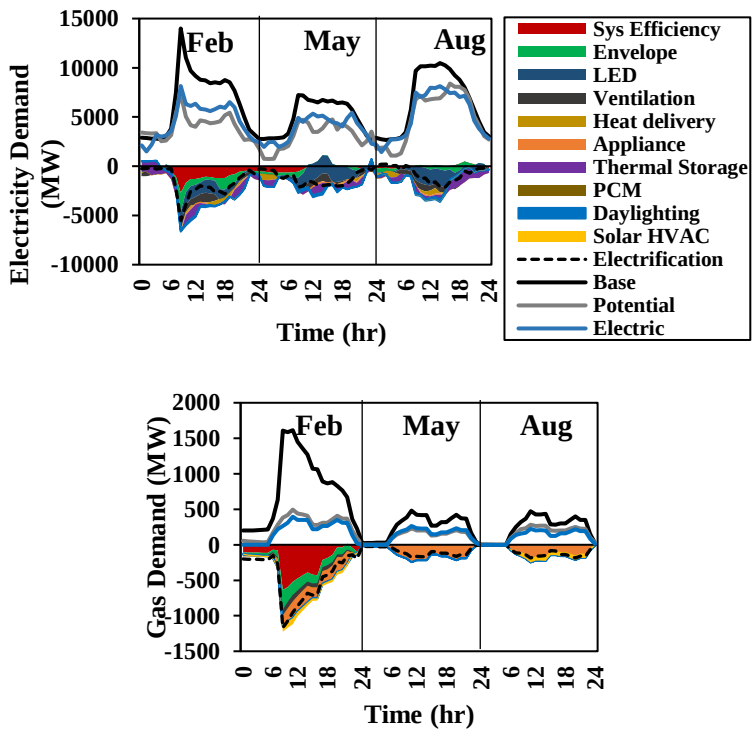

Figure 4-5. Average hourly regional electricity and gas demand considering seasonal changes and the impact of various measures on commercial building stock (Note: negative values indicate the reduction induced by each measure between the transition of pathway).

3) BIPV potential estimation

To consider different levels of the penetration rate of BIPV on the supply-side, key design and planning parameters, PV generation threshold, cell efficiency, and utilization factor, were considered to perform the sensitivity analysis for selecting the most feasible supply scenarios. Figure 4-6 shows the sensitivity analysis of key design and planning parameters of BIPV on yearly supply potential. The cell efficiency shows a strong correlation with PV potential in comparison to other parameters. Moreover, the PV rooftop has a dominant role in the energy generation potential of BIPV. The roof-façade pairwise analysis shows that the utilization factor is more critical in the deployment of PV rooftop, whereas the deployment of PV façade is more sensitive to generation threshold criteria. Overall, it is found that generation threshold criteria of 1000-400 kWh/(m^2·year) for roof-façade and 30% utilization of rooftop are selected in terms of deployment suitability and yearly potential output. Hence, two BIPV supply strategies are considered to further perform demand-supply assessment: (1) 1000 kWh/(m^2·year) as PV roof threshold and 400 kWh/(m^2·year) as PV façade threshold, 20% cell efficiency and 30% utilization factor (S1), and (2) No roof-façade threshold, 30% cell efficiency and No utilization factor (S2).

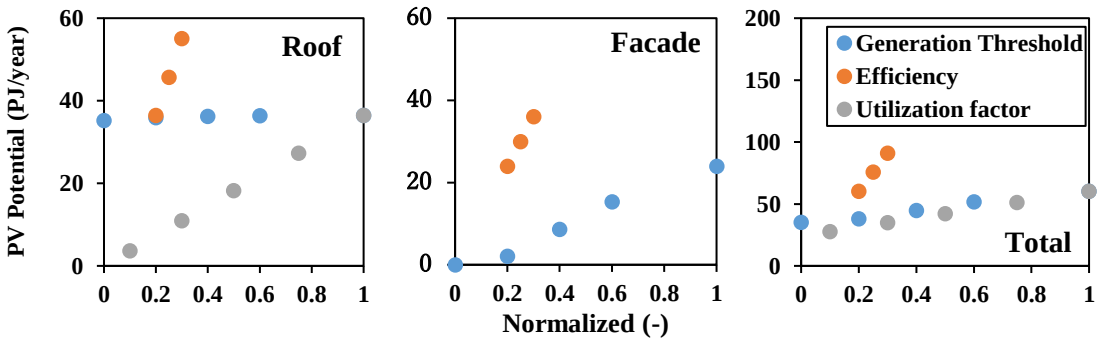

Figure 4-6. Sensitivity analysis of key design and planning parameters of BIPV on a yearly supply potential.

Figure 4-7 shows the composition and annual generation of BIPV for different supply strategies. The installed capacity of BIPV increased from 78 to 243 million m^2 area in S1 and S2 strategies respectively, which showed a four-fold increase in the overall potential of yield area. The area of the roof accounted for 23% to 26% of the total installed capacity, while the PV generation accounted for 42% and 60% in S1 and S2 strategies respectively. This indicated the high yield of PV rooftop that signify the importance of utilization of roof area in a high-density urban environment. Moreover, the duration curve shows a considerable difference in supply peak with a steep gradient observed in the overall potential estimation (or S2) strategy.

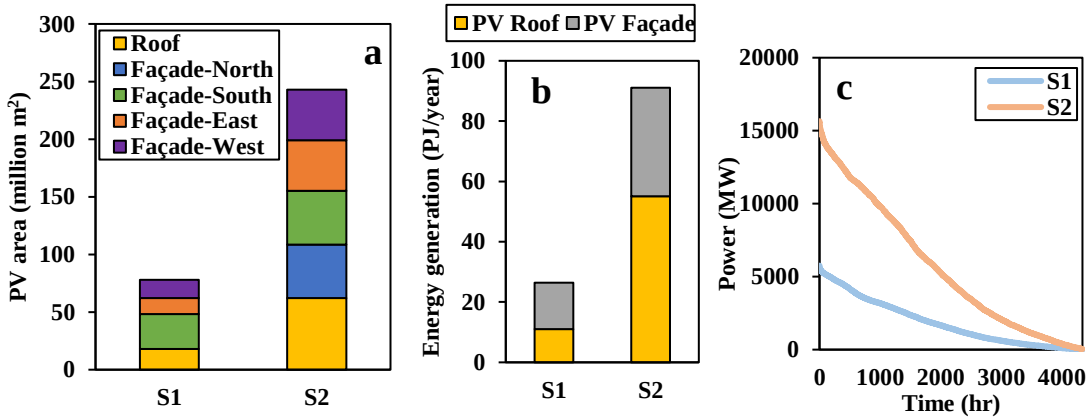

Figure 4-7. (a) Composition of BIPV module area for different supply strategies; (b) BIPV annual generation for different supply strategies at the regional level; and (c) load duration curve of different supply strategies.

4) Carbon neutrality assessment

The annual energy balance and emission reduction potential of commercial building stock across different demand and supply-side strategies are shown in Figure 4-8. At a regional level, SS improved from 0.16 to 0.63 with 2.5 times improvement among both scenarios that show higher utilization of BIPV yield higher SS. In terms of emission reduction potential under different intensities (CEI), it is found that the annual CO_2 emissions decreased by 84% with the adoption of ambitious demand-supply strategies illustrating that carbon neutrality of the commercial building stock requires further concrete measures. Moreover, the demand-side efficiency measures resulted in the largest emission reduction potential, ranging from 10.3 to 15.4 $MtCO_2$/year reduction, whereas the share of BIPV ranges from 2.2 to 10.1 $MtCO_2$/year reduction.

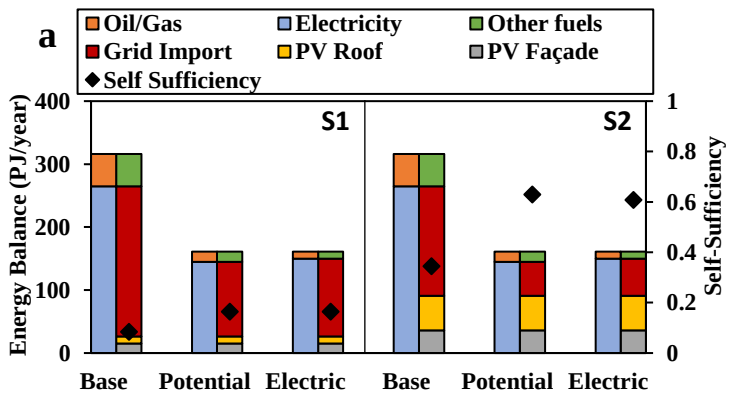

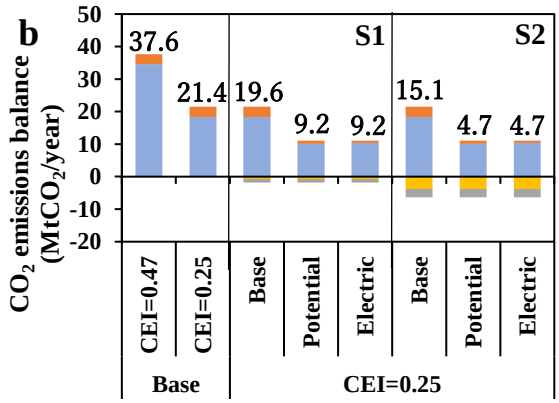

Figure 4-8. Annual energy balance (a) and emission reduction potential (b) of commercial building stock across different demand and supply-side strategies at the regional level.

As per dynamic energy balance analysis, as shown in Figure 4-9a, it is observed that the peak value of grid import reduces by 21% and 59% with the adoption of ambitious demand-supply strategies in the summer and winter seasons respectively, whereas the time-duration of grid import occurred at both day-time and night-time. The peak value of grid export increased manifold with maximum resource utilization of BIPV, whereas the time-duration of grid export mostly occurred during the daytime. Moreover, the difference in onsite consumption is mainly due to the difference in PV generation and demand levels. In terms of performance assessment (Figure 4-9b), the highest total number of hours of grid export is observed during the spring season, whereas EI improved up to 2.43 at noon time with the adoption of ambitious demand-supply strategies. Moreover, Fig. 8c shows the load duration curve of commercial building stock across different demand and supply-side strategies at the regional level. The negative net load duration increased from 0.8% (Base-S1) to 23% (Potential-S2) with the total number of hours with grid export increasing from 78 hrs to 2020 hrs in the year respectively.

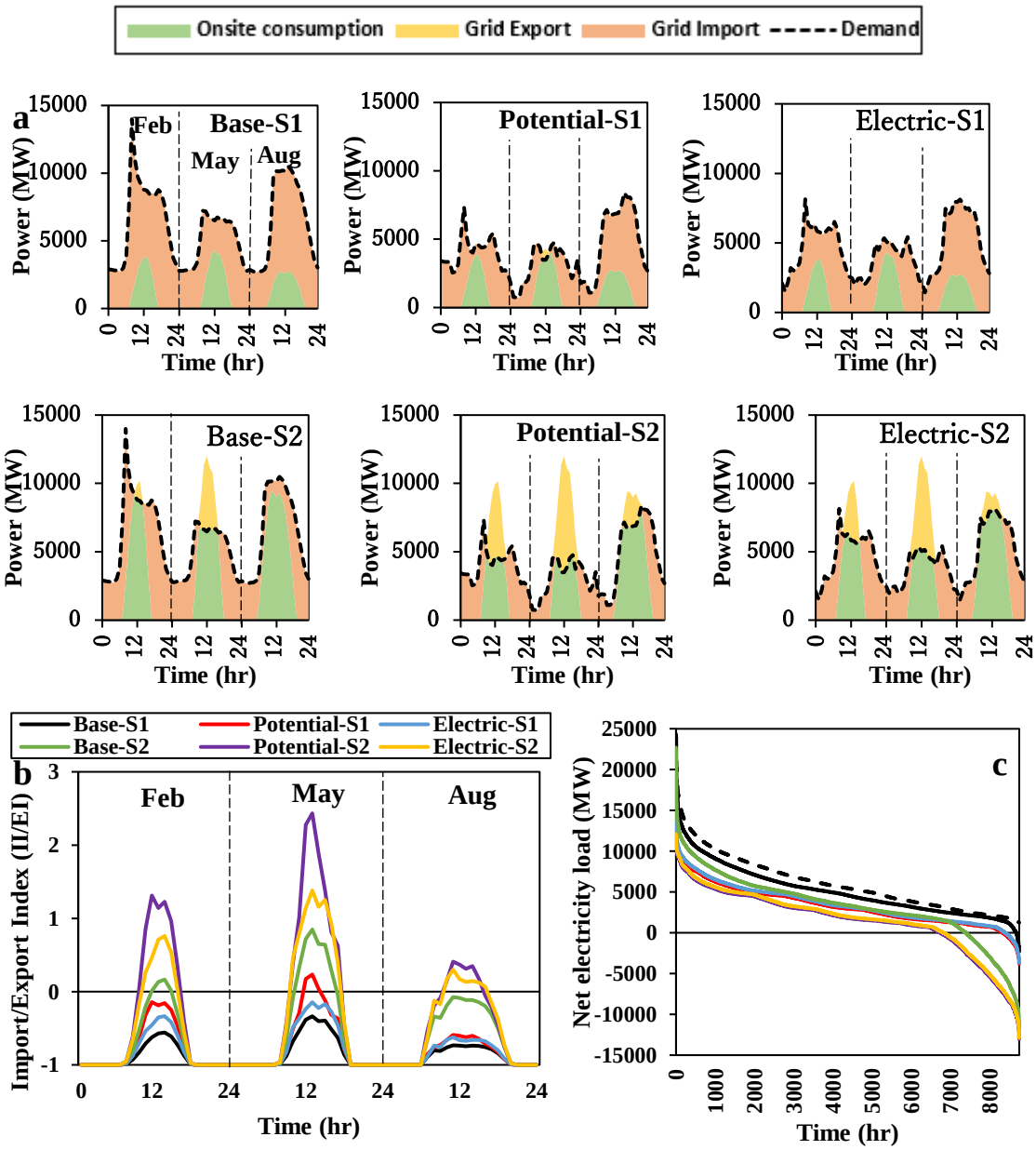

Figure 4-9. (a) Average monthly dynamic energy balance; (b) performance assessment; and (c) load duration curve of commercial building stock across different demand and supply-side strategies at the regional level.

4.3.3 Multi-scale evaluation

1) Energy demand

Figure 4-10 shows the scale-level distribution of EUI and the average daily load factor. In terms of variation in energy demand, it is observed that the larger the description of a scale, the lower the EUI. This was because of varying building stock compositions that exhibit energy hot spots in a few districts of each city. In terms of peak demand analysis, it showed a significant deviation

of load factor that varied between the range of 0.22 to 0.82. This also demonstrated higher variability of load factor with the transition from larger to smaller scale, whereas peak damping is observed at a larger scale. Moreover, the load factor seems to be more sensitive to seasonal changes resulting in more deviation and lower load factor in the winter season that demonstrates the pronounced effect of heating demand on peak load.

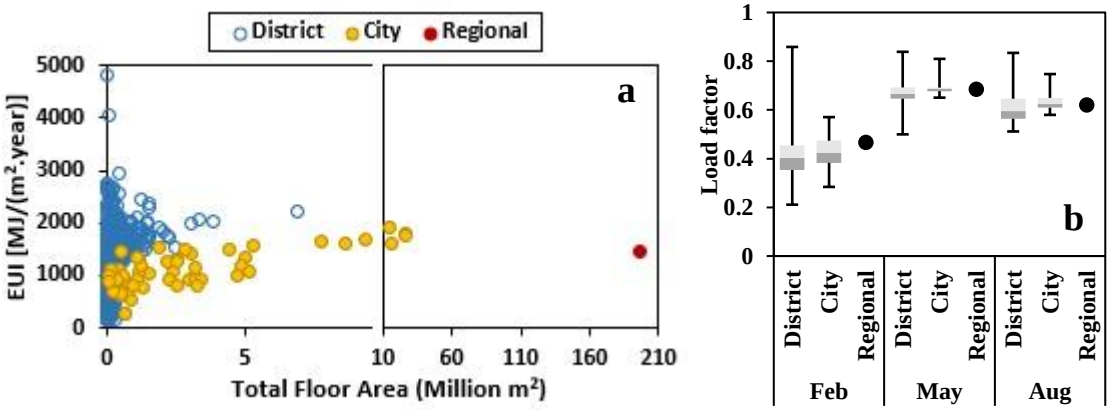

Figure 4-10. (a) Distribution of EUI; and (b) Comparison of average daily load factor across different scales.

2) Reduction potential

Figure 4-11 shows the spatial distribution of primary energy consumption at the city scale for different pathways. The primary energy consumption has a strong spatial dependence with higher variance in dense urban areas, whereas the spatial distribution for electric and potential scenarios as expected are nearly identical due to the maximization of building efficiency. The distribution of primary energy consumption of the districts and cities indicated more skewness and stacking with the incorporation of demand-side efficiency measures (see Supplementary Fig. S1). The percentage of districts ranged lower than 50 TJ/year increased from 59% in the base case to 71.6% and 73.6%, whereas in the case of cities, the primary energy consumption lower than 2000 TJ/year increased from 53% in the base case to 73% and 75% for electric and potential scenarios respectively.

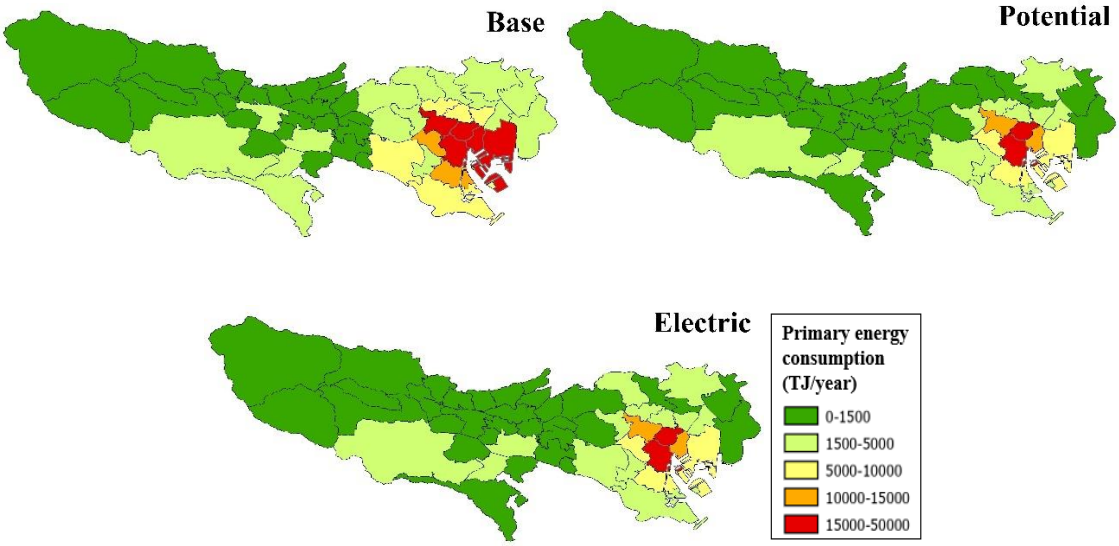

Figure 4-11. Illustrative city scale map of the spatial distribution of primary energy consumption for various pathways.

The measure-by-measure comparison, as shown in Figure 4-12, showed that the most impactful decarbonization measures are system efficiency improvement, and the upgradation of lighting and appliances that varies across the scales. In contrast, PCM and daylighting control caused negligible impact due to internal heat gain and loss effects. The active-passive measures pairwise comparison shows that only 10% reduction potential was attributed to passive design measures, whereas 90% reduction potential is due to active design measures. This demonstrates that simply focusing on passive design measures, envelope insulation, and natural ventilation, is not enough to decarbonize commercial building stock.

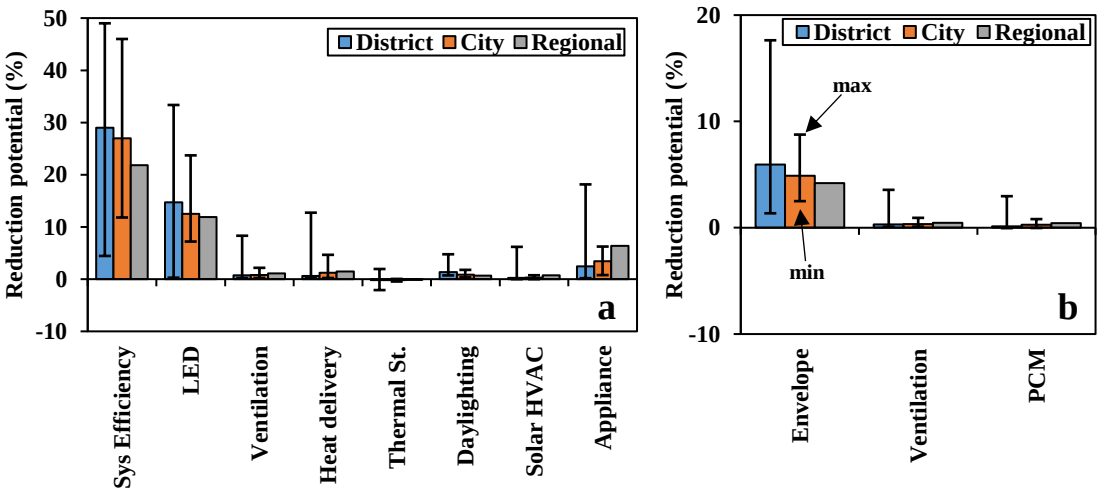

Figure 4-12. Reduction potential of demand-side measures across different scales: a) Active; and b) passive measures.

3) BIPV potential estimation

Comparing different BIPV supply strategies at various scales, it is found that the total PV potential of districts ranged greater than 50 TJ/year increased from 8.9% to 34.7%, whereas in the case of cities, the total PV potential greater than 1000 TJ/year increased from 20.4% to 51.8% for S1 and S2 supply scenarios respectively (see Supplementary Fig. S2). Figure 4-13 shows the temporal variation of BIPV generation across different scales. The maximum absolute deviation (MAD) is also shown on both sides of the generation pattern to indicate the diurnal variability across the number of districts and cities. The total BIPV potential changes in the order of magnitude of 29 to 54 with the variation of scale that presents a favourable transitional decarbonization supply choice to incorporate BIPV at a large scale. The highest electricity yield is observed in spring with generation variability across the whole year due to changes in climate conditions. In terms of roof-façade pairwise hourly analysis, it is observed that the PV façade gives an added value by providing a similar and steady supply during the period of low potential output (early morning or late afternoon) in comparison to the rooftop. The high potential supply period increases with the relaxation of threshold and utilization factor constraints. Overall, this demonstrates the dominant role of maximum resource utilization of building roof and façade on total BIPV potential.

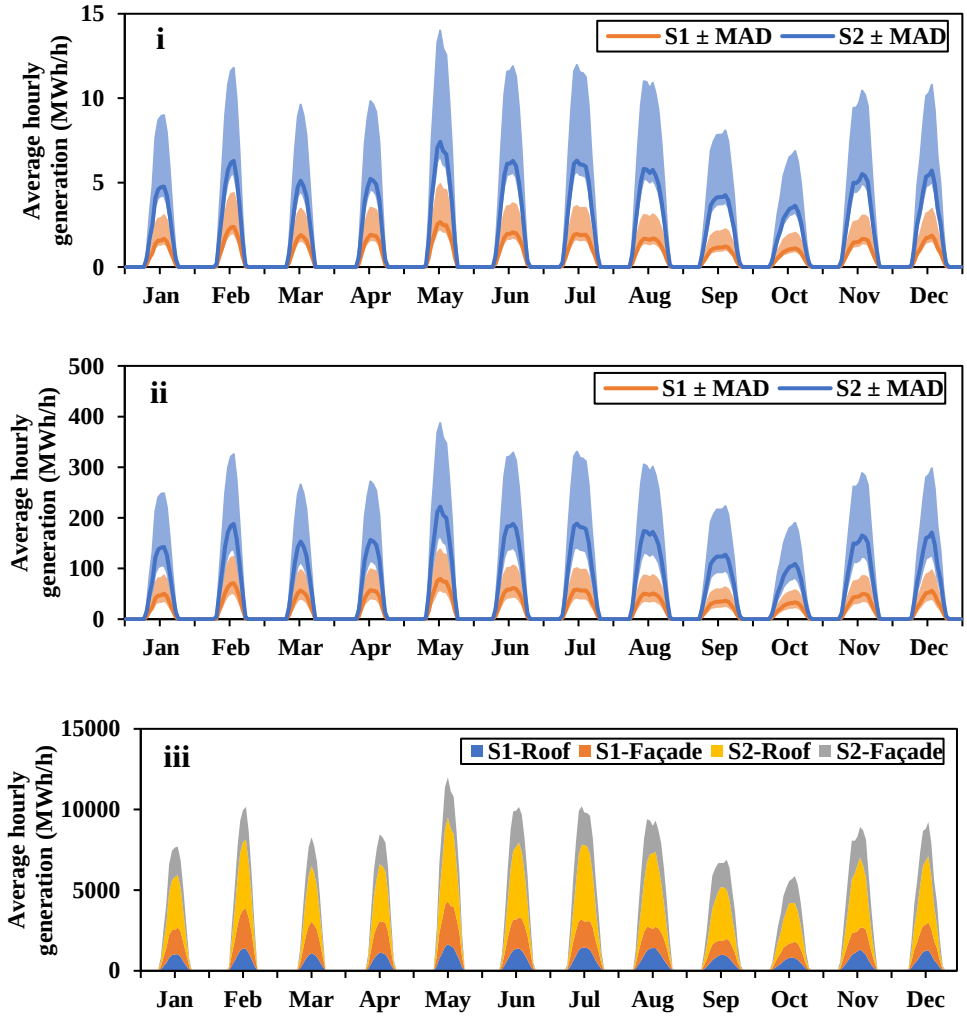

Figure 4-13. Average hourly BIPV generation across different scales: i) District; ii) city; and iii) regional level (showing the amount of added potential with the change in integration level).

4) Carbon neutrality assessment

As per the scale-bounded emission reduction potential analysis, as shown in Figure 4-14, it is observed that the annual carbon peak reduced by 59.4% and 61.5% with the adoption of demand-side efficiency improvement and integration of BIPV at district and city scales respectively. The improvement of CEI resulted in a further reduction of the annual carbon peak from the range of 0.72-1.74 $MtCO_2$/year to 0.40-0.97 $MtCO_2$/year at the district scale, whereas the annual carbon peak reduced from the range of 2.24-5.55 $MtCO_2$/year to 1.24-3.09 $MtCO_2$/year at city scale. In the Base-S1 scenario, the annual carbon emissions of most districts and cities that presented 40% of the stock TFA were below 0.12 and 1.67 $MtCO_2$/year, whereas in the Electric-S2 scenario, the annual carbon emissions of most districts and cities that presented 40% of the stock TFA were

below 0.04 and 0.5 $MtCO_2$/year respectively. This highlights the significant spatial variation of annual emission reduction potential that depicted the analytical capability of the UBEM model.

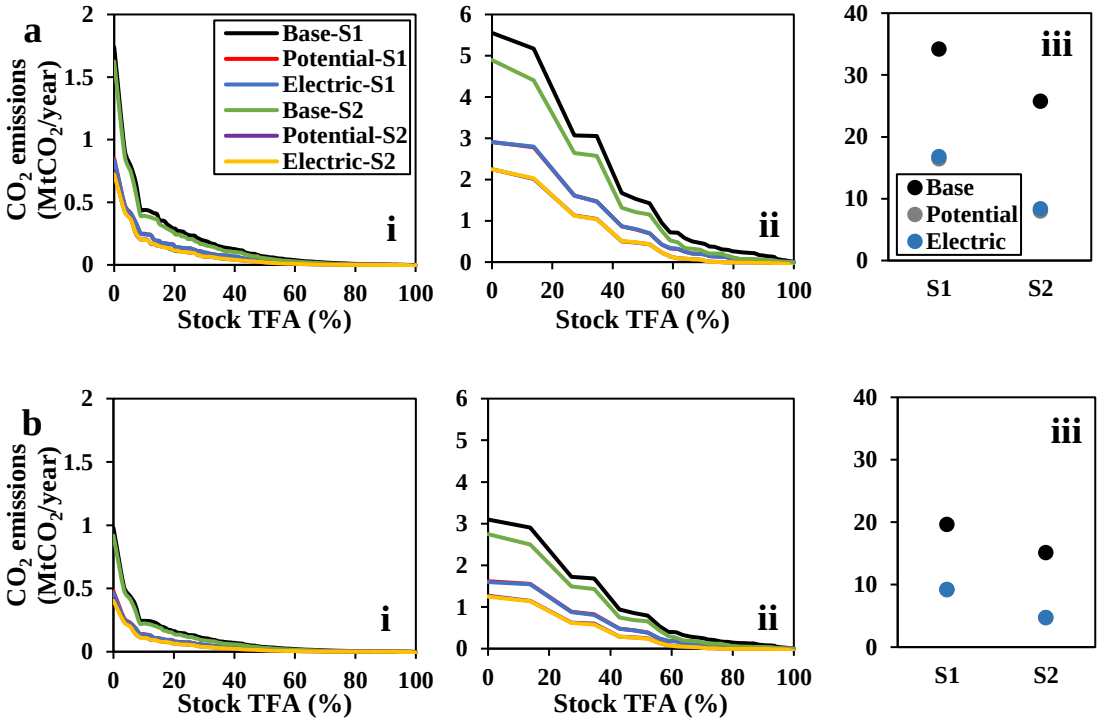

Figure 4-14. Annual emission reduction potential under different intensities, (a) CEI=0.47 and (b) CEI=0.25, for different scales: i) District; ii) city; and iii) regional level.

Figure 4-15 illustrates the spatial distribution of SS at the city scale for various demand-supply pathways. In the Base-S1 scenario, the SS of most cities were below 0.4, and in some cities, the SS were above 0.6, whereas in the Electric-S2 scenario, the SS of most cities were above 1, and in some cities, the SS were below 0.4. This highlights the significant spatial variation of SS with the adoption of demand-side efficiency improvement and integration of BIPV.

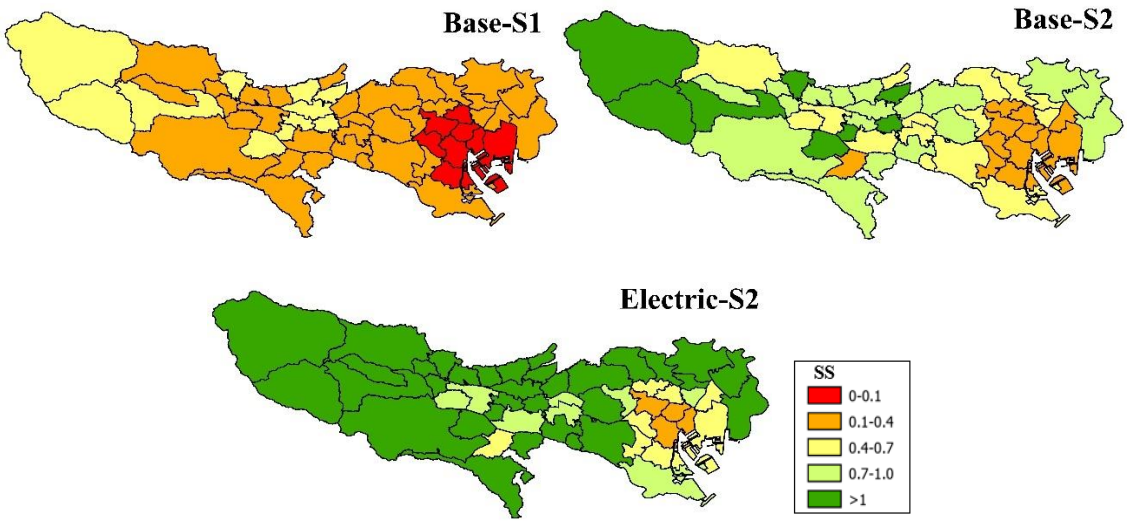

Figure 4-15. Illustrative city scale map of the spatial distribution of SS for various demand-supply pathways.

The scale-bounded comparison, as shown in Figure 4-16(a), shows that the ambitious demand-supply strategies, Potential-S2 or Electric-S2 scenarios, resulted in sharp skewness of SS percentage at the building-by-building level. Among the different demand-supply strategies, SS greater than 1 increased from 14.4% in the Base-S1 scenario to 70.1% in the Potential-S2 scenario at the building-by-building level. At other scales, 28% of districts transition into net positive energy districts, whereas, at the city scale, 22% of cities become net positive energy cities with the implementation of ambitious demand-supply strategies. In terms of average performance assessment (Figure 4-16b), the grid indexes showed similar temporal patterns with the variation of the magnitude across the scale. In the S1 scenarios, BIPV generation is mostly self-consumed at the regional level with maximum time-duration of grid import happening even in daytime, whereas most of the districts and cities showed much higher grid export in the daytime with the peak EI at 1.12 and 0.82 respectively. Meanwhile, the implementation of the ambitious demand-supply strategies, S2 scenarios, resulted in maximum time-duration of grid export in the daytime with the peak EI reaching up to 4.42, 3.92 and 2.43 for districts, cities and regional levels.

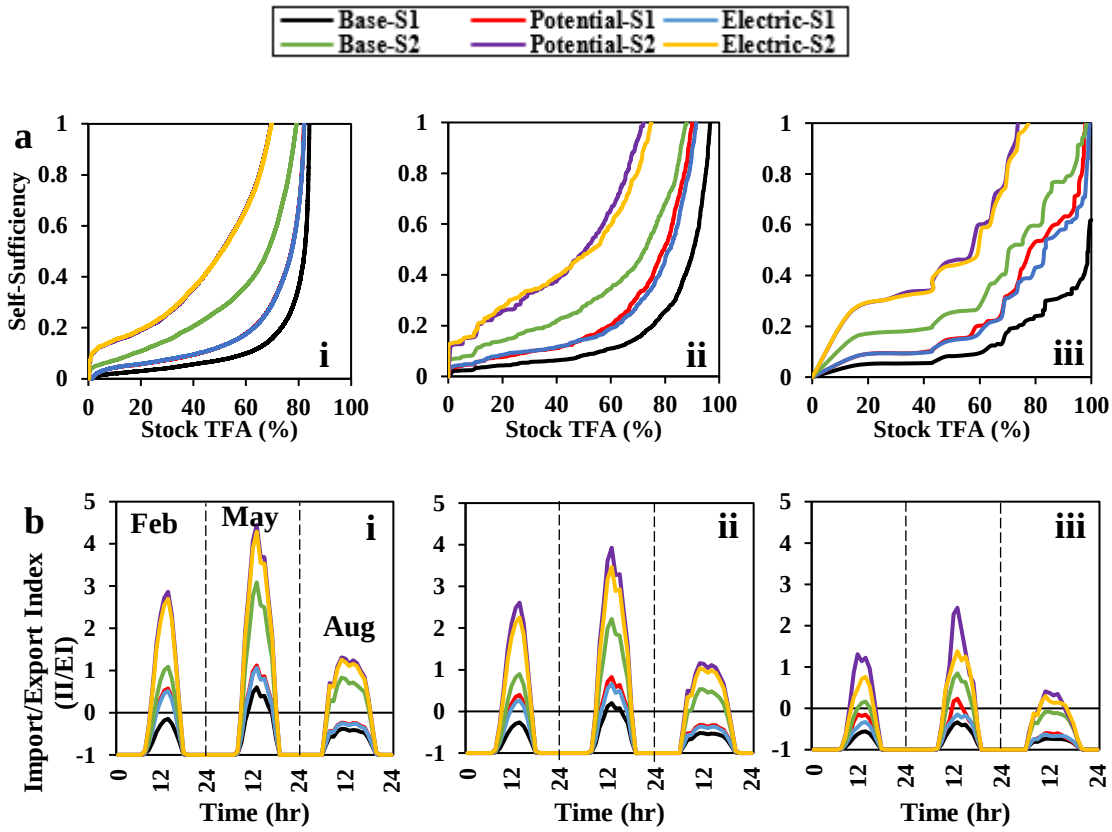

Figure 4-16. (a) Self-sufficiency analysis of commercial building stock across different scales: i) Building-by-building; ii) district; and iii) city level; (b) average dynamic performance assessment of different demand and supply-side strategies across different scales: i) District; ii) city; and iii) regional level.

4.4 Discussion

4.4.1 Development of UBEM-BIPV coupled approach

With the development of the proposed hybrid UBEM workflow, the model builds upon the building-level data obtained from GIS to facilitate consideration of a series of geometric and non-geometric parameters, and further utilized synthetic element modelling to assign technical elements to the commercial building stock. As shown in Section 4.3.1, this multi-stage process enhanced the analytical capability of the model by concurrently incorporating physical, technical, and socio-behavioral factors within a commercial building stock. Moreover, the integration of the physical-based approach of BIPV potential estimation resulted in the calculation of the point-based solar irradiance at a range of spatial scales with reduced computational time. From a practical implementation process, this further informs the stakeholders about the varying aspect of the adoption of BIPV technologies in the urban environment. Overall, this UBEM-BIPV coupled scheme enables the coordination among different methodological characterizations to

adequately manage the degree of complexity and modelling resolution for the energy transition of the commercial building stock.

4.4.2 Relationship between decarbonization strategies

In terms of reduction potential, the incorporation of multiple active and passive design measures resulted in a reduction potential of 49% with a significant decrease in gas consumption by 68% to 78%. The comparison of the reduction potential of these design measures in commercial building stock shows that only 10% reduction potential was attributed to passive design measures, whereas 90% reduction potential is due to active design measures. This demonstrates that simply focusing on passive design measures, envelope insulation, and natural ventilation, is not enough to achieve carbon neutrality in commercial buildings. Thus, the concurrent consideration of active and passive design measures needs to be investigated when performing a carbon neutrality assessment of commercial building stock. Moreover, it is worth noting that when all the decarbonization strategies are simultaneously deployed, it is found that the annual CO_2 emissions decreased by 84% with the simultaneous implementation of all the measures illustrating that carbon neutrality of the commercial building stock requires further concrete measures.

4.4.3 Scalability

Considering the evaluation capabilities, Section 4.3.3 shows that the differences in the demand reduction and BIPV potential exist across different scales due to varying structural and system stock composition, and urban morphological characteristics. However, the research gap of coupling the UBEM-BIPV scheme exists in the previous multi-scale studies that either only established UBEM models for a different scope (like residential building stock) (Nutkiewicz et al. (2018); Yang et al. (2022)) or focused only on estimating BIPV potential in an urban environment (Cheng et al. (2020); Liu et al. (2023)). This implies that the proposed coupled scheme identifies various drivers and determinants to better understand the mechanisms and conditions leading to different demand and supply levels across the scale. Additionally, the carbon neutrality assessment of commercial building stock (Section 4.3.3(4)) indicates that the maximum co-benefit of demand-side efficiency improvement and integration of BIPV is observed at building-by-building level with 70% of buildings has SS greater than 1 while at other scales, 28% and 22% of districts and cities transition into net positive energy districts and cities respectively. This spatial imbalance is mainly due to typological utilization constraints and diverse functionalities of commercial buildings. Therefore, those studies focusing on the optimization of a single building model result in insignificant or redundant findings at a larger scale.

4.4.4 Future work and limitations

Although the developed coupled scheme demonstrated improved adequacy at the multi-scale level and could be further applied to different regions, there are still some limitations that need to be addressed. An auto-calibration framework needs to be developed that can transform the existing multi-scale UBEM model into a scalable model, ensuring transparency at a granular level by providing a comprehensive insight into uncertainties at the spatial level. In a physical-based BIPV potential estimation approach, an anisotropic hourly diffuse radiation model is used without considering the ground-reflected irradiance that needed to be involved. Moreover, future work will be extending this GIS model to perform techno-economic analysis of physical energy infrastructure, electric vehicles, storages, and synthetic gas generation, for assessment of emerging technologies, and in terms of modelling capabilities, lifestyle changes (teleworking and relaxation of room set point temperature) and effect of socioeconomic factors on the implementation of decarbonization strategies need to be considered.

4.5 Conclusion

This study presents a GIS-synthetic hybrid UBEM model coupled with a physical-based approach of BIPV potential estimation to incorporate a building-level energy model at a large scale that could further evaluate the feasibility of carbon neutrality of commercial building stock at a multi-scale level. As a case study, the proposed coupled scheme is applied to the commercial building stock of Tokyo to evaluate the cofound influence of active and passive design measures, and BIPV on the overall decarbonization potential. Results show that the annual CO2 emissions can be reduced by 84% with the simultaneous implementation of all the measures. The measure-by-measure comparison showed that the most impactful demand-side efficiency measures are system efficiency improvement, and the upgradation of lighting and appliances while passive design measures only contribute a 10% reduction potential which is not enough to achieve carbon neutrality in commercial buildings. BIPV has a dominant role that satisfies 8% to 16% and 34% to 63% of electricity demand if threshold constraints and full exploitation of building surfaces are considered respectively. However, BIPV contributes 16% to 40% of the decarbonization potential which is less than demand-side efficiency measures. The scale-bounded comparative analysis shows that total PV potential changes in the order of magnitude of 29 to 54 with the variation of scale (with reference to district scale) and higher self-sufficiency are observed at the building-by-building level in comparison to district and city scales. This demonstrates that this coupled approach can provide a purpose-driven perspective of the energy transition at multiple scales with reduced computational time. Overall, this analysis provides a multi-level perspective to energy

modelers and policymakers on how to achieve the carbon-neutral goal in commercial building stock.

4.6 Appendix

4.6.1 Appendix A. Development of a physical-based BIPV potential estimation

This approach is developed by initially using a 3D GIS database and then sensor points were generated at a specified distance to calculate the point-wise irradiation (Shono et al. (2023)). For solar irradiance estimation, the direct solar irradiance (B) was calculated as follows:

$$\mathrm{B} = \mathrm{B_o} \cos \mathrm{i} \qquad \text{A-1}$$

where B_0 is the direct normal radiation and i is the incidence angle. To consider the effects of shadow, the maximum shaded angle was determined by:

$$\theta_{max} = \tan^{-1} \frac{z_{max} - z_p}{dis(P, Q_{max})} \qquad \text{A-2}$$

where z_{max} is the elevation of the highest surrounding building point Q_{max} for each sensor point and dis(P, Q_i) is the horizontal distance between the two points. The diffuse solar irradiance was estimated by using the anisotropic diffuse model as proposed by Perez et al. (1986 & 1987). The sky view factor (F_{sky}) was calculated as follows:

$$F_{sky} = \frac{1}{\pi} \int_{0}^{2\pi} \int_{v(\lambda)}^{\pi/2} \sin(\theta_z) \cos(\theta_z) \, d\theta_z \, d\lambda \qquad \text{A-3}$$

where θ_z is the zenith angle, λ is the azimuth angle, and $v(\lambda)$ is the maximum shading angle θ_{max} in direction λ. For PV potential estimation, the equivalent power capacity was calculated as follows:

$$P = G \times \eta_t \times \eta_c \times \left(\frac{A}{cos\beta}\right) \qquad \text{A-4}$$

where G is the global irradiance (Wh/m^2), A is the representative area (m^2) of each sensor point, η_c is the conversion efficiency of the PV module, η_t is the temperature coefficient of the PV module, and β is the slope angle of the PV module.

4.6.2 Appendix B. Types of HVAC systems and other measures.

Table B.1. Types of heat source in HVAC system.

Type		Heat source for cooling	Heat source for heating	Thermal storage
Decentralized system	Elec-VRF	Electricity-driven VRF	Same as cooling	
	Gas-VRF	Gas-driven VRF	Same as cooling	
	Mix-VRF	Both Elec-VRF and Gas-VRF	Same as cooling	
Centralized system	AirS-HP	Air-source heat pump	Same as cooling	
	AirS-HPS	Air-source heat pump	Same as cooling	Yes
	E-C&G-B	Electricity-driven chiller	Gas boiler	
	Gas-AbCB	Absorption chiller	Gas boiler	
	Gas-AbCH	Absorption chiller-heater	Same as cooling	
	Comb-EG	Electricity-driven chiller and absorption chiller-heater	Absorption chiller-heater	
	WaterS-CS	Electricity-driven chiller and absorption chiller-heater	Absorption chiller-heater	Yes

Table B.2. Types of air-conditioning system.

Type		Heating and cooling	Ventilation
Decentralized system	VRF	Variable refrigerant flow (VRF) system is used	The ventilation system is independently installed
Centralized system	FCU	Fan coil unit (FCU) is used	Same as VRF
	CAV	Air handling unit (AHU) with constant air volume (CAV) control is used	Air-intake is mixed in AHU
	VAV	AHU with variable air volume (VAV) control	Same as CAV
	CAV+FCU	Same as in CAV but perimeter zone is controlled by FCU	Same as CAV
	VAV+FCU	Same as CAV+FCU but VAV is used in AHU.	Same as CAV
	OHU+FCU	FCU is used in both interior and perimeter zones.	Outdoor air handling unit (OHU) is used

Table B.3. System efficiency of various sources.

Sources		Base		Potential/Electric	
		Rated COP (W/W)	Efficiency (%)	Rated COP (W/W)	Efficiency (%)
Electricity-driven chillers		5.5		7.0	
Absorption chillers		1.1		1.6	
Air source heat pump	Cooling	3.1		4.0	
	Heating	3.2		4.1	
Gas-driven VRF	Cooling	1.0		1.5	
	Heating	1.2		1.6	
Electricity-driven VRF	Cooling	3.0		3.8	
	Heating	3.4		4.2	
Heat pump water (HPWH)		4.3		4.3	
Electric water heater			90		90
Gas/oil boilers			86		93
Fan efficiency			36-63		46-75
Heat exchanger for air-intake			60		65

Table B.4. List of ventilation and heat delivery measures.

Type	Measure	Combination
Ventilation related measures	Heat exchanger as air-intake (HEX) Natural ventilation using an economizer (OA) Air-intake quantity control based on CO_2 concentration (CO_2)	All combinations of the three measures
Centralized system	Variable water volume control (VWV)	The adoption of VWV control

4.6.3 Appendix C. Description of commercial RBMs for UBEM model

Table C.1. Description of commercial RBMs of Tokyo.

Segment	Cluster	GFA (m^2)	Floors (Nos)	Height (m)	Shape Coefficient (S/V)	Aspect ratio	Orientation (^{0})
Office	CL1	118	4	13.6	0.36	0.55	-2
	CL2	213	8	24.5	0.27	0.53	-2.1
	CL3	373	8	28	0.18	0.47	-2.6
	CL4	1056	9	29.6	0.12	0.46	-2
	CL5	2761	23	94.6	0.07	0.42	-3.2
Hotel	CL1	130	4	13.6	0.34	0.53	0.3
	CL2	363	8	27.2	0.20	0.44	-6.2
	CL3	465	11	37	0.18	0.41	-4.4
	CL4	1654	14	49.4	0.10	0.34	-6.7
	CL5	4298	30	110.2	0.06	0.31	-0.8
Hospital	CL1	171	2	7	0.32	0.50	-0.2
	CL2	868	5	18.5	0.13	0.40	-6.1
	CL3	1149	6	19	0.12	0.28	-1.4
	CL4	4160	11	42	0.06	0.27	-2.7
School	CL1	1731	4	11.4	0.11	0.44	0.2
	CL2	2221	6	15.2	0.1	0.36	3.1
	CL3	2837	7	19	0.09	0.23	-0.1

Note: Positive orientation is considered as clockwise.

4.7 Supplementary data

Supplementary data to this chapter can be found online at:
https://doi.org/10.1016/j.enbuild.2023.113086

5 Integrated discussion

In the following chapter, an integrated discussion is presented to illustrate the critical overview of the research questions in terms of data acquisition, modelling capability and purpose-driven perspective. Initially, the chapter outlines the novel contributions to the field of BSEM and then, analyses the limitations and uncertainties of developed models.

The thesis aim is to assist the regional (or city) level energy planners and policy makers in understanding the role of data acquisition on the energy performance of BSEM, the analytical capability of multi-scale modelling using BSEM and further support them in evaluating the carbon neutrality of commercial building stock at multiple scales. This thesis resulted in three-fold contributions with the advancement of data acquisition and modelling techniques for commercial building stock. Firstly, to understand the transitional limitations of various BSEM approaches, a comparative study of three major bottom-up BSEMs was performed to evaluate the accuracy and added-value of these approaches for use in the bottom-up engineering model. Secondly, a hybrid BSEM is developed to facilitate the concurrent consideration of physical and technical elements and further extend the model to different spatial resolutions. This provided a multi-tier framework using spatial intelligence building stock approach to develop long-term energy efficiency monitoring strategies for commercial building stock at multiple scales. Thirdly, a UBEM-BIPV coupled approach is developed to consider the SER framework for the evaluation of carbon neutrality of commercial building stock. The coupled approach resulted in a purpose-driven perspective of the energy transition at multiple scales with reduced computational time. Moreover, a detailed description of the main contributions and limitations related to developed models is discussed below:

5.1 Role of data acquisition

The accuracy and reliability of BSEM mainly depend on the quality and quantity of data due to the interlinkage between the availability of input data and the use of computational methods. Thus, data acquisition is one of the main processes in the development of BSEM due to challenges associated with the retrieval of geometric, non-geometric, socio-behaviour, meteorological and measured energy data at a scale. In terms of best practices and use cases, it is important to select a model based on the availability and quality of data as well as the relevant system features required to develop a discrete representation of building stock. Moreover, most of the previous BSEM studies used a specific approach to quantitatively improve the robustness and accuracy of models but have not focused on identifying the impact of these approaches on the performance level of BSEMs. There is a lack of knowledge about the influence of data acquisition techniques on the model's accuracy. Hence, there is a need to focus on exploring the comparative

performance of these approaches to further assess the evaluation of accuracy in predicting the energy demand and carbon emissions of the commercial building stock.

To assess the comparative performance of BSEM approaches, Chapter 2 provided a detailed overview of the cross-over framework of the three major building stock approaches, sample-free synthetic, sample-based synthetic and geo-referenced, to quantify the accuracy and added-value of each approach in terms of heterogeneity, data dimensionality, integration and non-linear interactions within the stock. As discussed in Section 2.4, the sample-based synthetic method can incorporate multiple input distributions using a survey micro-dataset, while the geo-referenced method provides additional key determinants such as building typology (shape coefficient, aspect ratio and orientation) and morphological attributes. This implies that these are data-enriched methods which resulted in better performance in terms of building stock development and simulated building energy use that signifies the accuracy and added-value of these methods. However, a sample-based synthetic method provides a better compromise between data availability and simulation accuracy in comparison to other methods. This shows that the synthetic approach can be extended to commercial building stock, which mostly has a poorer data availability than residential building stock, which further allows to encompass modelling of a typical mixed-use urban environment. Moreover, this cross-over analysis will provide a granular level framework to assist the city-level planners and policy makers in choosing the right building stock modelling approach for predicting the energy demand and carbon emissions of the commercial building stock.

5.2 Multi-scale modelling

Urban energy planners and policymakers mostly experience scalability issues due to a lack of coordination in terms of availability and incomplete coverage of stock data. This hinders the implementation of target-based urban planning that requires intensive information at the granular level to identify the target areas where the energy policymakers can conduct target-based planning and decision-making. The selection and description of spatial resolution of the model mainly depend on the use case, availability of measured energy data and quality of data. To address these challenges, multi-scale modelling is one of the possible techniques that can improve the analytical capability of conventional BSEM by involving end-use energy processes (function and boundary of the systems), practices (socio-behavioural interaction, such as occupancy patterns and resource usage), and context (structure and conditions of systems) across a range of scales and sectors. However, for energy modelling of the commercial building stock, several methodologies were developed focusing on technology alternatives and retrofits for climate change mitigation, but they often have limitations to involve a differentiated description of practices and policies across a range of scales and sectors. Hence, there is a need to address the

limitations of existing commercial BSEMs, such as non-scalable framework and fragmented consideration of influencing factors (focusing on either physical or technological attributes), by establishing a multi-layer model across the scale.

To incorporate granularity and multi-dimensionality within BSEM, chapter 3 presented a novel GIS-synthetic hybrid model by integrating spatial and synthetic modelling approaches to facilitate the concurrent consideration of multiple building-oriented elements at multiple scales. As discussed in Section 3.3, the differences in the energy end usages and reduction potential exist due to varying structural and stock composition across different scales. This implies that the hybrid models capture these variations, which a conventional non-scalable model could not distinguish. From a practical implementation perspective, this further helps address the data limitations and context-specific issues to overcome the disparate coordination between the local and national level stakeholders, which could identify priority areas for implementing target-based energy efficiency strategies. Moreover, the selection and description of the appropriate spatial boundary are critical for the base year and long-term studies related to building stock energy modelling. The long-term studies are more sensitive to an adequate spatial boundary than the base year studies and show significantly different energy consumption patterns, 10–17%, and reduction potential, 2–3 times, when a non-representative scale is applied to other scales. This implies a need to develop multi-tier long-term building stock strategies to promote the adoption of ESMs and alternative technologies for achieving net-zero emissions in the building sector. Additionally, the two most critical building-oriented elements are geometry and plug loads when the non-representative scale is applied at other scales. This suggests that these elements lead to higher scale-bounded uncertainties, induced due to structural heterogeneity, typological complexities, and diverse functionalities associated with the stock composition of commercial buildings. This granular-level framework uses a spatial intelligence approach that can assist urban energy planners and policymakers in developing long-term energy efficiency monitoring strategies at multiple scales. The framework could further open new avenues in building stock methodologies by integrating conventional approaches with emerging information technologies. Such strategies are crucial to achieving valuable advances by incorporating emerging modelling techniques, and treatment of additional modelling dimensions within commercial BSEM.

5.3 Purpose-driven coupling

In order to mitigate the effect of climate change and meet carbon emission targets, there is a paradigm shift towards the shared global goal of achieving carbon neutrality. Recently, more aggressive national mitigation commitments have been adopted to meet the target of net-zero carbon emissions by 2050 (UNFCC COP 26, 2021). The transitional pathway to carbon-neutral

building stock includes an interplay of planetary and non-planetary boundaries, technological and non-technological options, and dispatchable and non-dispatchable energy resources. These interlinkages can not be captured by a singular or focal model with limited external coordination. Therefore, there is a need to develop a multi-model framework to illustrate the process of model coupling for the assessment of carbon-neutral building stock, which can involve a higher degree of coordination to adequately manage the modelling functionality and integration, resolution and data coherence.

To demonstrate purpose-driven model coupling, chapter 4 presented a coupled workflow that facilitated the homogenous use of a comprehensive GIS dataset to provide the necessary coordination of a hybrid UBEM model with a physical-based BIPV estimation approach at the multi-scale level, leading to further improvement in the methodological characterization to evaluate the carbon neutrality of commercial building stock. As discussed in Section 4.3, the differences in the demand reduction and BIPV potential exist across different scales due to varying structural and system stock composition, and urban morphological characteristics. This implies that the proposed coupled scheme identifies various drivers and determinants to better understand the mechanisms and conditions leading to different demand and supply levels across the scale. Additionally, in terms of modelling resolution, the maximum co-benefit of demand-side efficiency improvement and integration of BIPV is observed at the building-by-building level with 70% of buildings having Self-sufficiency (SS) greater than 1 while at other scales, 28% and 22% of districts and cities transition into net positive energy districts and cities respectively. This spatial imbalance is mainly due to typological utilization constraints and diverse functionalities of commercial buildings. Therefore, those studies focusing on the optimization of a single building model result in insignificant or redundant findings at a larger scale. This demonstrated that this coupled approach can provide a purpose-driven perspective of the energy transition at multiple scales with reduced computational time. Overall, this UBEM-BIPV coupled scheme will provide a multi-level perspective to energy modelers and policymakers on how to achieve the carbon-neutral goal in the commercial building stock.

5.4 Future work and limitations

Although the developed BSEMs demonstrated the comparative analysis of interlinkage between the availability of input data and use of the computational method, improved adequacy at the multi-scale level and could be further applied to different regions, and also provided purpose-driven coupling perspective of BSEM, there are still some limitations that need to be addressed. A summary of those limitations is provided as follows:

1. The segmentation process of data-driven modelling needs to be improved by overcoming the issue of homogeneity across the scale. The same number of classifiers are used to perform

the segmentation, resulting in an equal number of clusters at different scales. This scheme needs further improvement by implementing it at a specific granular level to obtain the optimum number of classifiers as per the specifications.

2. In synthetic modelling, a multi-nominal statistical approach is applied to a large sample dataset to fill the energy modelling gap due to a lack of information related to the technical factors. This requires further effort to conduct a multi-scale field survey for validating the probabilistic building systems stock model by comparing it with actual stock.
3. An auto-calibration framework needs to be developed that can transform the existing multi-scale UBEM model into a scalable model, ensuring transparency at a granular level by providing a comprehensive insight into uncertainties at the spatial level.
4. In a physical-based BIPV potential estimation approach, an anisotropic hourly diffuse radiation model is used without considering the ground-reflected irradiance that needed to be involved.
5. The developed BSEMs model mainly focused on physical and technical factors while the effect of lifestyle changes and socioeconomic factors are not considered within the model.

This thesis provided significant improvement in the analytical capability of BSEM in terms of building stock characterization and evolution, and further extended the scope and use case of BSEM. However, further future work can be performed to extend these research contributions as follow:

1. The development of multi-scalable reduced-order models for commercial building stock, which could speed up the development cycle by minimizing computational resources.
2. The dynamics of building stock transition also involve non-technological options that need to be assessed for the effective implementation of decarbonization measures. Urban energy planners and policymakers have to consider energy vulnerability and poverty issues for target-based urban planning to streamline the uptake of decarbonization measures. Further research can focus on the incorporation of lifestyle changes (teleworking and relaxation of room set point temperature) and the effect of socioeconomic factors on the implementation of decarbonization strategies.
3. The UBEM-BIPV coupled scheme can be further extended to perform techno-economic analysis of physical energy infrastructure, electric vehicles, storages, and synthetic gas generation, for assessment of emerging technologies on demand-supply synergy.

6 Conclusion

BSEM has gained a lot of attention recently with the development of a range of methodologies for various use cases by evaluating the trends of energy demand and carbon emissions, implementation of building efficiency retrofits, energy system integration and the effect of climate change. With the advancement of data-driven techniques, BSEMs involve a higher degree of complexity with the varying model structure and output that requires comprehensive reporting guidelines to improve the transparency and consistency of BSEM. In BSEM, several bottom-up methodologies have been developed to assess the energy demand and emission reduction potential of the stock but, often have transitional limitations either to shift from aggregated to disaggregated stock boundary conditions or involve a differentiated description of practices and policies across a range of scales and sectors. This thesis developed multiple BSEM methodologies to identify the best practices for minimum viable model guidelines that can provide transparency and capture value with the least cost and effort. To this extent, the comparative analysis of BSEM approaches was performed to assess the accuracy and added-value of quality and quantity of data on the model performance. Additionally, to improve the analytical capability of conventional BSEM, a GIS-synthetic hybrid model is developed to involve a differentiated description of practices and policies across a range of scales and sectors. This provided a multi-tier framework using spatial intelligence building stock approach to develop long-term energy efficiency monitoring strategies for commercial building stock at multiple scales. Moreover, to demonstrate a process of purpose-driven coupling, a multi-model framework of UBEM-BIPV coupled scheme is developed to illustrate the process of model coupling for the assessment of carbon-neutral building stock, which can involve a higher degree of coordination to adequately manage the modelling functionality and integration, resolution and data coherence. The coupled workflow facilitated the homogenous use of a comprehensive GIS dataset to provide the necessary coordination of building stock interventions with renewable DERs at the multi-scale level. The summary of findings related to formulated research objectives is given below:

1) How can the data acquisition influence the performance level and applicability of bottom-up BSEM in predicting the energy demand and carbon emissions of the commercial building stock.

A comparative analysis of BSEM approaches showed that the sample-based synthetic method provides a better compromise between data availability and simulation accuracy in comparison to other methods. The sample-based synthetic method can incorporate multiple input distributions using a survey micro-dataset, while the geo-referenced method provides additional key determinants such as building typology (shape coefficient, aspect ratio and orientation) and morphological attributes. This implies that these are data-enriched methods which resulted in better performance in terms of building stock characterization and estimation of building energy

use that signifies the accuracy and added-value of these methods. Moreover, it is observed that the combination of sample-based synthetic and geo-referenced approaches can provide cross-sectional and longitudinal enrichment within the model.

2) How can bottom-up BSEM be modelled to incorporate scalability and multiple building-oriented elements characterization within the model.

The proposed multi-scale model identifies various drivers and determinants of energy end-uses and resource usages to provide a better understanding of mechanisms and conditions that lead to different levels of demand for commercial building stock across the scale. This addresses the underlying complexity associated with the BSEMs by examining influencing factors that cause different levels of outcomes at different scales. As per the quantitative analysis, disregarding the physical and technical factors drops cumulative performance by up to 32%. This signifies the need for a concurrent consideration of these factors within BSEM. Moreover, the scale-bounded comparative approach indicates that the larger the description of the scale, the higher the error uncertainty when applied to a smaller representative scale. This scale variability seems significant due to relatively higher thermal dynamics induced by the building typology and functional composition of the commercial building stock. In terms of model complexity, a more integrated model is needed at a large scale than other scales because of the modular and diversified distribution of large-scale building stock, which leverages variability within the model output. The results imply that the performance gap increases significantly up to 21% when the description of a scale shifts from a smaller to a larger one. Overall, the developed model provides a comprehensive understanding of selecting and describing the minimum viable requirements for a specific scale by considering the effect of various influencing parameters on scale-bounded uncertainties.

3) How does the SER framework be considered for the evaluation of carbon neutrality of commercial building stock.

A GIS-synthetic hybrid UBEM model is coupled with a physical-based approach of BIPV potential estimation for the consideration of the SER framework in estimating the overall decarbonization potential of the commercial building stock. Results show that the annual CO_2 emissions can be reduced by 84% with the simultaneous implementation of all the measures. The measure-by-measure comparison showed that the most impactful demand-side efficiency measures are system efficiency improvement, and the upgradation of lighting and appliances while passive design measures only contribute a 10% reduction potential which is not enough to achieve carbon neutrality in commercial buildings. BIPV has a dominant role that satisfies 8% to 16% and 34% to 63% of electricity demand if threshold constraints and full exploitation of

building surfaces are considered respectively. However, BIPV contributes 16% to 40% of the decarbonization potential which is less than demand-side efficiency measures. The scale-bounded comparative analysis shows that total PV potential changes in the order of magnitude of 29 to 54 with the variation of scale (with reference to district scale) and higher self-sufficiency are observed at the building-by-building level in comparison to district and city scales. This demonstrates that this coupled approach can provide a purpose-driven perspective of the energy transition at multiple scales with reduced computational time.

Overall, this thesis has contributed to the advancement of BSEM by providing comprehensive reporting guidelines in terms of accuracy, granularity and multi-dimensionality aspects. This has enhanced the capability of the BSEM to be further extended to any demographic landscape or spatial resolution and evolve into a long-term transitional workflow. Thus, enabling long-term spatial energy resource planning and decision-making for commercial building stock across various scales. From a practical perspective, this thesis develops a multi-level framework using spatial intelligence to assist the urban energy planners and policymakers in: (1) the selection of the BSEM approach on the basis of availability and quality of data; (2) the development of long-term energy efficiency monitoring strategies at multiple scales; and (3) how to achieve the carbon-neutral goal in the commercial building stock.

References

Abbasabadi N, Ashayeri M, Azari R, Stephens B, Heidarinejad M. (2019). An integrated data-driven framework for urban energy use modeling (UEUM). Applied Energy, vol. 253, 113550. https://doi.org/10.1016/j.apenergy.2019.113550

Akenji L, Bengtsson M, Toivio V, Lettenmeier M, Fawcett T, Parag Y, Saheb Y, Coote A, Spangenberg JH., Capstick S, Gore T, Coscieme L, Wackernagel M, Kenner D. (2021). 1.5-Degree Lifestyles: Towards A Fair Consumption Space for All. Hot or Cool Institute, Berlin.

Ala-Juusela M, Crosbie T, Hukkalainen M. (2016). Defining and operationalising the concept of an energy positive neighbourhood. Energy Conversion and Management, vol. 125, pp. 133-140. https://doi.org/10.1016/j.enconman.2016.05.052

Ali U, Shamsi MH, Bohacek M, Purcell K, Hoare C, Mangina E, et al. (2020). A data-driven approach for multi-scale GIS-based building energy modeling for analysis, planning and support decision making. Applied Energy, vol. 279, 115834. https://doi.org/10.1016/j.apenergy.2020.115834

Ali U, Shamsi MH, Hoare C, Mangina E, O'Donnell J. (2019). A data-driven approach for multi-scale building archetypes development. Energy and Buildings, vol. 202, 109364. https://doi.org/10.1016/j.enbuild.2019.109364

Ali U, Shamsi MH, Hoare C, Mangina E, O'Donnell J. (2021). Review of urban building energy modeling (UBEM) approaches, methods and tools using qualitative and quantitative analysis. Energy and Buildings, vol. 246, 111073. https://doi.org/10.1016/j.enbuild.2021.111073

Amasyali K, El-Gohary N. (2022). Hybrid approach for energy consumption prediction: Coupling data-driven and physical approaches. Energy and Buildings, vol. 259, 111758. https://doi.org/10.1016/j.enbuild.2021.111758

Amjad F, Shah LA. (2020). Identification and assessment of sites for solar farms development using GIS and density based clustering technique- A case of Pakistan. Renewable Energy, vol. 155, pp. 761-769. https://doi.org/10.1016/j.renene.2020.03.083

Ang YQ, Berzolla ZM, Reinhart CF. (2020). From concept to application: A review of use cases in urban building energy modeling. Applied Energy, vol. 279, 115738. https://doi.org/10.1016/j.apenergy.2020.115738

ANSI/ASHRAE Standard 90.1-2022. (2022). Energy Standard for Buildings except Low-Rise Residential Buildings. American Society of Heating, Refrigerating and Air Conditioning Engineers (Atlanta, Georgia). ASHRAE: New York, NY, USA.

Ashie Y, Kagiya K. High resolution numerical simulation on the urban heat island of the entire 23 wards of Tokyo using the earth simulator. Technical note of National Institute for Land and Infrastructure Management 583, 2010. (http://www.nilim.go.jp/lab/bcg/siryou/tnn/tnn0583pdf/ks0583.pdf)

Azar E, Menassa CC. (2014). A comprehensive framework to quantify energy savings potential from improved operations of commercial building stocks. Energy Policy, vol. 67, pp. 459–472. https://doi.org/10.1016/j.enpol.2013.12.031

Basaraner M, Cetinkaya S. (2017). Performance of shape indices and classification schemes for characterising perceptual shape complexity of building footprints in GIS. International Journal of Geographical Information Science, vol. 31, pp. 1952–77. https://doi.org/10.1080/13658816.2017.1346257

Biljecki F, Ledoux H, Stoter J. (2016). An improved LOD specification for 3D building models. Computers, Environment and Urban Systems, vol. 59, pp. 25-37. https://doi.org/10.1016/j.compenvurbsys.2016.04.005

Borràs IM, Neves D, Gomes R. Using urban building energy modeling data to assess energy communities' potential. (2023). Energy and Buildings, vol. 282, 112791. https://doi.org/10.1016/j.enbuild.2023.112791

Buso T, Corgnati SP. (2017). A customized modelling approach for multi-functional buildings – Application to an Italian Reference Hotel. Applied Energy, vol. 190, pp. 1302–1315. https://doi.org/10.1016/j.apenergy.2017.01.042

Cabeza LF, Bai Q, Bertoldi P, Kihila JM, Lucena AFP, Mata É, Mirasgedis S, Novikova A, Saheb Y. (2022). Buildings. In IPCC, 2022: Climate Change 2022: Mitigation of Climate Change. Contribution of Working Group III to the Sixth Assessment Report of the Intergovernmental Panel on Climate Change, Cambridge University Press, Cambridge, UK and New York, NY, USA, 2022. (doi: 10.1017/9781009157926.011)

Cai B, Zhang L. (2014). Urban CO_2 emissions in China: Spatial boundary and performance comparison. Energy Policy, vol. 66, pp. 557-567. https://doi.org/10.1016/j.enpol.2013.10.072

Chang M, Lund H, Thellufsen JZ, Østergaard PA. (2023). Perspectives on purpose-driven coupling of energy system models. Energy, vol. 265, 126335. https://doi.org/10.1016/j.energy.2022.126335

Chatzipoulka C, Compagnon R, Kaempf J, Nikolopoulou M. (2018). Sky view factor as predictor of solar availability on building façades. Solar Energy, vol. 170, pp. 1026-1038. https://doi.org/10.1016/j.solener.2018.06.028

Chen X, Yang H, Peng H. (2019). Energy optimization of high-rise commercial buildings integrated with photovoltaic facades in urban context. Energy, vol. 172, pp. 1-17. https://doi.org/10.1016/j.energy.2019.01.112

Chen Y, Hong T, Piette MA. (2017). Automatic generation and simulation of urban building energy models based on city datasets for city-scale building retrofit analysis. Applied Energy, vol. 205, pp. 323–35. https://doi.org/10.1016/j.apenergy.2017.07.128

Chen Y, Hong T. (2018). Impacts of building geometry modeling methods on the simulation results of urban building energy models. Applied Energy, vol. 215, pp. 717–735. https://doi.org/10.1016/j.apenergy.2018.02.073

Cheng L, Zhang F, Li S, Mao J, Xu H, Ju W, Liu X, Wu J, Min K, Zhang X, Li M. (2020). Solar energy potential of urban buildings in 10 cities of China. Energy, vol. 196, 117038. https://doi.org/10.1016/j.energy.2020.117038

Chong A, Lam KP, Pozzi M, Yang J. (2017). Bayesian calibration of building energy models with large datasets. Energy and Buildings, vol. 154, pp. 343–55. https://doi.org/10.1016/j.enbuild.2017.08.069

Chong A, Menberg K. (2018). Guidelines for the Bayesian calibration of building energy models. Energy and Buildings, vol. 174, pp. 527–47. https://doi.org/10.1016/j.enbuild.2018.06.028

Dabirian S, Panchabikesan K, Eicker U. (2022). Occupant-centric urban building energy modeling: Approaches, inputs, and data sources - A review. Energy and Buildings, vol. 257, 111809. https://doi.org/10.1016/j.enbuild.2021.111809

D'Agostino D, D'Agostino P, Minelli F, Minichiello F. (2021). Proposal of a new automated workflow for the computational performance-driven design optimization of building energy need and construction cost. Energy and Buildings, vol. 239, 110857. https://doi.org/10.1016/j.enbuild.2021.110857

Dahlström L, Broström T, Widén J. (2022). Advancing urban building energy modelling through new model components and applications: A review. Energy and Buildings, vol. 266, 112099. https://doi.org/10.1016/j.enbuild.2022.112099

Davila CC, Reinhart CF, Bemis JL. (2016). Modeling Boston: A workflow for the efficient generation and maintenance of urban building energy models from existing geospatial datasets. Energy, vol. 117, pp. 237–50. https://doi.org/10.1016/j.energy.2016.10.057

Deng Z, Chen Y, Yang J, Causone F. (2023). AutoBPS: A tool for urban building energy modeling to support energy efficiency improvement at city-scale. Energy and Buildings, vol. 282, 112794. https://doi.org/10.1016/j.enbuild.2023.112794

Duffie JA, Beckman WA. Solar engineering of thermal processes. Wiley, 2013.

Electric commercial kitchen design information committee (ECKDIC). Guidelines for electric commercial kitchen design. 2000.(In Japanese)

Energy Data and Modeling Center, Institute of Energy Economics J. EDMC handbook of Japan's and world energy and economic statistics. Energy Conservation Center, Japan; 2017.

Esri Japan, 2015. ArcGIS Geo Suite.

Fathizad H, Mobin MH, Gholamnia A et al. (2017). Modeling and mapping of solar radiation using geostatistical analysis methods in Iran. Arabian Journal of Geosciences, vol. 10, 391. https://doi.org/10.1007/s12517-017-3130-x

Fernandez N, Katipamula S, Wang W, Xie Y, Zhao M. (2018). Energy savings potential from improved building controls for the US commercial building sector. Energy Efficiency, vol. 11, pp. 393–413. https://doi.org/10.1007/s12053-017-9569-5

Fonseca JA, Schlueter A. (2015). Integrated model for characterization of spatiotemporal building energy consumption patterns in neighborhoods and city districts. Applied Energy, vol. 142, pp. 247–65. https://doi.org/10.1016/j.apenergy.2014.12.068

Freitas S, Catita C, Redweik P, Brito MC. (2015). Modelling solar potential in the urban environment: State-of-the-art review. Renewable and Sustainable Energy Reviews, vol. 41, pp. 915-931. https://doi.org/10.1016/j.rser.2014.08.060

Gaspard A, Chateau L, Laruelle C, Lafitte B, Léonardon P, Minier Q, Motamedi K, Ougier L, Pineau A, Thiriot S. (2023). Introducing sufficiency in the building sector in net-zero scenarios for France. Energy and Buildings, 278, 112590. https://doi.org/10.1016/j.enbuild.2022.112590

Gassar AAA, Cha SH. (2021). Review of geographic information systems-based rooftop solar photovoltaic potential estimation approaches at urban scales. Applied Energy, vol. 291, 116817. https://doi.org/10.1016/j.apenergy.2021.116817

Geraldi MS, Ghisi E. (2020). Building-level and stock-level in contrast: A literature review of the energy performance of buildings during the operational stage. Energy and Buildings, vol. 211, 109810. https://doi.org/10.1016/j.enbuild.2020.109810

Geraldi MS, Melo AP, Lamberts R, Borgstein E, Yukizaki AYG, Maia ACB, Soares JB, Junior ADS. (2022). Assessment of the energy consumption in non-residential building sector in Brazil. Energy and Buildings, vol. 273,112371. https://doi.org/10.1016/j.enbuild.2022.112371

Ghaleb B, Asif M. (2022). Application of solar PV in commercial buildings: Utilizability of rooftops. Energy and Buildings, vol. 257, 111774. https://doi.org/10.1016/j.enbuild.2021.111774

Goldstein M, Uchida S. (2016). A comparative evaluation of unsupervised anomaly detection algorithms for multivariate data. PLoS One, vol. 11, pp. 1–31. https://doi.org/10.1371/journal.pone.0152173

Groppi D, Santoli L, Cumo F, Garcia DA. (2018). A GIS-based model to assess buildings energy consumption and usable solar energy potential in urban areas. Sustainable Cities and Society, vol. 40, pp. 546-558. https://doi.org/10.1016/j.scs.2018.05.005

Happle G, Fonseca JA, Schlueter A. (2020). Impacts of diversity in commercial building occupancy profiles on district energy demand and supply. Applied Energy, vol. 277, 115594. https://doi.org/10.1016/j.apenergy.2020.115594

Heidarinejad M, Mattise N, Dahlhausen M, Sharma K, Benne K, Macumber D, et al. (2017). Demonstration of reduced-order urban scale building energy models. Energy and Buildings, vol. 156, pp. 17–28. https://doi.org/10.1016/j.enbuild.2017.08.086

Heidelberger E, Rakha T. (2022). Inclusive urban building energy modeling through socioeconomic data: A persona-based case study for an underrepresented community. Building and Environment, vol. 222, 109374. https://doi.org/10.1016/j.buildenv.2022.109374

Hermes K, Poulsen M. (2012). A review of current methods to generate synthetic spatial microdata using reweighting and future directions. Computers, Environment and Urban Systems, vol. 36, Issue 4, pp. 281-290. https://doi.org/10.1016/j.compenvurbsys.2012.03.005

Hietaharju P, Pulkkinen J, Ruusunen M, Louis JN. (2021). A stochastic dynamic building stock model for determining long-term district heating demand under future climate change. Applied Energy, vol. 295, 116962. https://doi.org/10.1016/j.apenergy.2021.116962

Hirvonen J, Heljo J, Jokisalo J, Kurvinen A, Saari A, Niemelä T, et al. (2021). Emissions and power demand in optimal energy retrofit scenarios of the Finnish building stock by 2050. Sustainable Cities and Society, vol. 70, 102896. https://doi.org/10.1016/j.scs.2021.102896

Hiyama K, Srisamranrungruang T. Low-carbon assessment of building facades using dynamic CO_2 intensity of electricity generation in Japan. Energy and Buildings, vol. 278, 112637, 2023. https://doi.org/10.1016/j.enbuild.2022.112637

Hong T, Piette MA, Chen Y, Lee SH, Taylor-Lange SC, Zhang R, et al. (2015). Commercial Building Energy Saver: An energy retrofit analysis toolkit. Applied Energy, vol. 159, pp. 298–309. https://doi.org/10.1016/j.apenergy.2015.09.002

Horan W, Byrne S, Shawe R, Moles R, O'Regan B. (2020). A geospatial assessment of the rooftop decarbonisation potential of industrial and commercial zoned buildings: An example of Irish cities and regions. Sustainable Energy Technologies and Assessments, vol. 38, 100651. https://doi.org/10.1016/j.seta.2020.100651

Huo T, Xu L, Feng W, Cai W, Liu B. (2021a). Dynamic scenario simulations of carbon emission peak in China's city-scale urban residential building sector through 2050. Energy Policy, vol. 159, 112612. https://doi.org/10.1016/j.enpol.2021.112612

Huo T, Ma Y, Cai W, Liu B, Mu L. (2021b). Will the urbanization process influence the peak of carbon emissions in the building sector? A dynamic scenario simulation. Energy and Buildings, vol. 232, 110590. https://doi.org/10.1016/j.enbuild.2020.110590

IEA. (2019). Perspectives for Clean Energy Transition. The Critical Role of Buildings. Int Energy Agency 2019:117.

Ivanova D, Büchs M. (2020). Household Sharing for Carbon and Energy Reductions: The Case of EU Countries. Energies, 13(8), 1909. https://doi.org/10.3390/en13081909

Japan Meteorological Agency (JMA), Historical Weather Data, 2022. (https://www.data.jma.go.jp/gmd/risk/obsdl/index.php)

Japan Meteorological Agency (JMA), The Automated Meteorological Data Acquisition System (AMeDAS), (2014). (In Japanese).

Japan Sustainable Building Consortium (JSBC). (2017). Open Source Data-base for Energy Consumption of Commercial Building. (http://www.jsbc.or.jp/decc_english/index.html)

Japanese Association of Building Mechanical and Electrical Engineering (JABMEE). (2010). ELPAC data. (http:/www.jabmee.or.jp/seihin/elpac/)

Jinko Solar, 2021. Product Catalogue 2021. (https://www.jinkosolar.com/uploads/00012.pdf)

Jokinen I, Lund A, Hirvonen J, Jokisalo J, Kosonen R, Lehtonen M. (2022). Coupling of the electricity and district heat generation sectors with building stock energy retrofits as a measure to reduce carbon emissions. Energy Conversion and Management, vol. 269, 115961. https://doi.org/10.1016/j.enconman.2022.115961

Karl-Hermann W, Marco G, Johann J, Christian R, Monika E, Matthias B, et al. Erich. MPI-M MPIESM1.2-LR model output prepared for CMIP6 CMIP. (Version 20190710)

Kavgic M, Mavrogianni A, Mumovic D, Summerfield A, Stevanovic Z, Djurovic-Petrovic M. (2010). A review of bottom-up building stock models for energy consumption in the residential sector. Building and Environment, vol. 45, Issue 7, pp. 1683-1697. https://doi.org/10.1016/j.buildenv.2010.01.021

Kim B, Yamaguchi Y, Kimura S, Ko Y, Ikeda K, Shimoda Y. (2020). Urban building energy modeling considering the heterogeneity of HVAC system stock: A case study on Japanese office building stock. Energy and Buildings, vol. 199, pp. 547-561. https://doi.org/10.1016/j.enbuild.2019.07.022

Kim MK, Kim YS, Srebric J. (2020). Impact of correlation of plug load data, occupancy rates and local weather conditions on electricity consumption in a building using four back-propagation neural network models. Sustainable Cities and Society, vol. 62, 102321. https://doi.org/10.1016/j.scs.2020.102321

Kobashi T, Choi Y, Hirano Y, Yamagata Y, Say K. (2022). Rapid rise of decarbonization potentials of photovoltaics plus electric vehicles in residential houses over commercial districts. Applied Energy, vol. 306, Part B, 118142. https://doi.org/10.1016/j.apenergy.2021.118142

Kondo T, Nagai T, Kawase T, Sakamoto Y, Masukawa Y, Sato M, Niwa K, Matsunawa K, Sawachi MMT. (2011). Comprehensive study on equipment use and on energy consumption for purpose of revision of the energy conservation standards: (Part 8) setting standard schedules of room and equipment use. Technical Paper. Annual Meeting of Society of Heating, Air-Conditioning and Sanitary Engineering (SHASE) Japan, pp. 2425-28. https://doi.org/https://doi.org/10.18948/shasetaikai.2011.3.0_2425

Koutra S, Denayer N, Galatoulas N, Becue N, Ioakimidis S. (2021). The zero-energy challenge in districts. Introduction of a methodological decision-making approach in the case of the district of Cuesmes in Belgium. International Journal of Urban Sustainable Development, vol. 13:3, pp. 585-613. https://doi.org/10.1080/19463138.2021.1985504

Langevin J, Harris CB, Reyna JL. (2019). Assessing the Potential to Reduce U.S. Building CO_2 Emissions 80% by 2050. Joule, vol. 3, pp. 2403–24. https://doi.org/10.1016/j.joule.2019.07.013

Langevin J, Reyna JL, Ebrahimigharehbaghi S, Sandberg N, Fennell P, Nägeli C, et al. (2020). Developing a common approach for classifying building stock energy models. Renewable and Sustainable Energy Reviews, vol. 133, 110276. https://doi.org/10.1016/j.rser.2020.110276

Lausselet C, Rokseth LS, Lien SK, Bergsdal H, Tønnesen J, Brattebø H, Sandberg NH. (2022). Geo-referenced building stock analysis as a basis for local-level energy and climate mitigation strategies. Energy and Buildings, vol. 276, 112504. https://doi.org/10.1016/j.enbuild.2022.112504

Ledesma G, Pons-Valladares O, Nikolic J. (2021). Real-reference buildings for urban energy modelling: A multistage validation and diversification approach. Building and Environment, vol. 203, 108058. https://doi.org/10.1016/j.buildenv.2021.108058

Lenormand M, Deffuant G. (2013). Generating a synthetic population of individuals in households: sample-free vs sample-based methods. Journal of Artificial Societies and Social Simulation, vol. 16, pp. 1–10. https://doi.org/10.18564/jasss.2319

Li X, Yao R. (2021). Modelling heating and cooling energy demand for building stock using a hybrid approach. Energy and Buildings, vol. 235, 110740. https://doi.org/10.1016/j.enbuild.2021.110740

Liang Y, Pan Y, Yuan X, Yang Y, Fu L, Li J, Sun T, Huang Z, Kosonen R. Assessment of operational carbon emission reduction of energy conservation measures for commercial buildings: Model development. Energy and Buildings, vol. 268, 112189, 2022. https://doi.org/10.1016/j.enbuild.2022.112189

Liu Z, Liu X, Zhang H, Yan D. (2023). Integrated physical approach to assessing urban-scale building photovoltaic potential at high spatiotemporal resolution. Journal of Cleaner Production, vol. 388, 135979. https://doi.org/10.1016/j.jclepro.2023.135979

Ma J, Cheng JCP. (2016). Estimation of the building energy use intensity in the urban scale by integrating GIS and big data technology. Applied Energy, vol. 183, pp. 182–92. https://doi.org/10.1016/j.apenergy.2016.08.079

Madhusanka HWN, Pan W, Kumaraswamy MM. (2022). Constraints to low-carbon building: Perspectives from high-rise high-density cities. Energy and Buildings, vol. 275, 112497. https://doi.org/10.1016/j.enbuild.2022.112497

Mata É, Sasic Kalagasidis A, Johnsson F. (2014). Building-stock aggregation through archetype buildings: France, Germany, Spain and the UK. Building and Environment, vol. 81, pp. 270–282. https://doi.org/10.1016/j.buildenv.2014.06.013

Mghouchi El Y, Bouardi El A, Choulli Z, Ajzoul T. (2016). Models for obtaining the daily direct, diffuse and global solar radiations. Renewable and Sustainable Energy Reviews, vol. 56, pp. 87-99. https://doi.org/10.1016/j.rser.2015.11.044

Ministry of Economy Trade and Industry (METI). General rules of recommended lighting levels (JIS-Z-9110), 2011. http://www.jisc.go.jp/app/jis/general/GnrJISNumberNameSearchList?toGnrJISStandardDetailList (In Japanese).

Ministry of Environment (MOE), Japan. Overview of the Plan for Global Warming Countermeasures, 2016. (https://www.env.go.jp/press/files/en/676.pdf)

Moazzen N, Ashrafian T, Yilmaz Z, Karagüler ME. (2020). A multi-criteria approach to affordable energy-efficient retrofit of primary school buildings. Applied Energy, vol. 268, 115046. https://doi.org/10.1016/j.apenergy.2020.115046

Mohammadiziazi R, Copeland S, M. Bilec M. (2021). Urban building energy model: Database development, validation, and application for commercial building stock. Energy and Buildings, vol. 248, 111175. https://doi.org/10.1016/j.enbuild.2021.111175

Morewood J. (2023). Building energy performance monitoring through the lens of data quality: A review. Energy and Buildings, vol. 279, 112701. https://doi.org/10.1016/j.enbuild.2022.112701

Nageler P, Zahrer G, Heimrath R, Mach T, Mauthner F, Leusbrock I, Schranzhofer H, Hochenauer C. (2017). Novel validated method for GIS based automated dynamic urban building energy simulations. Energy, vol. 139, pp. 142–54. https://doi.org/10.1016/j.energy.2017.07.151

Nägeli C, Camarasa C, Delghust M, Fennell P, Hamilton I, Jakob M, Langevin J, Laverge J, Reyna JL, Sandberg NH, Webster J. (2022). Best practice reporting guideline for building stock energy models. Energy and Buildings, vol. 260, 111904. https://doi.org/10.1016/j.enbuild.2022.111904

Nägeli C, Camarasa C, Jakob M, Catenazzi G, Ostermeyer Y. (2018). Synthetic building stocks as a way to assess the energy demand and greenhouse gas emissions of national building stocks. Energy and Buildings, vol. 173, pp. 443-460. https://doi.org/10.1016/j.enbuild.2018.05.055

Nägeli C, Jakob M, Catenazzi G, Ostermeyer Y. (2020). Towards agent-based building stock modeling: Bottom-up modeling of long-term stock dynamics affecting the energy and climate impact of building stocks. Energy and Buildings, vol. 211, 109763. https://doi.org/10.1016/j.enbuild.2020.109763

Nutkiewicz A, Yang Z, Jain RK. (2018). Data-driven Urban Energy Simulation (DUE-S): A framework for integrating engineering simulation and machine learning methods in a multi-scale urban energy modeling workflow. Applied Energy, vol. 225, pp. 1176–89. https://doi.org/10.1016/j.apenergy.2018.05.023

Österbring M, Mata É, Thuvander L, Mangold M, Johnsson F, Wallbaum H. (2016). A differentiated description of building-stocks for a georeferenced urban bottom-up building-stock model. Energy and Buildings, vol. 120, 78-84. https://doi.org/10.1016/j.enbuild.2016.03.060

Panagiotidou M, Brito MC, Hamza K, Jasieniak JJ, Zhou J. (2021). Prospects of photovoltaic rooftops, walls and windows at a city to building scale. Solar Energy, vol. 230, pp. 675-687. https://doi.org/10.1016/j.solener.2021.10.060

Pasichnyi O, Wallin J, Kordas O. (2019). Data-driven building archetypes for urban building energy modelling. Energy, vol. 181, pp. 360–377. https://doi.org/10.1016/j.energy.2019.04.197

Perez R, Seals R, Ineichen P, Stewart R, Menicucci D. (1987). A new simplified version of the perez diffuse irradiance model for tilted surfaces. Solar Energy, vol. 39, Issue 3, 1987, pp. 221-231. https://doi.org/10.1016/S0038-092X(87)80031-2

Perez R, Stewart R, Arbogast C, Seals R, Scott J. (1986). An anisotropic hourly diffuse radiation model for sloping surfaces: Description, performance validation, site dependency evaluation. Solar Energy, vol. 36, Issue 6, pp. 481-497. https://doi.org/10.1016/0038-092X(86)90013-7

Perwez U, Yamaguchi Y, Ma T, Dai Y, Shimoda Y. (2022). Multi-scale GIS-synthetic hybrid approach for the development of commercial building stock energy model. Applied Energy, vol. 323, 119536. https://doi.org/10.1016/j.apenergy.2022.119536

Perwez U, Yamaguchi Y, Shimoda Y. (2020). Development of Geo-spatial building stock model for Japanese Commercial Buildings. Proceedings of 2nd Annual Conference of Society of Airconditioning and Sanitary Engineering (SHASE), vol. 10. https://doi.org/10.18948/shasetaikai.2020.10.0_25

Perwez UB, Yamaguchi Y, Shimoda Y. (2021). Cross-over analysis of building-stock modelling approaches for bottom-up engineering model. Proceedings of Building Simulation 2021: 17th Conference of IBPSA, vol. 17, pp. 1781-1788. https://doi.org/10.26868/25222708.2021.30586

Prataviera E, Vivian J, Lombardo G, Zarrella A. (2022). Evaluation of the impact of input uncertainty on urban building energy simulations using uncertainty and sensitivity analysis. Applied Energy, vol. 311, 118691. https://doi.org/10.1016/j.apenergy.2022.118691

Rasool MH, Perwez U, Qadir Z, Ali SMH. (2022). Scenario-based techno-reliability optimization of an off-grid hybrid renewable energy system: A multi-city study framework. Sustainable Energy Technologies and Assessments, vol. 53, Part A, 102411. https://doi.org/10.1016/j.seta.2022.102411

Reinhart C, Davila C. (2016). Urban building energy modeling – A review of a nascent field. Building and Environment, vol. 97, pp. 196-202. https://doi.org/10.1016/j.buildenv.2015.12.001

Reinhart CF, Dogan T, Jakubiec JA, Rakha T, Sang A. (2013). UMI - An urban simulation environment for building energy use, daylighting and walkability. Proceedings of Building Simulation 2013: 13th Conference of IBPSA, vol. 13, pp. 476–83.

Robinson C, Dilkina B, Hubbs J, Zhang W, Guhathakurta S, Brown MA, et al. (2017). Machine learning approaches for estimating commercial building energy consumption. Applied Energy, vol. 208, pp. 889–904. https://doi.org/10.1016/j.apenergy.2017.09.060

Rodríguez LR, Duminil E, Ramos JS, Eicker U. (2017). Assessment of the photovoltaic potential at urban level based on 3D city models: A case study and new methodological approach. Solar Energy, vol. 146, pp. 264-275. https://doi.org/10.1016/j.solener.2017.02.043

Roth J, Martin A, Miller C, Jain RK. (2020). SynCity: Using open data to create a synthetic city of hourly building energy estimates by integrating data-driven and physics-based methods. Applied Energy, vol. 280, 115981. https://doi.org/10.1016/j.apenergy.2020.115981

Saretta E, Caputo P, Frontini F. (2019). A review study about energy renovation of building facades with BIPV in urban environment. Sustainable Cities and Society, vol. 44, pp. 343-355. https://doi.org/10.1016/j.scs.2018.10.002

Sartori I, Napolitano A, Voss K. (2012). Net zero energy buildings: A consistent definition framework. Energy and Buildings, vol. 48, pp. 220-232.

Sartori I, Sandberg NH, Brattebø H. (2016). Dynamic building stock modelling: General algorithm and exemplification for Norway. Energy and Buildings, vol. 132, pp. 13–25. https://doi.org/10.1016/j.enbuild.2016.05.098

Shono K, Yamaguchi Y, Perwez U, Ma T, Dai Y, Shimoda Y. (2023). Large-scale building-integrated photovoltaics installation on building façades: Hourly resolution analysis using commercial building stock in Tokyo, Japan. Solar Energy, vol. 253, pp. 137-153. https://doi.org/10.1016/j.solener.2023.02.025

Society of Heating, Air-Conditioning and Sanitary Engineers of Japan (SHASE-J). (2017). Archi-tec consulting Co. Ltd, A&S Data. (http:/www.archi-tec.jp/#secA)

Sokol J, Cerezo Davila C, Reinhart CF. (2017). Validation of a Bayesian-based method for defining residential archetypes in urban building energy models. Energy and Buildings, vol. 134, pp. 11–24. https://doi.org/10.1016/j.enbuild.2016.10.050

Statistical Bureau of Japan (SBJ), e-Stat. (2017). The Result of the Survey on Land and Buildings. (http://www.estat.go.jp/SG1/estat/GL08020101.do?toGL08020101&tstatCode=000001020939)

Sun C, Perwez U, Yamaguchi Y, Shimoda Y. (2021). Impact of urban morphology on building energy use and solar potential of the commercial building stock in Tokyo. Proceedings from 37th JSER: Energy System/Economic/Environmental Conference. Building Simulation and Optimisation Conference.

The Illuminating Engineering Institute of Japan (IEIJ). Lighting handbook. 2006.

Thebault M, Desthieux G, Castello R, Berrah L. (2022). Large-scale evaluation of the suitability of buildings for photovoltaic integration: Case study in Greater Geneva. Applied Energy, vol. 316, 119127. https://doi.org/10.1016/j.apenergy.2022.119127

Tokyo Electric Power Company (TEPCO), CO2 Emissions, CO2 Emissions Intensity and Electricity Sales, 2016. (https://www.tepco.co.jp/en/corpinfo/illustrated/environment/emissions-co2-e.html)

Tokyo Gas (TG), Sustainability report, 2021. (https://www.tokyo-gas.co.jp/sustainability/download/pdf/en/e-sr2021_all.pdf)

Tokyo Metropolitan Government (TMG), 2020. Tokyo carbon reporting program for SMFs. (In Japanese).

Tokyo Statistical Yearbook (TSY), 2019. Construction and Housing.

Tokyo Urban Development Bureau (TUDB), 2017. Tokyo city planning geographic information system.

U.S. EIA. (2020). Commercial Demand Module of the National Energy Modeling System: Model Documentation 2020:187.

United Nations Framework Convention on Climate Change (UNFCCC) Annual Conference of the Parties (COP) 26. Glasgow climate pact, 2021. (https://unfccc.int/sites/default/files/resource/cma3_auv_2_cover%20decision.pdf)

United States Department of Energy (DOE), EnergyPlus Ver.8.6, 2016. (https://www.energyplus.net/)

Vaisi S, Firouzi M, Varmazyari P. (2023). Energy benchmarking for secondary school buildings, applying the Top-Down approach. Energy and Buildings, vol. 279, 112689. https://doi.org/10.1016/j.enbuild.2022.112689

Walch A, Castello R, Mohajeri N, Scartezzini J. (2020). Big data mining for the estimation of hourly rooftop photovoltaic potential and its uncertainty. Applied Energy, vol. 262, 114404. https://doi.org/10.1016/j.apenergy.2019.114404

Wang C, Ferrando M, Causone F, Jin X, Zhou X, Shi X. (2022). Data acquisition for urban building energy modeling: A review. Building and Environment, vol. 217, 109056. https://doi.org/10.1016/j.buildenv.2022.109056

Yadav AK, Chandel SS. (2015). Solar energy potential assessment of western Himalayan Indian state of Himachal Pradesh using J48 algorithm of WEKA in ANN based prediction model. Renewable Energy, vol. 75, pp. 675-693. https://doi.org/10.1016/j.renene.2014.10.046

Yamaguchi Y, Kim B, Kitamura T, Akizawa K, Chen H, Shimoda Y. (2022). Building stock energy modeling considering building system composition and long-term change for climate change mitigation of commercial building stocks. Applied Energy, vol. 306, 117907. https://doi.org/10.1016/j.apenergy.2021.117907

Yamaguchi Y, Miyachi Y, Shimoda Y. (2017). Stock modeling of HVAC systems in Japanese commercial building sector using logistic regression. Energy and Buildings, vol. 152, pp. 458–71. https://doi.org/10.1016/j.enbuild.2017.07.007

Yang X, Hu M, Heeren N, Zhang C, Verhagen T, Tukker A, et al. (2020). A combined GIS-archetype approach to model residential space heating energy: A case study for the Netherlands including validation. Applied Energy, vol. 280, 115953. https://doi.org/10.1016/j.apenergy.2020.115953

Yang X, Hu M, Zhang C, Steubing B. (2022). Key strategies for decarbonizing the residential building stock: Results from a spatiotemporal model for Leiden, the Netherlands. Resources, Conservation and Recycling, 184, 106388. https://doi.org/10.1016/j.resconrec.2022.106388

Ye Y, Chen Y, Zhang J, Pang Z, O'Neill Z, Dong B, et al. (2021). Energy-saving potential evaluation for primary schools with occupant-centric controls. Applied Energy, vol. 293, 116854. https://doi.org/10.1016/j.apenergy.2021.116854

Yoshino H, Hong T, Nord N. (2017). IEA EBC annex 53: Total energy use in buildings—Analysis and evaluation methods. Energy and Buildings, vol. 152, pp. 124–36. https://doi.org/10.1016/j.enbuild.2017.07.038

Yu FW, Ho WT. (2021). Tactics for carbon neutral office buildings in Hong Kong. Journal of Cleaner Production, vol. 326, 129369. https://doi.org/10.1016/j.jclepro.2021.129369

Yu H, Wang M, Lin X, Guo H, Liu H, Zhao Y, Wang H, Li C, Jing R. (2021). Prioritizing urban planning factors on community energy performance based on GIS-informed building energy modelling. Energy and Buildings, vol. 249, 111191. https://doi.org/10.1016/j.enbuild.2021.111191

Zhang A, Bokel R, Dobbelsteen AVD, Sun Y, Huang Q, Zhang Q. (2017). Optimization of thermal and daylight performance of school buildings based on a multi-objective genetic algorithm in the cold climate of China. Energy and Buildings, vol. 139, pp. 371-384. https://doi.org/10.1016/j.enbuild.2017.01.048

Zhang N, Luo Z, Liu Y, Feng W, Zhou N, Yang L. (2022). Towards low-carbon cities through building-stock-level carbon emission analysis: a calculating and mapping method. Sustainable Cities and Society, vol. 78, 103633. https://doi.org/10.1016/j.scs.2021.103633

Zhang S, Ma M, Xiang X, Cai W, Feng W, Ma Z. (2022). Potential to decarbonize the commercial building operation of the top two emitters by 2060. Resources, Conservation and Recycling, vol. 185, 106481. https://doi.org/10.1016/j.resconrec.2022.106481

Zhang X, Wang F. (2016). Assessment of embodied carbon emissions for building construction in China: Comparative case studies using alternative methods. Energy and Buildings, vol. 130, pp. 330-340. https://doi.org/10.1016/j.enbuild.2016.08.080

Zheng Y, Weng Q. (2019). Modeling the effect of climate change on building energy demand in Los Angeles county by using a GIS-based high spatial- and temporal-resolution approach. Energy, vol. 176, pp. 641–655. https://doi.org/10.1016/j.energy.2019.04.052

Zhu L, Wang B, Sun Y. (2020). Multi-objective optimization for energy consumption, daylighting and thermal comfort performance of rural tourism buildings in north China. Building and Environment, vol. 176, 106841. https://doi.org/10.1016/j.buildenv.2020.106841

Zhu W, Feng W, Li X, Zhang Z. (2020). Analysis of the embodied carbon dioxide in the building sector: A case of China. Journal of Cleaner Production, vol. 269, 122438. https://doi.org/10.1016/j.jclepro.2020.122438